MECHANISTIC CHARACTERIZATION OF THIN ASPHALT OVERLAYS FOR PAVEMENT PRESERVATION USING THE FINITE ELEMENT MODELING APPROACH

FINAL PROJECT REPORT

by

Imad Al-Qadi
Hasan Ozer
Jaime Hernandez
Heena Dhasmana

University of Illinois at Urbana-Champaign

for

Center for Highway Pavement Preservation
(CHPP)

In cooperation with US Department of Transportation Research and Innovative Technology Administration (RITA)

August, 2018

Disclaimer

The contents of this report reflect the views of the authors, who are responsible for the facts and the accuracy of the information presented herein. This document is disseminated under the sponsorship of the U.S. Department of Transportation's University Transportation Centers Program, in the interest of information exchange. The Center for Highway Pavement Preservation (CHPP), the U.S. Government and matching sponsor assume no liability for the contents or use thereof.

Technical Report Documentation Page

1. Report No. ICT-18-008	2. Government Accession No. N/A	3. Recipient's Catalog No. N/A	
4. Title and Subtitle Mechanistic Characterization of Thin Asphalt Overlays for Pavement Preservation Using the Finite Element Modeling Approach		5. Report Date June 2018 6. Performing Organization Code N/A	
7. Author(s) Imad Al-Qadi, Hasan Ozer, Jaime Hernandez, Heena Dhasmana		8. Performing Organization Report No. ICT-18-008 UILU-ENG-2018-2008	
9. Performing Organization Name and Address CHPP Center for Highway Pavement Preservation, Tier 1 University Transportation Center Michigan State University, 2857 Jolly Road, Okemos, MI 48864		10. Work Unit No. (TRAIS) N/A 11. Contract or Grant No. N/A	
12. Sponsoring Organization Name and Address United States of America Department of Transportation Research and Innovative Technology Administration		13. Type of Report and Period Covered Final Report 9/30/2013-9/30/2018 14. Sponsoring Agency Code N/A	
15. Supplementary Notes Report uploaded at http://www.chpp.egr.msu.edu/			

16. Abstract

Thin asphalt concrete (AC) overlays are commonly used as a preservation technique for rigid and flexible pavement because of their ability to improve riding quality, extend service life, and reduce noise level. Many state highway agencies are currently using thin overlays routinely as part of their planned preservation and maintenance operations. Despite the widespread use of thin overlays, there is a gap in the literature related to their life expectancy and potential role in improving pavement's structural capacity and functional properties. This research work aimed at characterizing the performance of thin AC overlays using a mechanistic approach. The analysis of thin overlay poses significant challenges compared with the conventional techniques commonly used in the analysis of layered pavement systems. Considering the fact that the overlays are directly exposed to non-uniform and three-dimensional truck loads resulting in complex stress states mostly in compression and shear, some of the fundamental assumptions used in the mechanistic analysis of pavements are violated. In addition, the AC mixture's heterogeneity and microstructural characteristics can govern the response within these surface layers under complex environmental and traffic loading conditions. A three dimensional (3-D) finite element (FE) modeling approach coupled with domain analysis were used to address some of these challenges. Domain analysis allows better characterization of complex stress and strain states within the thin overlays by providing a more representative response spectrum. It also incorporates the material's failure characteristics to represent different types of AC mixtures or damage in existing pavement layers. As a result, a correlation was developed between the service life and domain analysis output demonstrating a variation of allowable service lives between seven and approximately 15 years. The outcome provides guidance to agencies to predict the service life of a thin overlay treatment when major variables such as existing pavement condition and AC thickness and mixture characteristics are known.

17. Thin overlay, mechanistic, finite element, domain analysis		18. Distribution Statement No restrictions.	
19. Security Classification (of this report) Unclassified.	20. Security Classification (of this page) Unclassified.	21. No. of Pages 74 pp.	22. Price NA

Form Reproduction of completed page authorized

TABLE OF CONTENTS

List of Figures

List of Tables

List of Abbreviations

FHWA: Federal Highway Administration
UIUC: University of Illinois at Urbana-Champaign
CHPP: Center for Highway Pavement Preservation
ICT: Illinois Center for Transportation
ATREL: Advanced Transportation Research and Engineering Laboratory
NMAS: Nominal Maximum Aggregate Size

Acknowledgments

This publication is based on the results of the CHPP sponsored project, Mechanistic Characterization of Thin Asphalt Overlays for Pavement Preservation using the finite element modeling approach, conducted in cooperation with the Illinois Center for Transportation (ICT).

The contents of this report reflect the view of the authors, who are responsible for the facts and the accuracy of the data presented herein. The contents do not necessarily reflect the official views or policies of Center for Highway Pavement Preservation or ICT.

Trademark or manufacturers' names appear in this report only because they are considered essential to the object of this document and do not constitute an endorsement of product by ICT.

Executive Summary

According to various reports published by the Federal Highway Administration (FHWA), almost 49.4 percent of vehicle miles traveled on the federal-aid highway system could not meet the established standard of good ride quality and almost 18 percent even failed to qualify for the "acceptable level" of riding quality. It was also emphasized that the condition of pavements has a direct and considerable impact on the vehicle operating costs and the entire transportation infrastructure performance (Keenan et al., 2012, USDOT, 2013). Thin overlays have been recently considered as one of the preservation strategies which have been increasingly used to improve pavement performance and maintain acceptable ride quality in a cost-effective manner.

Thin overlays are popular primarily due to their ability to improve ride quality and aesthetics at a cost much lower than conventional overlays. According to conducted surveys, many construction agencies have been using thin overlays not only because of the benefits they might provide but mostly because of their cost effectiveness. However, there is a great deal of non-uniformity in the guidelines in definition and thickness selection of thin overlays. Thin overlays are usually not considered a structural component of a pavement system. Therefore, material and thickness selection is rather arbitrary, resulting in a wide range of service life for thin overlays.

This research project aims at developing a mechanistic approach first to understand the mechanics of thin overlays and to provide guidance to agencies to select materials and thickness for thin overlay applications. The mechanics of thin overlays are complicated due to complex stress states as a result of direct exposure to non-uniform tire contact stresses and environmental loadings. The loading within the surface layers can be primarily in compression and shear. There is no experimental method for asphalt mixtures to relate such field responses. Simple mechanistic models, including layered elastic or viscoelastic and 2-D axisymmetric finite element, may not describe the mechanics and physics of this problem. Therefore, the three-dimensional (3-D) finite element (FE) modeling approach was chosen in this study. The 3-D FE models were coupled with domain analysis instead of the critical point strain method. In addition, micromechanical modeling was used to incorporate mixes failure characteristics in the 3-D FE analysis.

A numerical analysis matrix was prepared to investigate major variables affecting thin overlay performance. These factors include thickness, mixture type, existing pavement condition, and removal of the deteriorated layers. Thin overlays are assumed to vary in thickness from a minimum value of 0.75 in to a maximum of 2 in. One stone mastic asphalt (SMA) with PG 70-22 binder and a dense-graded mix utilizing PG 64-22 and includes 20% recycled asphalt shingle (RAS) were used. A few inches are usually milled off from the surface before placing the thin overlay; therefore, analysis is usually conducted after an inch is reduced from the thickness of the asphalt layer directly beneath the thin overlay. This allows for a more realistic simulation of the actual design practice on the field.

Initially, traditional critical point response analysis was conducted using the results of 3-D FE models. According to the outcome of this analysis, it was found out that the longitudinal strains are always greater than transverse strains at the bottom of the overlay system that includes thin overlays and the rest of the asphalt concrete (AC) layers. Thin overlays up to 2 in are under heavy

influence of compression and shear type of stresses. For all the critical responses studied, as part of the overall pavement system, a decrease in values was observed with an increase in the thickness of the thin overlay. The structural contribution of thin overlays was manifested as a reduction in the vertical strains on top of the subgrade. However, point stress and strain analysis were found to be inadequate to describe complex stress and strain states within thin overlays. Hence, resulted in inconclusive service life predictions for thin overlay treatments.

As an alternative approach to the critical point stress or strain analysis, the domain analysis method was utilized to better understand the mechanics of thin overlays. The domain analysis method utilized was recently introduced by Gamez et al. (2018). Flexible pavement responses to tire loading, obtained using advanced FE models, are presented within nine subdomains. A scalar damage indicator is determined, which is unique to a pavement structure (layer thickness and material properties) and loading configuration (tire type, axle load, tire–inflation pressure). The domain method provided a more representative response spectrum covering the nine subdomains. Domain analysis method was used to represent different materials with distinctive failure characteristics or existing deteriorated layers prior to thin overlay application. When the effect of deterioration was considered in the existing AC section, it was found out that shear strains increase considerably for most of the zones in AC layers beneath the overlay. The increase was, however, more significant at the bottom of the AC section.

Finally, the outcome of the numerical analyses was used to predict the thin overlay service life. Four overlay thickness and 14 mixture types were considered in this study. A correlation developed between the service life and the pavement characteristics; with allowable service lives ranging from seven to approximately 15 years.

CHAPTER 1 - INTRODUCTION

1.1 INTRODUCTION

Thin overlays are considered one of the commonly used preservation techniques on low- and high-volume roads. Thin asphalt overlays are commonly used to increase the functional performance and durability of asphalt pavements, thus facilitating a smooth ride without increasing the structural capacity of pavements. The definition of thin overlay may vary among the states according to recent surveys. Surveys data reveal disagreements on the value of what is considered appropriate thickness by various agencies for thin overlays (Figure 1-1). For instance, many agencies do not define these overlays as a "thin "or "non-thin" asphalt overlay. Variations are also observed in the evaluation of average service life by various agencies; values for service life vary from seven to 11 years. The factors resulting in such a wide range may include traffic, weather, existing pavement conditions (extent and severity of distress) at the time of overlay construction, and the use of varying quality standards when thin overlays are placed on interstate highway projects versus secondary and local roads (Watson and Heitzman, 2014).

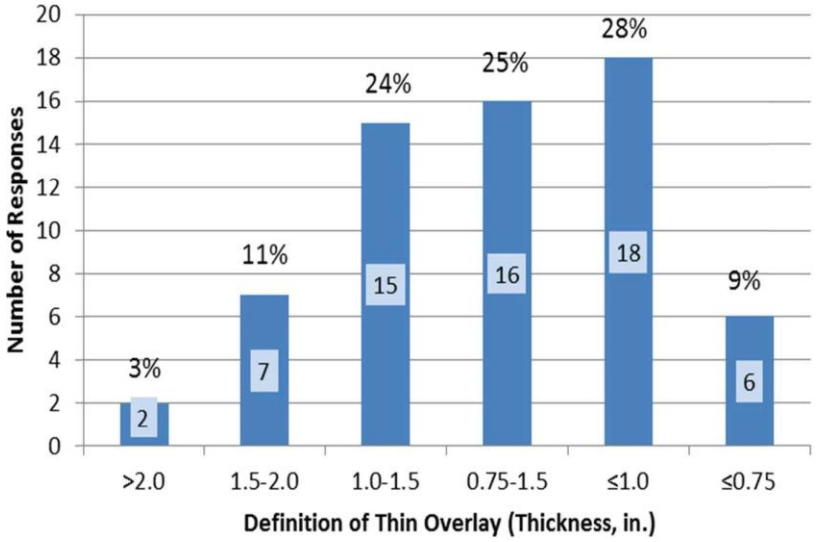

Figure 1-1 Definition of overlay thickness response by various agencies (Watson and Heitzman 2014).

Effective implementation of a preservation strategy with strategic planning and timing of activities, including thin asphalt overlays, can go a long way in ensuring the longevity of pavement at a cost lower than major rehabilitation costs. Thin asphalt overlays are generally more economical than relatively thicker dense-graded layers when applied at the right time and conditions (Watson and Heitzman, 2014). Thin layers at the pavement surface allow pavement engineers to overlay more lane-miles with the same resurfacing budget. As a result, thin overlays are often reported to have lower life-cycle costs than other available types of pavement preservation solutions (Table 1-1).

Table 1-1 Summary of Expected Lives and Costs for Preservation Treatments (Wang et al., 2012)

Preservation Treatment	Average Service Life (Years)	Cost Per Lane-Mile ($)
Thin overlay	8.4	14,600
Double chip seal	7.3	12,600
Micro-surfacing	7.4	12,600
Slurry seal	4.8	6,600

The National Asphalt Pavement Association (NAPA) information series 135 provides a detailed and updated summary of thin asphalt overlays, emphasizing the shift of focus from new pavement construction to more wide-scale maintenance and rehabilitation activities (Newcomb, 2009). Selection of pavement maintenance/preservation activities is project based, but agencies often have a set of activities designed for the lifetime of different pavement types. NCHRP Synthesis Report 222 summarizes three main approaches based on the pavement preservation activity selected, namely pavement condition analysis, priority assessment models, and network optimization models (Zimmerman, 1995). The report concludes that the most important basis for treatment selection is finding the technique that most effectively addresses the deficiencies of existing pavement. Efficiency is quantified mostly on the basis of total cost incurred, typical service life of the treatment, and life-cycle costs. Additional factors used in the evaluation of pavement choices include pavement condition, functional classification, and type of overlaid existing pavement (Watson and Heitzman, 2014).

According to a 1999 AASHTO survey conducted by the Lead States Team on Pavement Preservation, thin asphalt overlays were presented as the most popular preventive maintenance treatment for asphalt and composite pavements (AASHTO, 2009). This observation has led to an increase in the number of studies on the materials, design, and construction of thin overlays which not only focus on optimizing pavement preservation strategies, but also on the development of new technologies and improved materials to help extend the service life of pavements; works by Cooley and Brown (2003), Walubita and Scullion (2008), and Chou et al. (2008) are only a few examples.

Two major distresses that have been observed in thin asphalt overlays are reflective and thermal cracking. Thermal cracks develop as a result of high cooling rates and/or low pavement temperature resulting from changes in the weather. Damage is triggered when the thermal stresses exceed the strength and fracture resistance of the mix in the overlays. Overlays are also exposed to cracking due to traffic loading and temperature variations at the joints and cracks in the underlying pavement layer. As a result, reflective cracks are generated in the overlay which provides a path for water to penetrate inside the pavement structure, thus leading to roughness, spalling, etc. (Son and Al-Qadi, 2014).

Different evaluation methods have been proposed for the design of thin asphalt overlays under various conditions. The earliest technique involved empirical models in which a threshold was created with respect to the existing conditions in order to design certain aspects of pavement. Empirical methods are often limited to the conditions (traffic, environment, and materials) where

they are developed and cannot be easily generalized to the situations where any one of these conditions are outside the expected range. Therefore, the use of empirical method to design and understand thin overlay behavior is restricted. To overcome this issue, mechanistic empirical pavement design methods were developed in the 1990s (Thompson and Elliott, 1985; Thompson, 1996; Smith et al. 1986). Along with the nationwide attempt to develop a mechanistic empirical method to design new pavements, the concept was also applied to major maintenance treatment techniques such as overlays. An attempt by Texas Transportation Institute (TTI) was made to develop mechanistic empirical rutting and reflection cracking models for overlay design and analysis which were thereafter integrated in an asphalt overlay thickness design and analysis system (Zhou et al., 2009). Different analytical approaches, ranging from the simple closed from solutions to the complex FE models, have been developed to-date to effectively understand the performance of different combinations of overlays in the construction of composite pavements. However, none of these mechanistic methods were applied to the thin overlays as they are considered non-structural components of pavement structure.

1.2 PROBLEM STATEMENT

Despite the progress in developing advanced methods to design new pavements and understand pavement's structural response to make more accurate predictions, our understanding of how thin overlays behave is limited. There is no mechanistic based design method so far developed for thin overlays. There is number of difficulties and complexities that could be attributed to the lack of use of proper mechanistic analysis methods in the case of thin overlays. First of all, surface layers are under direct exposure to tire contact stresses, temperature, and aging gradients. All of these factors can generate a complex 3-D stress and strain field much more different than the rest of the layers where the mechanistic design methods often extract critical response. Therefore, classical structural analysis methods such as the layered elastic or 2-D FE used in the design of flexible pavements may not capture the mechanics of thin overlay behavior. Therefore, our understanding of near-surface failure primarily taking place within the thin overlay is limited.

Due to the lack of understanding and proper design methods, thickness of thin overlays is often determined based on mix type (governed by minimum or maximum lift thickness that can be constructed by the selected mix design) or past experiences. Therefore, there exists a wide range of service life expected from thin overlays as reported in the literature. It is imperative to improve our understanding of the factors affecting the performance of thin overlays to make more efficient designs that improve the service life of thin overlays. Therefore, this study proposes the use of advanced modeling techniques to understand the behavior of thin overlays and develop tools to predict the performance of thin overlays more accurately.

1.3 RESEARCH OBJECTIVE AND SCOPE

The principal objective of this study was to investigate the structural response of thin overlays using mechanistic methods. The ultimate aim of the project was to provide state highway agencies with objective tools to make a decision with respect to the design of thin asphalt overlays. For this purpose, certain design variables, including overlay thickness, mix characteristics, existing condition of pavement structure before overlay application were considered and their impact on asphalt overlays was evaluated. Because thin asphalt overlay consists of the pavement layer which

is directly affected by exterior stresses, the analysis was performed on the micro as well as macro scales considering mix heterogeneity and non-uniform, 3-D contact stresses.

In order to accomplish the ultimate goal of the study, a multi-scale modeling approach was developed. The research scope includes the following:

- Local materials scale micromechanical modeling of selected asphalt concrete (AC) mixes to quantify contribution of microscale features to cracking of thin overlay mixes (Volume I)
- Global scale pavement modeling to evaluate mechanics of thin overlays and failure mechanisms with consideration of microscale features obtained from the micromechanical modeling (Volume II)
- Laboratory testing to provide input to both modeling stages at micromechanical local and global pavement scale (Volumes I and II)

1.4 RESEARCH TASKS AND METHODOLOGY

The study consisted of modeling tasks at the micromechanical scale and global pavement scale. There are various types of laboratory tests conducted to provide input to the modeling efforts. The experiments included dynamic shear rheometer for complex modulus of binders, direct tensile testing equipment for binder-mortar adhesion property, and complex modulus testing of AC mixes. Subsequently, results obtained at small scale are projected on to the global scale using linear viscoelastic functions to maintain computational efficiency. The computational models at the continuum level can generate efficient responses for different variables that may be critical for thin asphalt overlay performance.

1.5 ORGANIZATION OF THE REPORT

Chapter 1 provides the introduction and objectives of the project. Chapter 2 provides detailed review of the literature in the field of thin asphalt overlays characterization. A detailed summary of the experimental, empirical as well as computational methods is also provided. Thereafter, information about the experimental programs conducted for this study and the mixes used for analysis is given in Chapter 3. Results of the 3-D pavement FE model with and without thin overlays are presented in Chapter 4. Values of certain critical responses along the depth of the pavement structure are generated and studied to gauge the impact of certain variables affecting the performance of thin asphalt overlays. Chapter 5 presents the domain analysis technique and its results for this project. Finally, Chapter 6 highlights the importance of the failure criteria defined for any pavement problem.

CHAPTER 2 - LITERATURE REVIEW

A thin surface pavement can be defined as either a single or multiple application bituminous surface treatment or a layer of hot-mix asphalt less than 2 in thick over an unbound base (Anderson et al. 2014). Thin asphalt overlays are useful among the maintenance/pavement preservation treatments due to various reasons. One of their most attractive features is that they are generally more economical than thicker, dense-graded layers (Watson and Heitzman, 2014). Thin layers also allow pavement engineers to overlay more lane-miles using the same weight material. Lower life-cycle costs of thin overlays demonstrating satisfactory performance have led to their use as a standard practice across agencies. A 2012 survey on pavement preservation treatments in cold regions found that in conditions of heavy studded tire usage, crack sealing, patching, and thin overlays are the most common treatments used (Zubeck et al., 2012). Apart from the usage of traditional dense-graded AC layers, various other specialty mixes have also been developed.

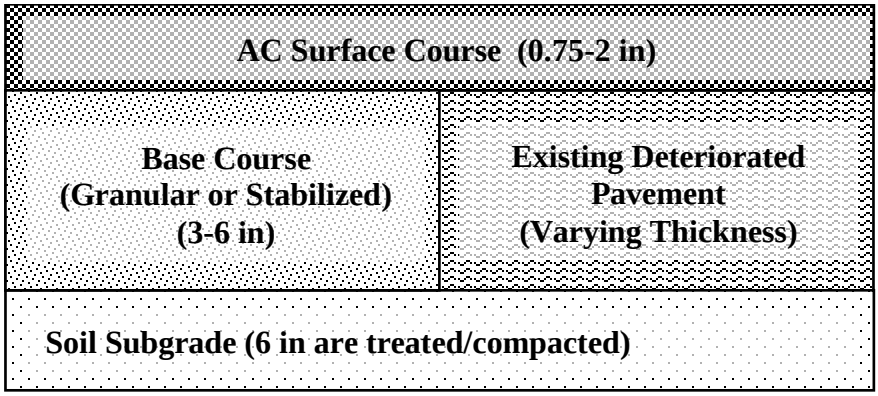

Figure 2-1 Typical cross section of a surface treatment (Anderson et al., 2014).

According to the survey conducted as part of NCHRP Synthesis Report 222, it was found out that the average service life of a thin overlay constructed in the prescribed situations ranges from seven to 11 years (Watson and Heitzman, 2014). The attributes generally responsible for this outcome could be traffic, weather, existing pavement condition (and level of distress) at the time of overlay construction, and the use of different quality standards when thin overlays are placed on interstate projects versus secondary and local roads (Watson and Heitzman, 2014). This may be because most pavement structural design procedures facilitate a wearing surface with some structural value, whereas thin overlays do not provide any structural potential to the pavement. Hence, no structural design methods are directly applicable where thin overlays are constructed.

In the NCHRP survey, 61% of the agencies mentioned using thin-surfaced pavements because they had the lowest first cost for a hard-surface pavement, while 54% indicated their

selection was based on budget limitations. Survey results were consistent, indicating that 91% of local government agencies stated that a thin-surfaced pavement was all they could manage on a restricted budget and 81% of the states pointed out that they chose thin-surfaced pavements because of low initial costs. Furthermore, only 60% of the agencies indicated that they based the thickness and structural design of their pavements on experience and not on a published procedure. This percentage was fairly consistent at all levels, except at the federal level (Geoffroy, 1998).

2.1 FACTORS AFFECTING THIN ASPHALT OVERLAY CONSTRUCTION

Performance of thin asphalt overlays can be affected on a major or minor scale by any of the following (Watson and Heitzman, 2014; Newcomb, 2009; Geoffroy, 1998; Eshan, 2009):

1. Existing pavement condition and extent/severity of distresses
2. Traffic loads and volumes
3. Environmental and climatic conditions (e.g., dust control, temperature, moisture, etc.)
4. Material availability and selection
5. Subgrades and drainage
6. Use of recycled materials
7. Construction quality

Design and material selection criteria for maintenance treatments including thin overlays may include some or all of the following considerations (Newcomb, 2009):

1. Provides a smooth surface
2. Increases frictional resistance
3. Reduces noise at tire–pavement interface when fine-graded mixtures are used
4. Increases safety
5. Reduces agency maintenance costs
6. Reduces vehicle operating and maintenance costs
7. Reduces the amount of moisture entering the pavement structure
8. Eliminates or reduces the loss of surface aggregate
9. Availability of local materials and work force skilled in applying materials
10. Maintains grade and slope geometry with little environmental impact
11. Can be recycled
12. Can be easily maintained
13. Increases cost effectiveness
14. Minimizes life-cycle costs

The immediate benefits of improvement in performance with a thin asphalt overlay are the improvement in ride quality, pavement condition, decreased noise level, and in some cases, friction. Labi et al. concluded that the direct gain in ride quality ranges from 18 to 36% decrease in the International Roughness Index (IRI); 5 to 55% reduction in rut depth; and 1 to 10% improvement in the pavement surface condition rating (Labi et al., 2005). It was also reported in a FHWA study that thin asphalt rubber overlays in the Phoenix area resulted in noise reduction by 5dB (FHWA, 2005). Chou et al. studied thin overlays which were 2 in or less and found out that the range of expected performance was quite stable among different projects and did not seem to be affected significantly by varying climate and traffic levels (Chou et al., 2008). It was also

concluded that overlays of asphalt pavements apparently last longer than those placed on either concrete or composite pavements. Belshe et al. analyzed the thin asphalt rubber open-graded overlays in Arizona and deduced that they hold the potential for prolonging the jointed concrete pavement life by reducing the curling stress in the concrete slabs by reducing the temperature differential in the pavement (Belshe et al., 2007). Bausano et al. observed that the thin asphalt overlays maintain a high level of service in comparison to chip seals and crack sealing (Bausano et al., 2004). Overall, thin overlays can be regarded among the most promising preservation method as far as ascertaining performance improvement and longevity are concerned.

2.2 THIN OVERLAY PAVEMENT DESIGN

Thickness is considered one of the major design parameters for thin asphalt overlays. In order to select a specific thickness for thin overlays, the factors responsible can be ranked in the decreasing order of importance: traffic volume, truck volume, classification of the road, costs, public policy, and ease of implementation. As such, it is practically impossible to come up with a universal plan or chart to easily pick a thickness for a given situation because the fundamental aspects affecting the design themselves vary greatly over the length and life of pavement. The most practical strategy is thus to compare a pavement design with the design and performance of previously constructed treatments and make an up-to-date engineering decision with respect to the adequacy of the design. As seen in various studies, agencies have actually provided their opinion regarding the measures that can be taken to improve the performance of thin asphalt overlays (Geoffroy, 1998; Watson and Heitzman, 2014). One practice is selecting the right candidate project for thin asphalt overlay construction. Sometimes thin overlays are used in mill-and-fill operations to cover up badly cracked pavements, simply because funding is insufficient to enable additional structures or perform the rehabilitation needed. In cases like these, not much reliability can be attached to the expected service life of the pavement. Thin overlays should be applied before the actual structural failure of the existing pavement starts and should not be placed over a rutted and structurally unsound pavement. In the case that all of these best practices are followed in conjunction with the existing condition, thin overlays can very well be expected to have a reasonable service life.

The general practice for classifying and selecting the thickness of thin overlays varies from state to state. In Alaska, for instance, the minimum thickness for an asphalt overlay is 2 in. Several other states define a thin overlay to be no more than 1 in. Some agencies consider 1-1.5 in as a conventional overlay instead of a thin bituminous surface treatment (Geoffroy, 1998). A number of agencies did not have a well-defined range for the thickness of thin asphalt overlays because the thickness allowed depends on the mix type used for surfacing. However, 86% of the respondents define thin asphalt overlays as surface courses placed no more than 1.5 in thick. In a study conducted by Lee et al., pavement response models were developed based on the idea that wearing course must not be considered a structural layer due to the relatively minimal thickness of the layers (Cewe, 1966 and Lee et al., 2007).

In a report by Barker et al., a detailed study of factors that help determine the thickness criteria of asphalt surface and base layers in airfield pavements was conducted (Barker et al., 2011). The fundamental concept behind the CBR-BETA$_{min}$ method was the development of a rational thickness design procedure using high quality materials in the asphalt and base courses to minimize rutting. This is made possible when the shear stresses in the granular base and sub-base have a

threshold value which is a function of layer strength. As a result, the design procedure adopted by the authors was simply based on the load-related aspects of the problem, i.e., limiting the shear stresses in the granular base layer. Similarly, the procedure for determining the base course required thickness was based on further reducing the stress to a limited value at the top of the sub-base. However, when the existing pavements are overlaid, the thickness of the overlay probably varies more than the thickness of a layer in a new pavement. During construction and particularly during layer compaction, air and mix temperature are important and critical for the construction of thin AC layers (Brown et al., 2004 and 2005). Thin AC layers tend to cool faster, thus rendering compaction more difficult. This restriction also places a limitation on the minimum thickness normally prescribed for thin asphalt overlay construction on the field.

2.2.1 Mix Design Criteria

Gap-grade SMA is considered the best performer as compared with conventional dense-graded mixes even in high traffic heavy load conditions. Commonly used SMA have 12.5 NMAS, whereas mixes with 0.37 and 0.18 in NMAS are increasingly used. The common and best practice for thin overlays mixes include the use of high polymer-modified asphalt binders at higher content (6-8.5%) in a fine and preferably gap-graded mixes. The mixes for such applications commonly have high VMA and lower design air voids to increase asphalt binder film thickness. High quality aggregates with low absorption is preffered. The use of additives such as lime and silicon dioxide (for moisture resistance and friction, respectively) can also improve the performance of thin overlay asphalt mixes considerably (Walubita et al, 2008).

2.2.2 Material Requirements

In general, the materials used can be selected same as those used for the thicker structural surface layers. The only difference is the use of a smaller NMAS for aggregates. However, it was shown that the type of aggregate may also affect the performance. In a study by Kansas State University, it was concluded that the thin overlay mix prepared with crushed gravel aggregates perform better t than that prepared with crushed limestone (Rahman et al., 2011). In a study by Texas DOT, granite mixes displayed superior performance in comparison to limestone mixes (Walubita et al, 2008). In a recent study by the TTI, it was found that using smaller, high-quality aggregate (e.g., Grade 5) results in thinner overlays and increases the longevity of the pavements (Pavement Preservation Journal, 2014 and Wilson et al., 2012). Further evaluation also showed that the pavements constructed using such high-quality aggregates demonstrated better rut and crack resistance. Using thinner overlays in this respect can lead to a net saving of about 30% per square yard in the road maintenance budgets. Also, thin overlays with 0.75 in thickness could also last longer than the 2 in overlays with these modifications in material specifications (Pavement Preservation Journal, 2014).

As far as binder is concerned, a high binder grade and content (around 6-8% for thin overlay mixes) is commonly used. The use of RAP or RAS is generally limited or not allowed by agencies in OGFC or SMA. Only Alabama allows as much as 15% RAP in SMA. Evaluation studies by Alabama DOT found out that high RAP could increase the mix tensile strength values but would reduce the fatigue life. Also, using high RAP may result in an increase in the potential for low temperature cracking; however, another study in Georgia resulted in no major affect even when 30% RAP was used in AC mixes (Watson and Heitzman, 2014 and Watson et al., 2008a). Texas also reported promising results with the cracking development within acceptable limits after

using RAP in AC mixes (Newcomb, 2009). Table 2-1 presents an overview of different mixes used in thin overlay mixes:

Table 2-1. Thin AC Overlay Mix Properties (Sauber, 2009).

Types of Thin AC Surface Mixes:
• Dense-graded systems (HPTO) • Open-graded systems (OGFC and AR-OGFC) • Gap-graded systems (SMA and SMAR) • Ultra-thin systems (Novachip)
Properties of Dense-Graded Mixes:
• Dense-graded mixes – Continuously graded, Superpave. high performance thin overlay (HPTO) • Open-graded mixes – 15-22% voids, fibers and polymer or crumb rubber. Used to reduce splash and spray, improve high speed friction and reduce tire noise • Gap-graded mixes – SMA and SMAR mixes (0.37 in and 0.49 in). Ultra-thin systems (Novachip)

2.2.3 Laboratory Compaction Level (N_{design})

For a long time, many agencies have used the Superpave specified gyration level for laboratory compaction as specified in AASHTO M 323. However, it is recommended that, especially in the case of thin asphalt overlays, an agency define the locking point of the aggregate structure in its AC mixtures and subsequently use that number of gyrations as its N_{design} level while maintaining the same binder type. The locking point can generally be defined as the first instant at which the specimen height remains the same for three successive gyrations. It was confirmed by the Georgia DOT that the locking point density correlated well with the on-field density (Watson et al., 2008b). It was also observed that the AC mixes designed at 60 gyrations had almost twice the fatigue life as those designed with 110 gyrations (Watson and Heitzman, 2014).

2.3 THIN OVERLAY MIX TYPES

Thin overlay SMA with 0.37 and 0.49 in NMAS are considered superior candidates among the commonly used alternative mix designs. These can be very cost effective as they can potentially last more than 20 years without resurfacing (Newcomb, 2009). Dense- and fine-graded 0.18 in or 0.37 in NMAS mix has also been used by various agencies. In a study by National Center for Asphlat Technology (NCAT), no difference was observed in the rutting resistance of the coarse and fine-graded Superpave mixes (Frank, 2013; Luelmo et al., 1971; West et al., 2006 and Kandhal et al., 2002). In addition, besides its early inception in Europe, SMA has gained reputation as a viable option. Finer AC mixes were found to be rut resistant, could be placed in thinner layers, and were less permeable than coarser mixes thus making them good candidates for thin overlays (Cooley and Brown, 2003). Agencies have also used OGFCs for thin layer construction to effectively reduce the temperature differential between the top and bottom of the slab (Watson et al., 2004). Another study in New Jersey reported that OGFC mixes deliver the most benefit for the least cost with a very good performance at wet friction numbers, ride quality, and cost effectiveness (Bennert et al., 2005). OGFC pavements along with the pavements with crumb rubber are observed

to be the quietest one-third of the entire conglomerate of the different kind of pavements (Rymer and Donavan, 2009).

2.4 EVALUATION TECHNIQUES FOR ASPHALT OVERLAYS

The methodologies used to evaluate thin asphalt overlays can be divided as mechanistic empirical (M-E) methods, experimental and field assessments, and computational and theoretical techniques. Mechanistic empirical models have been used to define the performance parameters of pavements for different applications. Various models have also been developed for asphalt overlays to characterize the reflective cracking phenomenon as early as 1932. Using different variables, several models have been created to-date, including empirical, extended multi-layer elastic, equilibrium-based equations, FE plus traditional fatigue equation based, FE plus fracture mechanics, crack band, non-local continuum damage mechanics-based and cohesive crack/zone models (Table 2-2). On the other hand, experimental efforts to characterize thin asphalt overlays can be at a large scale (on-field or with field extracted cores in the lab) or at a comparatively smaller scale (which might include tests on small amounts of AC mixes, binder, or aggregate alone).

In the laboratory, the Hamburg wheel tracking test equipment orasphalt pavement analyzer, and Texas overlay tester have been used for rutting and reflective cracking characterization, respectively. Indirect tensile tests and dynamic creep tests have also been used quite often (Cooley and Brown, 2003; Scullion et al., 2009 and Xie et al., 2005). No standard performance testing protocol is applied for thin overlay mixes. In recent years, with the increasing emphasis on balanced mix designs, various types of cracking tests were developed.

Interlayer mixes generally used in conjunction with the overlays were found ineffective as far as their tendency to prevent reflective cracking (Kim et al., 2009). However, in order to reduce the time and effort spent on experiments, various analytical approaches ranging from the simple closed form solutions to the complex FE models were used to understand the performance of different kinds of overlays in the construction of composite pavements. For example, Zhu et al. developed a 2-D micromechanical discrete element model based on Particle Flow Codes for evaluating the interlayer damages for an AC layer over Portland cement concrete (PCC) pavement (Zhu and Jia, 2009).

Baek et al. also utilized the usability of computational techniques by incorporating a linear viscoelastic model and bilinear cohesive zone model in a FE model to analyze continuum and fracture properties of AC overlays with and without sand mix interlayer which can be used to control reflection cracking in pavements (Baek and Al-Qadi, 2011). It was finally concluded that the sand mix interlayer increased the resistance to reflective cracking by a factor of 1.17 to 2.45 on account of the interlayer's high fracture toughness. A number of research initiatives were also undertaken with different combinations of overlays. Cable et al. performed a comparative study of results from FE models and field outputs for a case of white topping over asphalt pavements (Cable et al., 2005). Inconsistency of results was attributed to experimental errors and localized differences in the material properties on test sites.

Based on the aforementioned studies, it was concluded that overlay thickness is the most important factor in defining overlay performance, followed by the thickness of the existing AC

layer. A brief summary of the different types of models devised in different researches over time is given in Table 2-2:

Table 2-2 Available Mechanistic Empirical Models

Category	Researchers	Approach/Objective	Major Variables
Empirical models	Hall et al. (1989)	To predict the total length of medium and high severity reflection cracks in AC overlays	ESALs, thickness, age, freezing index, measure of PCC condition
	NCHRP 1-37 A Project (2007)	% of cracks in overlays as a function of time	Time, regression coefficients
Extended multi-layer linear elastic models	Eckman (1990)	Usage of MOEBIUS software	-
	VanGurp and Molenaar (1989)	Usage of FE modeling and BISAR	Effective modulus values for the overlay
Equilibrium equations based models	McCullough and Seeds (1982)	Equilibrium equations to estimate stress and strains in overlay	-
FE plus traditional fatigue equation based models	Coetzee and Monismith (1979)	2D FE to study stresses around a crack with and without SAMI[1]	-
	Chen et al. (1982)	2D linear plain strain FE under moving loads	-
	Francken and Vanelstraete (1992)	2D FE to study effect of interface systems on overlays	-
	Kim et al. (2009); Kim and Buttlar (2002)	3D nonlinear FE for critical responses in asphalt overlays	-
	Sousa et al. (2001)	Mechanistic empirical based overlay design method for reflective cracking	-
FE plus fracture mechanics models	Jayawickrama and Lytton (1987)	Repetitive crack propagation calculation until cracks stops growing or reaches the overlay surface	No. of days and calibration factors
	Owusu-Antwi et al. (1998)	Number of load repetitions to propagate a crack through an overlay	Thickness, SIF, material constants
	Al-Qadi et al. (2003)	Design model to predict service life using LEFM	Thickness, modulus
Crack band models	Joseph et al. (1987)	2D plain strain FE model to study effect of various treatments on	-

[1] Stress Absorbing Membrane Interlayer

		decreasing low temperature reflection cracking	
Non-local continuum damage mechanics based	Wu et al. (2006)	Implicit gradient formulation to replace local with non-local strains to characterize reflection cracking	-
Cohesive crack/zone model	The use of cohesive crack model by different researchers under monotonic loading. More work needed for impact under repeated loading.		

2.5 COST/ BENEFIT EVALUATION OF THIN OVERLAYS

In a survey by Wang et al., on comparing the different pavement preservation treatments, it was found that although thin asphalt overlays can be the most costly alternative with higher initial construction costs, they provided the greatest increase in pavement life (Wang et al., 2012; Newcomb, 2009 and Chou et al., 2008). A synthesis performed for the Montana DOT by Cuelho et al. summarized survey responses for expected service life and cost per lane-mile for several types of preventive maintenance treatments (Cuelho et al., 2006). Based on survey results, thin overlays extended pavement life by an average of 5.4 years, chip seals by 1.9 years, crack seals by 1.7 years, and slurry seals by 1.1 years. Bausano et al. used the PMS data collected on 240 preventive maintenance projects since 1992 by conducting a reliability-based analysis to determine the life expectancy (performance) of five different PM fixes including non-structural thin overlays (Bausano et al., 2004). The reliability value for non-structural bituminous overlay was relatively constant up to year 3, which then dropped at a fast rate. However, it was still high at year 6 (78%). These results were in agreement with MDOT's guidelines according to which life extension for thin overlays is around 5-10 years. For the pavements subjected to surface milling with a non-structural bituminous overlay, reliability value was close to 100% for the first 4 years. In both cases, a distressed pavement was not observed from year 1 to year 4-5.

Another study by Oregon found that thin asphalt overlays were the most cost-effective treatment on a life-cycle basis especially for heavy traffic conditions (Parker, 1993). But at the same time, survey responses showed a large variation in the service life of pavements. Some other comments from the survey suggested reasons for wide fluctuations in service life could be environmental conditions, changes in the construction quality standards (interstate versus secondary tracks), regional variations in the material and construction quality, and roads requiring rehabilitation identified as only mill and fill because of cost and other factors.

Seven DOTs reported that the thin asphalt overlays surpassed their expectations. Mixes, such as permeable friction course and ultra-thin bonded friction course were used. On the other hand, several agencies stated that thin asphalt overlays failed to perform as expected. In the two wet climate regions and in the dry no-freeze climate regions, agencies stated that significant instances of failure were observed. Three DOTs gave reasons for possible failure which included loopholes in pavement rehabilitation selection technique, construction, or traffic load estimation. In Massachusetts, it was noted that selection of the right treatment for the right pavement is a considerable factor in addition to surface preparation and application of adequate tack coat. In Georgia, reflective cracking was listed as a major concern for thin lift overlays. A recent comparison by Tennessee in the bid prices of micro-surfacing and thin asphalt overlays revealed that thin asphalt overlays are comparable in price to the micro-surfacing preservation treatment practice (Watson and Heitzman, 2014).

CHAPTER 3 - EXPERIMENTAL PROGRAM

3.1 MATERIAL DETAILS

The study utilized various AC mixes from some of the ongoing or completed projects at the Illinois Center for Transportation (ICT) of the University of Illinois at Urbana-Champaign (UIUC). Asphlat concrete mixes from different categories were selected and used for various purposes in the study. Table 3-1 provides a brief summary of the AC mixes considered:

Table 3-1 Asphlat concrete Mix Types Used for Thin Asphalt Overlay Project

Project Detail/ Task	**Mix Properties**	**Selection Criteria**
R27-128 Testing Protocols to Ensure Performance of High Asphalt Binder Replacement (ABR) Mixes Using RAP and RAS[2] (Al-Qadi et al., 2015) **Objective:** Development of a cost-effective cracking test. **Project Status:** Completed	N-90 Coarse Graded (**control mixes**) Binder PG = 64-22 NMAS = 0.37 in	This AC mix is well characterized utilizing several tests, including fracture, modulus, flow, and fatigue, as well as micromechanical characterization[3] (using Digital Image Correlation [DIC])
Specimens from FHWA's Accelerated Loading Facility (**ALF**) tested specimens (Ozer et al., 2018) **Objective:** Evaluate the effect of RAP and RAS field accelerated-loading fatigue behavior. **Project Status:** Completed	**Lane 1:** Binder PG = 64-22 NMAS = 0.49 in **Lane 3:** Binder PG = 64-22 NMAS = 0.49 in	Data from accelerated pavement testing are available, as well as data on loss in modulus and micro cracking damage. In addition, effect of aging on AC mixes was analyzed and extensive DIC test results And effect of AC air void content are available. AC mix performed significantly diffretent; especially lanes 1, 3 and 11, which performed relatively best, worst, and intermediate, respectively.

[2] Recycled Asphalt Pavement (RAP) and Recycled Asphalt Shingles (RAS)

[3] More details in section 4.2

R27-42 Development of an Economical, Thin, Quiet, Long-lasting, and High Friction Surface Layer (Al-Qadi et al., 2013) **Objective:** Development of new, cost effective, and locally available ACs for wearing courses. **Project Status:** Completed	SMA: Binder PG = 70-22 NMAS = # 4 (3/16 in)	Field sections of alternative high-friction AC surfaces with varying overlay thicknesses.

The properties of the aforementioned three AC mix are presented in detail in Table 3-2:

Table 3-2 Asphalt Concrete Mix Specifications for the Lab-Prepared Specimens

Project Name/Other Detail	**R27-128**	**ALF (Lane 1)**	**ALF (Lane 3)**	**R27-42**
Property	**Value**			
Bulk specific gravity, G_{mb}	2.392	2.632	2.631	-
Binder specific gravity, G_b	1.03	1.03	1.03	1.03
Maximum specific gravity, G_{mm}	2.496	2.734	2.742	2.454
Binder (%)	6.0	5.3	5.2	7.3
VMA (%)	15.3	16.3	16.3	18.5
VTM (%)	4.2	3.7	4.0	4.0
VFA (%)	72.7	77.1	75.1	78.4
ABR (%)	0.0	0.0	20	0.0

3.2 MODULUS CHARACTERIZATION

Complex modulus of each one of the AC mixes used in this study was determined. The modulus values were used directly as input into the FE simulations. Experimental data for the complex modulus were derived from other projects conducted at ICT or elsewhere (Al-Qadi et al., 2015). Testing was conducted in accordance with the AASHTO TP 79-15 to determine the linear viscoelastic properties of the selected AC mixes. Tests were either conducted using the Interlaken Hydraulic Testing Machine or similar hydraulic driven loading frames. Superpave Gyratory Compactor was used to produce cylindrical samples of about 6-in diameter and 7.1-in height. Asphalt concrete cylinders were then cored out and cut to a diameter between 3.9 and 4 in and a height ranging from 5.8 to 6 in. Air void content was generally kept at 7 ± 0.5%. In order to measure the axial displacement of these specimens, three 2.75-in extensometers were placed on to the surface. AASHTO TP 79-15 testing standard was followed for specimen conditioning and testing at temperatures of 14°F, 40°F, 70°F, 100°F, and 130°F. At each of these temperatures,

modulus testing was conducted at five frequencies, 25, 10, 5, 1, 0.5, and 0.1 Hz, in the indicated order. Average microstrain value at each temperature and frequency was maintained between 50 and 75. Appendix A provides a comparison of master curves of the AC mixes. The master curves, which represent linear viscoelastic constitutive relationship of these AC mixes, were used as inputs to the FE models.

3.3 ANALYSIS MATRIX

Major focus was given to evaluating the impact of parameters which generally affect the performance of thin asphalt overlays using FE modeling. The analysis matrix given in Table 3-3 was used throughout the project. Three AC mixes, ALF Lane 1 (L1), ALF Lane 3 (L3) and R 27-42, were used. Four different thicknesses, 0.75 in, 1.0 in, 1.5 in, and 2.0 in, were applied for each material. W and W' in the last row of the figure represent the original pavement structure and the one with a reduced AC layer (by milling off 1 in), respectively.

Table 3-3. Simulation matrix to include 4 overlay thickness, 3 mixes and pavement surface condition scenario

Thickness	Mixtures	ID for No Milling Scenario	ID for 1-in Milling Sceanario
0.75	ALF Lane 1 (A1) ALF Lane 3 (A3) R27-42 (R)	75A1, 75A3, 75R	75A1', 75A3', 75R'
1.0		1A1, 1A3, 1R	1A1', 1A3', 1R'
1.5		15A1, 15A3, 15R	15A1', 15A3', 15R'
2.0		2A1, 2A3, 25R	2A1', 2A3', 25R'

Thin overlay maintenance strategy is commonly recommended only when there is a fair amount of deterioration in the existing asphalt pavement wearing course. Hence, it is necessary to take into account in the analyses the effect of milling any of the pavement structure when thin overlays are applied after removal of deteriorated surface layer.

CHAPTER 4 - MECHANICS OF THIN ASPHALT OVERLAYS

This chapter introduces the FE model development and results of pavements with varying thickness of thin overlays. Three-dimensional FE modeling of pavements was used to evaluate the stress-strain fields within the thin overlays to understand the failure mechanisms. In addition, the contribution of thin overlays to overall structural capacity was investigated. Different materials were used as thin overlays with distinct modulus characteristics.

4.1 PAVEMENT 3-D FE MODEL

Three-dimensional FE models were developed for pavements with thin overlays. The objective of this numerical simulation was to characterize critical response parameters within thin overlays. These critical responses were used in models to predict permanent deformation and cracking. They critical responses are generally affected by environment, base support and underlying layer conditions, AC mixture properties, layer thicknesses, and layer densities. The effect of these variables were considered in the simulation.

4.1.1 Pavement 3-D FE Model Development

In the current pavement design model (Mechanistic Empirical Pavement Design Guide or MEPDG), a layered elastic analysis is used to obtain mechanistic responses assuming an axisymmetric model, linear elastic materials, uniform and static loading, circular contact area, and simplified layer interaction. However, the pavement model used for this research includes features such as linear viscoelastic AC, nonlinear cross-anisotropic base layer for thin pavement (and linear elastic behavior for both base and subgrade for thick pavements), dynamic analysis and measurement of 3-D contact stresses or loads (Hernandez et al., 2016). Linear viscoelastic material properties take into account the impact of temperature and loading variations on the pavement structure. In contrast to the conventional static loading conditions, an implicit dynamic analysis can efficiently account for the regular moving nature of the non-uniform, 3-D traffic loads across the pavement sections. As a result, an effective combination of 3-D contact loading in conjugation with viscoelastic AC and stress-dependent granular layers, appropriate representative of layer interaction, and temperature profiles along the AC layer were used in this study (Yoo et al., 2006). A 3-D pavement FE model with the wheel path and infinite boundary elements to simulate far-field behavior is shown in Figure 4-1. The pavement model used for analysis in this study is the result of continued efforts by various researchers at ICT over the years (Elseifi et al., 2006; Yoo et al., 2006; Al-Qadi and Yoo, 2007; Al-Qadi et al., 2008; Hernandez et al., 2016)

Figure 4-1 shows a plan view for the pavement model with three different zones highlighted as follows: 1) wheel path, 2) transition zone, and 3) infinite elements. The difference in mesh density was applied to account for sensitive responses under the wheel path. In fact, mesh sensitivity was carried out for each dimension in the plan view with respect to several variables including the maximum longitudinal and transverse tensile strains at the bottom of the AC, maximum surface strain, maximum vertical shear strain in each layer, and maximum vertical strain in each layer (Hernandez et al., 2016). Tire loading was represented by contact stresses in the vertical, longitudinal, and transverse directions. The continuous moving load was numerically implemented by specifying an increasing and decreasing amplitude of the contact load upon entry and exit on elements in the FE model, respectively. This provided a realistic simulation of a traffic

load traversing the pavement surface. To define the interface between different layers, a tied contact was used to simulate full bonding between AC layers, elastic slip between AC-to-base layers and coulomb friction model for the base-to-subgrade interfaces. Considering the aforementioned parameters, analysis matrix was developed and used in Abaqus for pavement modeling (Abaqus, 2014). Two pavement structures (introduced in the next section), with varying thin asphalt overlay thicknesses (0.75 in, 1 in, 1.5 in and 2 in), different material properties, and varying loading conditions were considered.

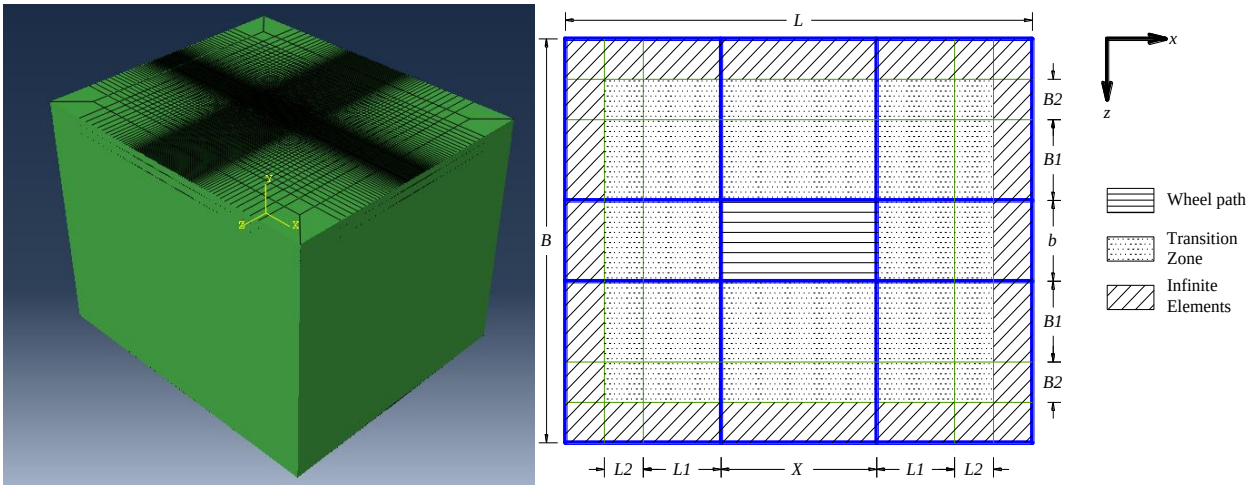

Figure 4-1 Three-dimensional and plan views of FE model.

4.1.2 Pavement Structures

For this research, one pavement structure simulated an interstate highway, referred to as a "thick" pavement structure. Two scenarios were considered for thin overlay pavement: Application of thin overlays on top of the existing surface, and application of thin overlays after milling 1 in from the existing pavement surface.

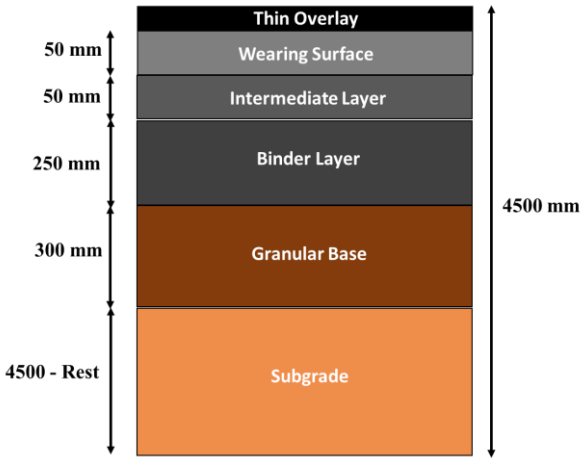

Figure 4-2 Thick pavement structure considered in this study.

4.1.3 Tire Loading

For the loading cases, the 3-D contact stresses, provided by the Michelin Americas Research Company for a separate study at ICT, were used (Al-Qadi et al., 2016). The data were generated with respect to tire characteristics, such as applied load, tire-inflation pressure, type, life, size, and centrifugation. Two different loading cases were applied: wide-base tire and dual-tire assembly. Basic information for the two cases is given in Table 4-1 as follows:

Table 4-1 Tire Loading Details

Case	Loading Cases	Applied Load (kip)	Inflation Pressure (psi)
L1	Wide-base tire Ref W445	8.5	100
L2	Dual-tire assembly D275	8.5	100

4.2 PAVEMENT 3-D FE MODEL ANALYSIS RESULTS

To evaluate the impact of various parameters on the performance of thin asphalt overlays, a pavement structure with a specific loading condition was assumed. Dual-tire assembly with a nominal width of 10.8 in, applied load of 8.5 kips and an inflation pressure of 100 psi was considered. Critical responses studied are the following:

- Tensile strains along longitudinal and transverse directions at the bottom of the thin overlay layer (ε_{11AC}, ε_{33AC});
- Tensile strains along longitudinal and transverse directions on the surface (ε_{11Surf}, ε_{33Surf});
- Vertical strains in the thin overlay, base and subgrade (ε_{22AC} , ε_{22Base}, ε_{22Subg});
- Vertical shear strains in the thin overlay, base and subgrade (ε_{23AC} , ε_{23Base}, ε_{23Subg}).

Normally, tensile surface strains are related to the near-surface fatigue cracking while those at the bottom of the AC layer are associated with bottom-up fatigue cracking. Vertical strains in each layer affect the permanent deformation behavior of the pavement structure. Figures 4-3 to 4-6 compare the responses for different thicknesses of the thin overlay for the two different AC mix types.

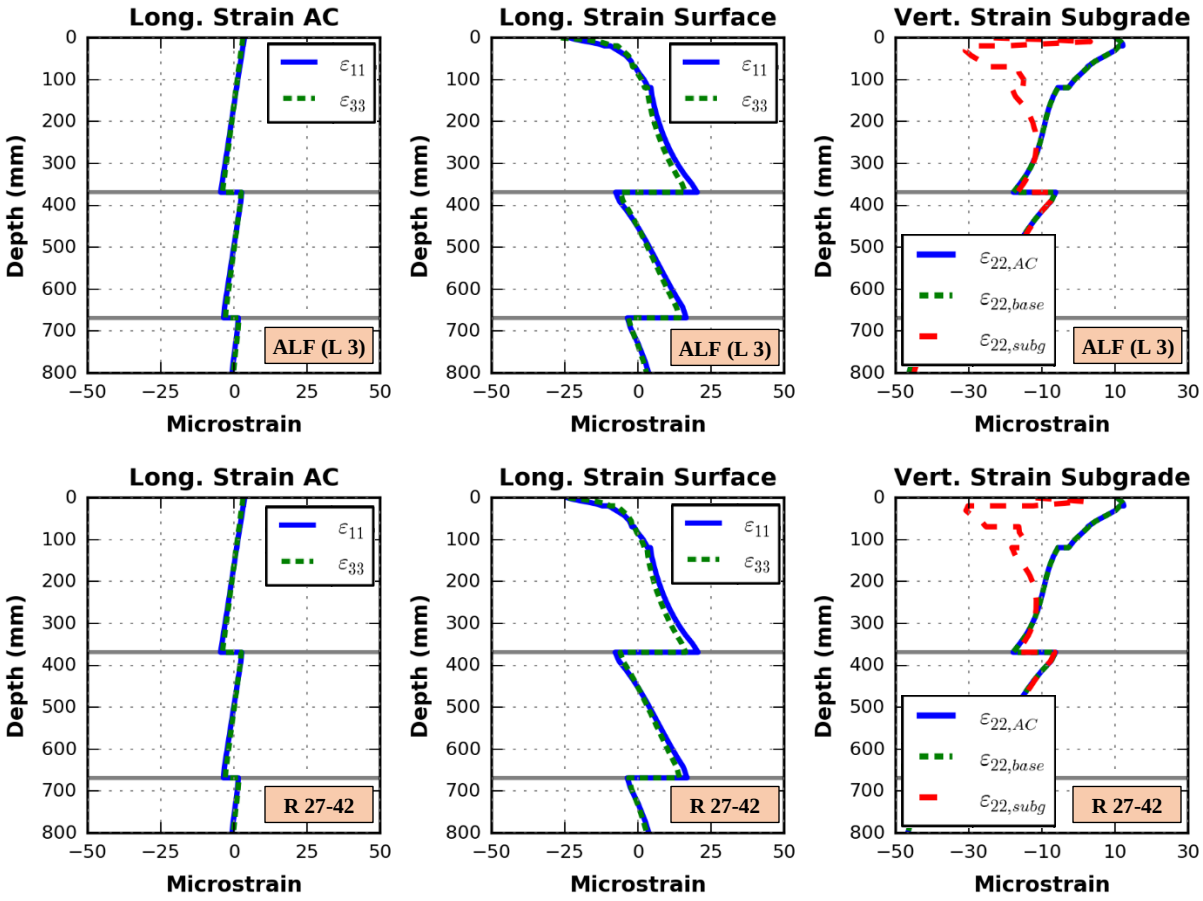

Figure 4-3 Critical responses predicted for the case of thin overlays with ALF (Lane 3) and R 27-42 AC mixes and a thin overlay thickness of .75 in.

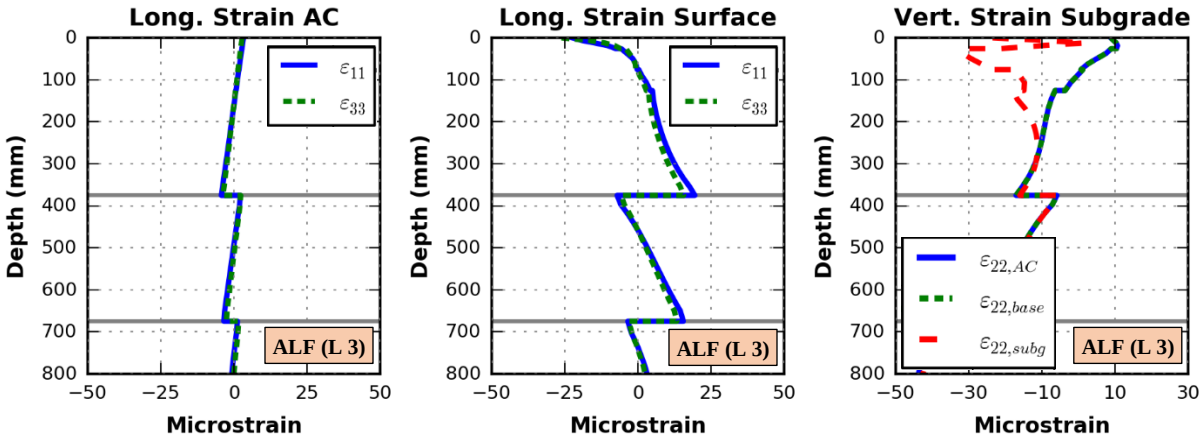

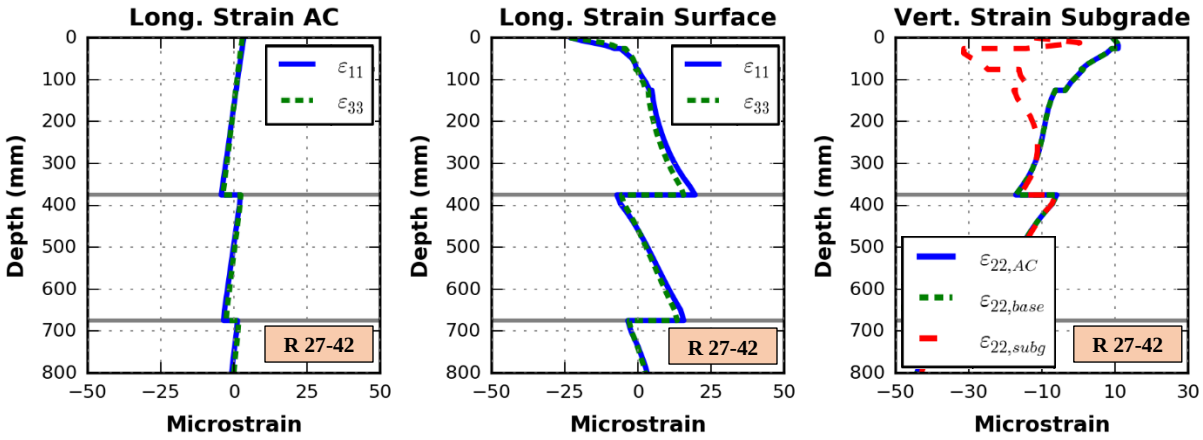

Figure 4-4 Critical responses predicted for the case of thin overlays with ALF (Lane 3) and R 27-42 AC mixes and a thin overlay thickness of 1.0 in.

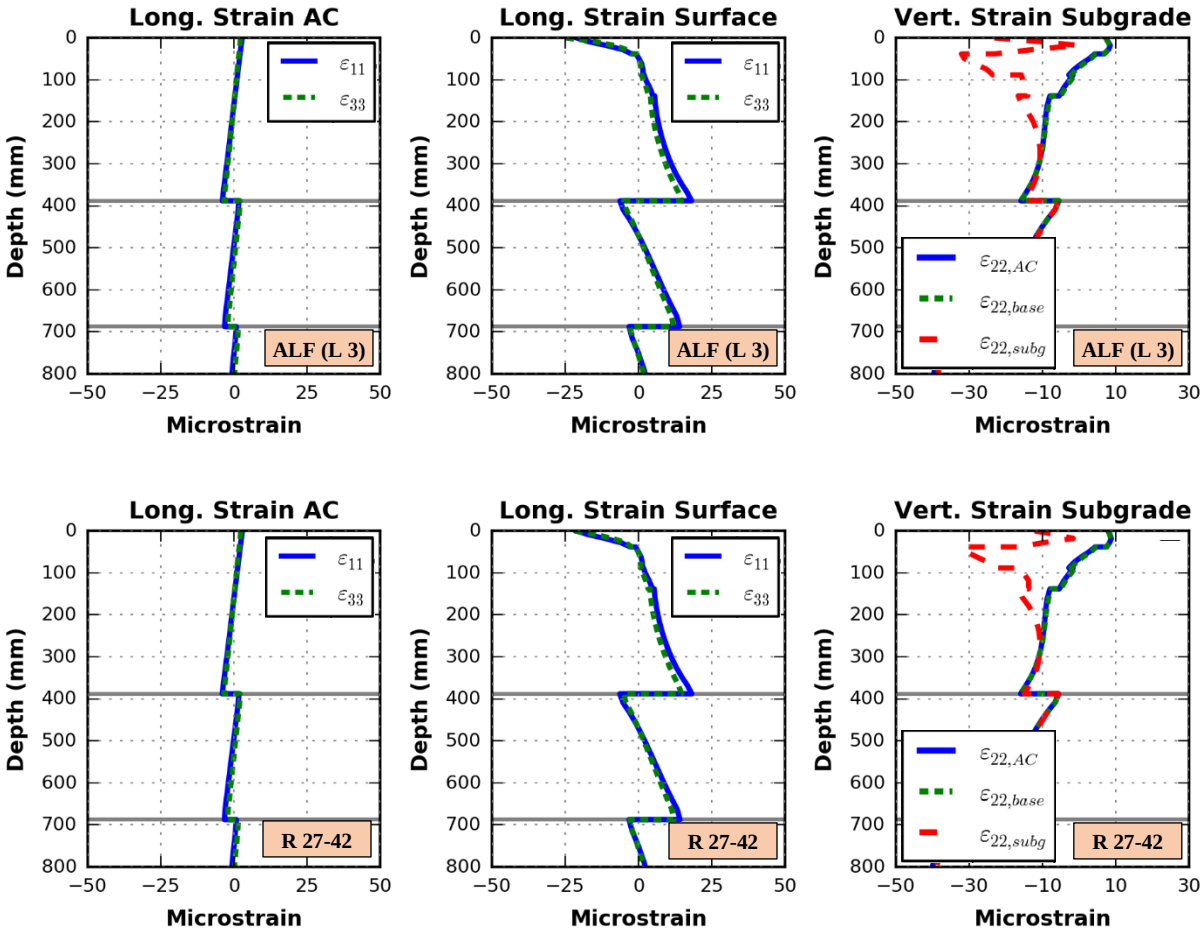

Figure 4-5 Critical responses predicted for the case of thin overlays with ALF (Lane 3) and R 27-42 AC mixes and a thin overlay thickness of 1.5 in.

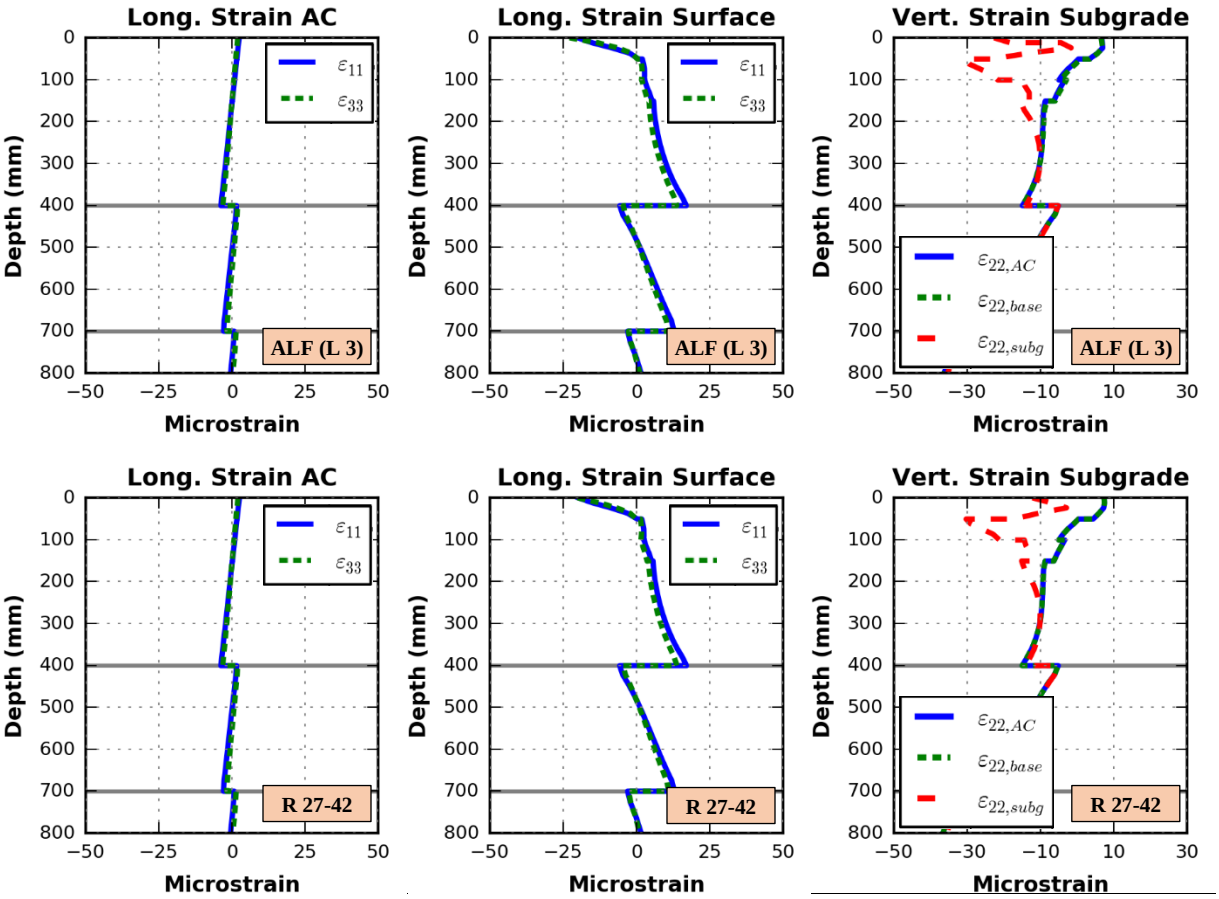

Figure 4-6 Critical responses predicted for the case of thin overlays with ALF (Lane 3) and R 27-42 AC mixes and a thin overlay thickness of 2.0 in.

Figures 4-7 to 4-9 show the variation of three different responses for four values of thickness for the thin overlay AC layer. Along the depth, as would be expected, compressive strains change to tensile trajectory. Vertical strains at top of the subgrade layer are significantly higher than those at bottom of base or AC layers due to the layer material properties. Longitudinal strains changed orientation at interfaces. The longitudinal strains were found to be greater than transverse strains at the bottom of the overlay layer in all cases. It should also be noted that the values obtained for the responses at the bottom of thin overlay layer were generally low.

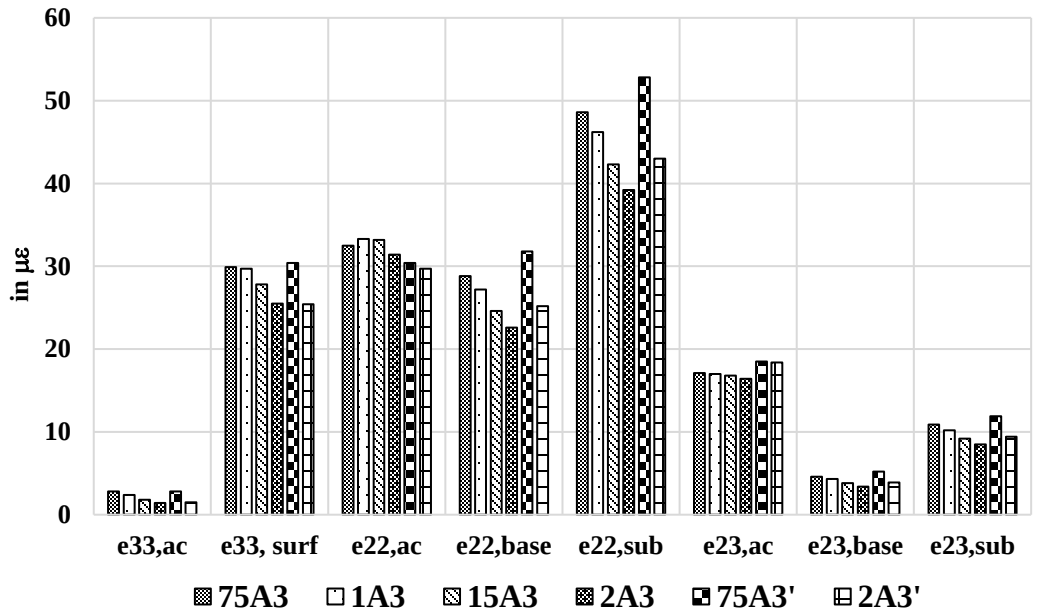

Figure 4-7 Critical responses for the thin overlays using ALF AC mixes.

Results for various critical responses for the thin AC overlay of the ALF mixes are presented in Figure 4-9. In the figure plots, the vertical axis represents the values of critical responses in $\mu\varepsilon$ at the base of thin overlay layer (ac), surface (surf), base (base), subgrade (sub), and the legend denotes the thickness of thin overlay layer with the specific mix type. As expected, higher vertical strains were calculated over subgrade where the overlay was the thinnest. As overlay thickness increased, the vertical pressure on the subgrade decreased. Transverse strains were very low at the bottom of the thin overlay layer while those on the surface were significantly higher in compression due to contact stresses. The overlay is not thick enough to develop tensile strains at the bottom. A similar behavior was observed in the thin SMA overlay as shown in Figure 4-8. A comparison of the ALF L3 and SMA is shown in Figure 4-9 for strains developed within the thin overlay. Due to modulus difference, responses varied slightly; however, a similar pattern with varying structures was observed for both materials.

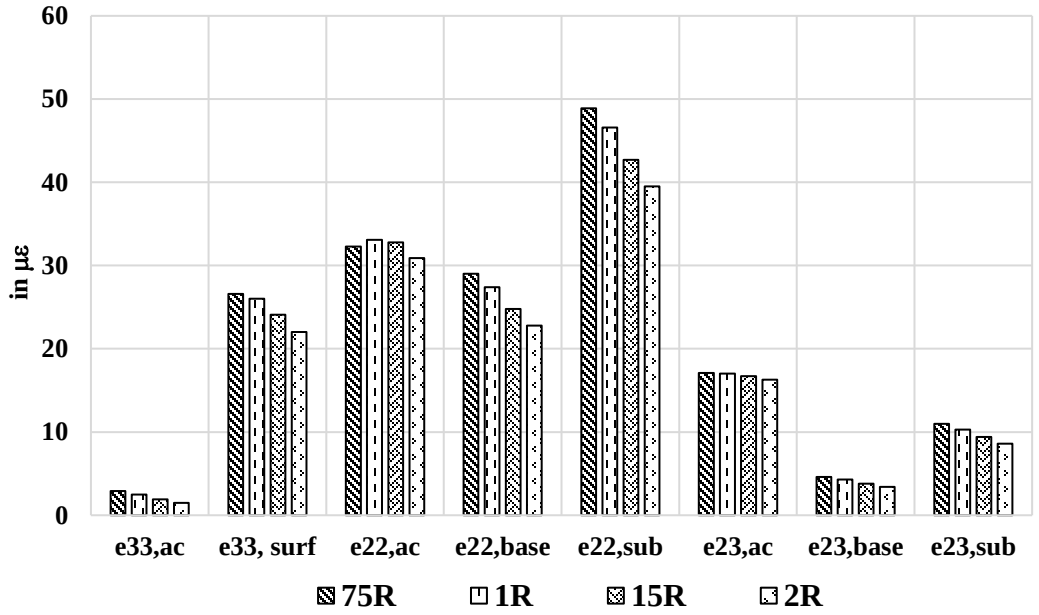

Figure 4-8 Critical responses for the thin SMA overlays.

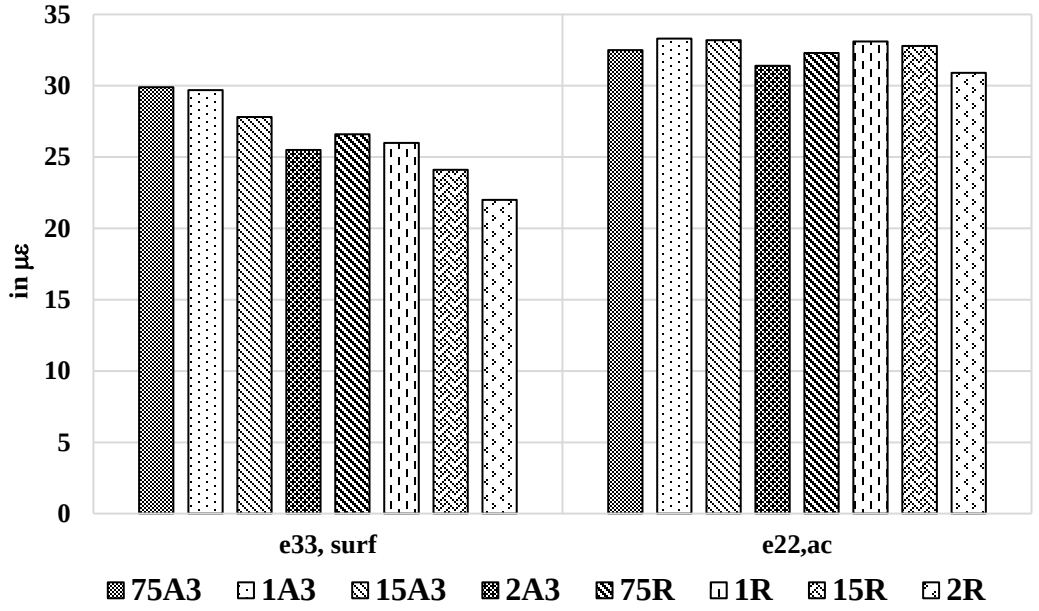

Figure 4-9 Comparison of transverse and vertical strains for different AC mixes and thin overlay thicknesses.

After analyzing the presented results, the following observations are made:

1. The effect of AC modulus properties on the thin AC overlay responses appeared to be minimal even though two distinct mixes were used in the simulations. This indicates that the response analysis with linear viscoelastic characterization may not explain the

differences in the performance of thin overlays. Failure characteristics such as strength and cracking of materials have to be incorporated into the analysis.

2. In contrast, a change in thin AC overlay thickness impacted the responses; especially in the lower layers of the structure. This manifests the structural contribution of thin overlays.
3. The strain response within thin overlays is mainly governed by compression and shear strains. The low thickness of the thin overlay results diminishing bending type tensile strains. This suggests that conventional experimental characterization and modeling methods relying on tensile cracking and fatigue damage may not be applicable to the analysis and design of thin overlays.

CHAPTER 5 - ANALYSIS OF THIN ASPHALT OVERLAYS USING DOMAIN ANALYSIS METHOD

As presented in Chapter 4, the FE analysis of a pavement with a thin overlay was conducted using traditional point stress and strain analysis. Traditional point stress or strain analysis was successfully used to translate critical pavement responses to pavements service life. However, point response analysis generally suffer for near-surface analysis of pavements where the 3-D complex stress and strain fields prevail due to non-uniform nature of tire contact stresses. Due to the relatively limited AC thickness of thin overlays to withstand vehicular and environmental loading, it is necessary to utilize a different approach. The domain analysis method was introduced recently to alleviate the problems emanating from traditional point response analysis (Gamez et al., 2018). The domain analysis is a volumetric analysis of the critical subregions in a pavement structure through a normalized scale parameter representing the multi-axial stress and strain state evolving in each region.

5.1 DESCRIPTION OF THE DOMAIN ANALYSIS CONCEPT

First of all, the underlying critical stresses and strains for any case are calculated from the FE pavement model as explained in Chapter 4. However, because the subdomain of the entire pavement model would be considered, it was necessary to study in full detail the stress state of an individual element. For any element, the stress states are characterized by normal and shear components in the Cartesian coordinate system or by principal stresses and strains along with the principal axes. Equations (5.1) and (5.2) define the hydrostatic (p_σ) and shear (q_σ) stresses calculated using the principal stresses. Similarly, equations (5.3) and (5.4) represent the hydrostatic and shear strains.

$$p_\sigma = \frac{1}{3}(\sigma_1 + \sigma_2 + \sigma_3) \tag{5.1}$$

$$q_\sigma = \sqrt{\frac{1}{2}((\sigma_1 - \sigma_2)^2 + (\sigma_2 - \sigma_3)^2 + (\sigma_1 - \sigma_3)^2)} \tag{5.2}$$

$$p_\varepsilon = \frac{1}{3}(\varepsilon_1 + \varepsilon_2 + \varepsilon_3) \tag{5.3}$$

$$q_\varepsilon = \sqrt{\frac{2}{9}[(\epsilon_1 - \varepsilon_2)^2 + (\varepsilon_2 - \varepsilon_3)^2 + (\varepsilon_1 - \varepsilon_3)^2]} \tag{5.4}$$

where: σ_1 = maximum principal stress, σ_2 = intermediate principal stress, σ_3 = minimum principal stress, ε_1 = maximum principal strain, ε_2 = intermediate principal strain, and ε_3 = minimum principal strain.

Using these definitions, the subdomains extracted from the pavement model were analyzed. These subdomains had an area of 10.7 ft^2 in the $x - z$ plane and to a depth of 39.3 in into the subgrade layer. The location of these domains is in the center of the wheel path and the critical loading step was assumed to be when the tire is in the middle of the path (. Initially it was

considered that the 2-D plane for analysis was situated in the middle of the length of the pavement model. But studies showed that for a moving tire, maximum stresses and strains might not be exactly in the middle of the tire footprint. These behaviors could be attributed to the viscoelastic nature of the AC mixes, which cause the strain response to follow the loading profile with a delay. As a result, the location of the maximum values of each critical response studied might vary in the FE subdomain. For this purpose, a volume averaging method was used to incorporate all possible values of the 3-D sample size.

The steps to perform domain analysis are described in details in the following section. Briefly, the procedure includes the following steps:

1. Calculate multi-axial stress and strain states using the FE analysis in each subregion;
2. Discretize the pavement domain to identify critical zones;
3. Extract principal values of stresses and strains in each element included in the subregions;
4. Compare stress and strain states with respect to a pre-defined failure criterion often described using principal stresses; and
5. Combine the failure potential of critical regions to obtain a scalar that indicates the level of damage potential.

5.1.1 Domains Defined in the Thin Asphalt Overlay Layer

For the thick pavement cases studied in this project, horizontal and vertical boundaries were defined for the subdomains only in the AC section of the pavement structure. A maximum horizontal limit equal to the thickness of the thin asphalt overlay was defined in each case. For the base and subgrade layers, a horizontal boundary was defined at 3.9 in from the top and bottom of each layer. Further, nine sub-zones were created within these larger domains to capture and analyze in details the near-surface and other critical layers.

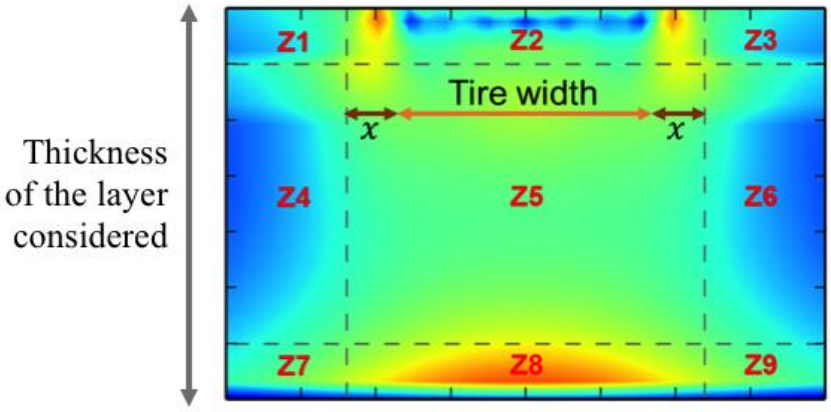

Figure 5-1 Zones created for each 2-D layer in the longitudinal direction.

For the thin overlay layer, the vertical boundary for the near-surface subdomains was determined around the rounded depth of the first FE in that layer. On the other hand, the horizontal boundary was defined by the tire width and an additional 1.9 in in the left and right directions. A clear depiction of the zones created for each 2-D layer in the traveling direction is provided in Figure 5-1. For the subdomains defined, hydrostatic and shear stresses and strains were calculated by obtaining principal values at the centroid of each FE. Figure 5-2 shows a typical pq -diagram derived in the stress domain for the case when thickness of the thin overlay layer is 1 in (with very low temperature profile in the pavement structure). The two other plots at the bottom panel of Figure 5-2 describe the shear and mean stress indicators for that particular case. According to the results presented in Figure 5-2, the layer is under the effect of compressive mean stresses (negative p values) and nearly equivalent magnitudes of shear stress indicator (q values). Which are intensified under each tire rib.

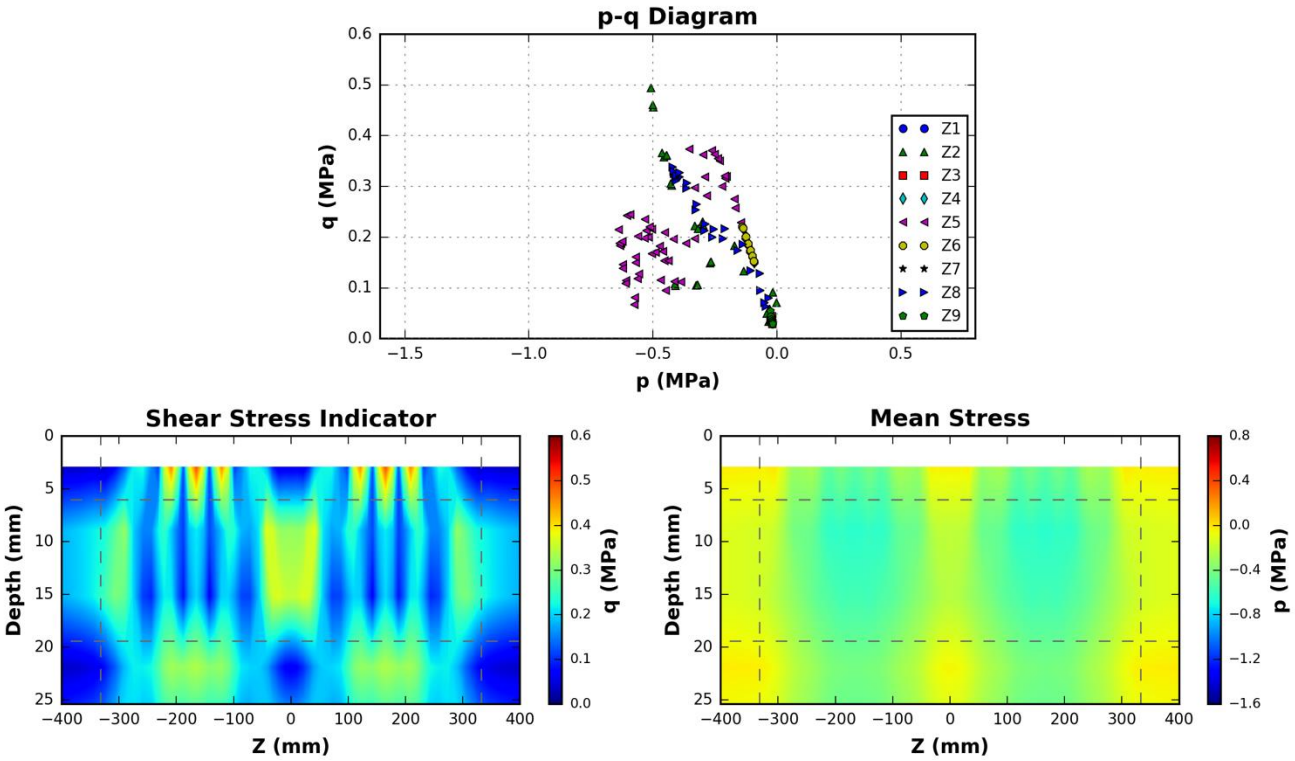

Figure 5-2 Stress distributions in the thin asphalt overlay.

In Figure 5-2, as would be expected, the maximum stress and strain values would be obtained near the surface of the pavement structure. High compressive and shear forces were evident from the purple triangle markers (pointing to the left) spread largely on the compressive side of the plot and the green markers depicting high shear values. It was expected that with the increasing thickness of the overlay, compressive stresses should diminish and turn to tensile stresses. However, since the thickness of thin overlay does not exceed 2 in in this study, the overlay could always be assumed under heavy influence of compressive and shear type of stresses. It should be noted that in order for all results to be presented for domain analysis in this project, tire load was positioned directly in the middle of the wheel path. More details are provided in Section 5.2.

5.1.2 Domain Parameters

Principal values of stresses or strains should be obtained and shear (q) and mean stress (p) indicators should be calculated for any domain analysis problem. However, in order to accurately map the p-q values into the space of the failure envelope, the values in Cartesian coordinates need to be transformed into polar coordinates. For this purpose, the values of the following parameters were extracted from the original plots:

1. Absolute magnitude of the vector drawn from the point of origin to the exact location of any coordinate on the plot;
2. Angle θ between the vector and the horizontal axis.

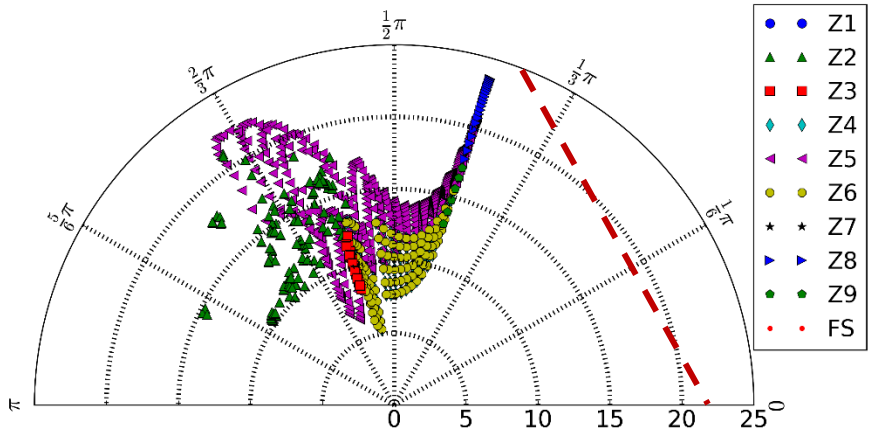

Figure 5-3 Polar plots generated from the Cartesian p-q plots.

The failure envelope shown by a red line in Figure 5-3 was also generated accordingly. The polar coordinate system was divided into 30 different sectors by defining the six radii and seven angle boundaries $(0, \frac{\pi}{6}, \frac{\pi}{3}, \frac{\pi}{2}, \frac{2\pi}{3}, \frac{5\pi}{6}, \pi)$. As the distance from the failure plane to any data point in the response point cloud was very critical in this analysis, a parameter was devised in direct correlation with the position of any particular stress/strain point. Weight factors for each of the 30 sectors in the polar coordinate system were defined. If the distance from the failure envelope to the midpoint of a specific sector is 'd', then the reciprocal 'r' is given as 1/d. Consequently, the sector closest to the failure envelope would have the highest value of the reciprocal. A weight factor, w_i, was then calculated by normalizing the reciprocals to the maximum reciprocal. Therefore, the sector nearest to the failure envelope had a weightage of 1.0. Using the value of these weights and the vector magnitude, the point cloud for any zone could be condensed into one single cumulative value. Using this concept, the following analysis generated values of cumulative responses for comparison. It should be noted that the weight factors were applied to the responses lying only within the envelope and the values of w_i remain constant for the individual sectors (irrespective of the geometry or loading parameters for any given case).

5.1.3 Failure Criteria Defined for Domain Analysis

According to Shin et al., in particulate materials shear properties are the most critical; whereas in bulk materials, tensile and hydrostatic are the defining parameters. Modified Drucker-

Prager Cap Model (MDPC) has been used extensively as the constitutive model to describe the particulate materials in many fields of engineering (Shin et al., 2015). The major variables in the MDPC model are parameters defining elastic behavior, shear failure surface, the cap parameters (the cap aspect ratio, R, and the transition surface parameter, α), which outline the shape of the cap and the transition surface, and the hydrostatic pressure vs. the inelastic volumetric strain relationship which controls the movement of the cap. Parameters R and α are considered the most significant variables in the MDPC model.

Modified Drucker-Prager model defines the yield surfaces in the pq plane where p is normally the mean stress (pressure) and q is the Mises-equivalent shear stress. As shown in Figure 5-4, there are three surfaces in the MDPC model: 1) the Drucker-Prager shear failure surface, 2) an elliptical cap limiting the hydrostatic pressure, and 3) a smooth transition zone between the failure surface and the cap.

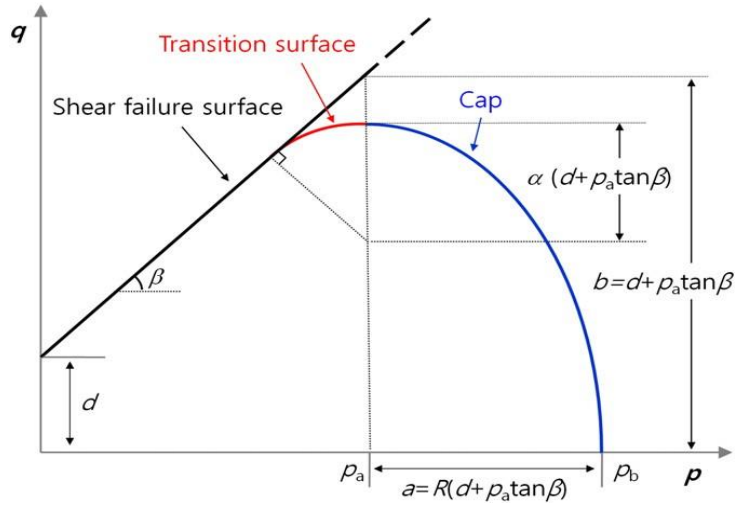

Figure 5-4 Yield surfaces of the MDPC Model in the pq -plane (Shin et al., 2015).

The Drucker-Prager shear failure surface is defined by the following:

$$F_s\,(p,q) = q - p\,tan\beta - d = 0 \tag{5.5}$$

where: β = angle of friction, and d = cohesion intercept.

Moreover, the cap and transition yield surfaces are calculated as follows:

$$F_c = \sqrt{(p - p_a)^2 + \left[\frac{Rq}{(1+\alpha+\alpha/cos\beta)}\right]^2} - R(d + p_a tan\beta) = 0 \tag{5.6}$$

$$F_t = \sqrt{(p - p_a)^2 + \left[q - (1 - \frac{\alpha}{cos\beta})(d + p_a tan\beta)\right]^2} - R(d + p_a tan\beta) = 0 \tag{5.7}$$

$$p_a = \frac{p_b - Rd}{1 + R\ tan\beta} \tag{5.8}$$

where: R = ratio of the horizontal span of the cap on the hydrostatic axis to the original cap height (when the transition surface does not exist) and is called the cap aspect ratio, α = cap parameter that defines the smooth transition surface between the Drucker-Prager shear failure surface and the cap and controls only the cap surface, and p_b = mean effective yield stress and defines position of the cap.

It can be observed from Figure 5-5 that the material behaves elastically when the stress state of the specimen lies within the region defined by the three surfaces. However, as soon as the stress state reaches the shear failure surface, specimen fails by shear action. A new yield surface is created when the critical stress responses reach the cap, in accordance with the hardening law which allows additional plastic deformation after the yielding of the concerned materials before the ultimate failure state depicted by the failure surface. At this point, the stress state is on the surface of the moving cap because logically it cannot lie anywhere outside the yield surface. Consequently, when the stress state reaches a failure surface which lies inside the cap, the cap contracts to the stress state on the failure surface. As a result, the position of p_b decreases, thus implying a reduction in the inelastic volume strain (or the dilation of the material) according to the hardening law. This dilation stops when the contracting cap reaches the stress state of the failure surface.

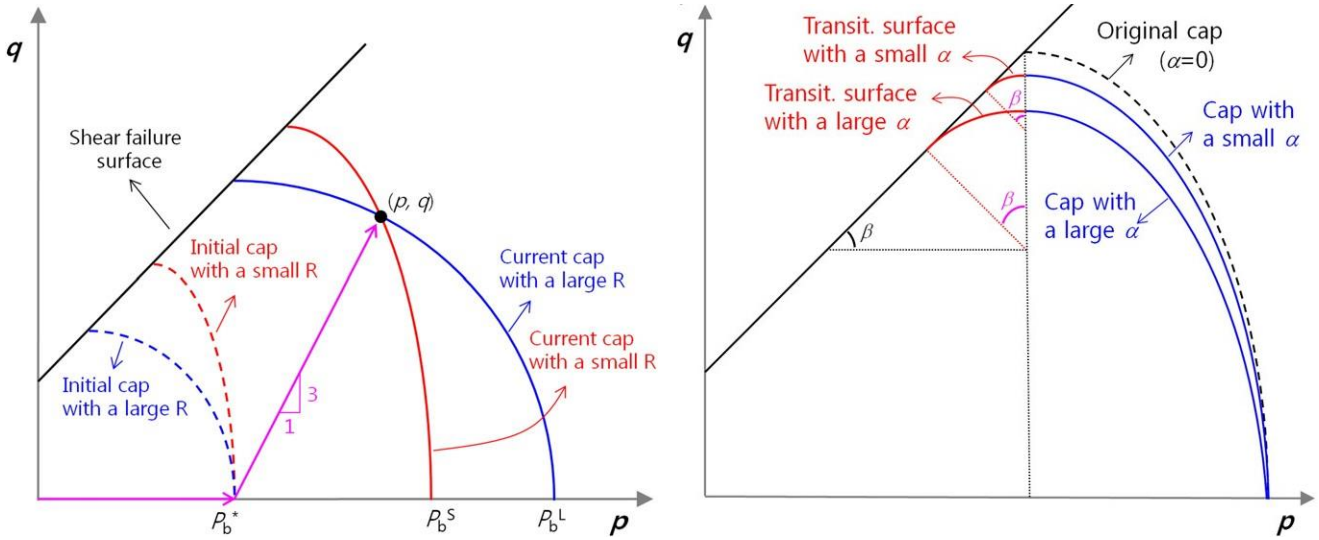

(a) Caps at two different R values at a given stress state when α is zero (b) Effect of the variation of α for a constant R value

Figure 5-5 Parametric study to analyze the impact of R and **α** in MDPC Model (Shin et al., 2015)

Shin et al. evaluated the effect of changes in the parameters R and α (Shin et al., 2015). Figure 5-5(a) shows that a given q value is achieved at a smaller strain value when R is small. However, the same q value can be attained albeit at a larger strain value with a larger R. Thus, the change in R value is actually only having an impact on the positioning of the cap in order to attain the ultimate shear stress level. As such, R is determined to have no impact on the maximum shear stress level that can be achieved in a specimen. As for the effect of variable α, Figure 5-5 (b) shows

that for a larger α, the cap is considerably squeezed, which creates issues as when it lowers the ultimate failure state excessively. In conclusion, it is recommended that R be determined in experimental schemes by taking the value of α as 0. The α value should be set as small as possible unless the results from the MDPC analysis does not produce a converged solution. For the current project, values of parameters used for the MDPC model are given in Tables 5-1 and 5-2.

Table 5-1 Failure Surface Parameters for the Stress Domain (Gamez et al., 2018)

Failure Surface Parameter	Pavement Layer		
	AC	Base	Subgrade
β	40°	35°	30°
d [ksi]	1.17	0.0058	0.004351
R	0.25	0.25	0.25
α	0.73	0.88	1.15

Table 5-2 Failure Surface Parameters for the Strain Domain (Gamez et al., 2018)

Failure Surface Parameter	Pavement Layer		
	AC	Base	Subgrade
β	50°	45°	45°
d [$\mu\varepsilon$]	100.0	100.0	100.0
R	0.69	0.70	0.67
α	0.32	0.26	0.36

5.2 DOMAIN ANALYSIS APPLICATION TO THIN ASPHALT CONCRETE OVERLAY

Two different materials from the ALF (Lane 3) and R 27-42 projects were used for thin AC overlays. In this section, domain analysis results for the eight different base cases are presented.

As shown in Figure 5-1, nine different subdomains were created within the thin overlay extracted from the main pavement structure. A standard location of the 2-D layer right at the middle of the wheel path was considered to evaluate the impact of thin overlay design parameters such as thickness and AC mix type. Failure envelope properties were considered the same as given in Tables 5-1 and 5-2 for all cases.

Figure 5-6 depicts a comparison of the cumulative strain values calculated using the ALF project mix properties. The first digit in the legend indicates the thickness of the overlay; the letter indicates that the project (A is for ALF project). The digit following the letter shows if Lane 1 or 3 from the ALF project is taken into account. The quote mark demarcates whether the effect of deterioration of existing pavement is considered or not (the "‘" sign indicates 1-in milled of existing pavement prior to overlay).

For any given pavement structure, it is expected that the zone closest to the surface should experience the highest possible stresses or strains in compressive mode. Very high and localized

compressive and shear stress values due to direct contact with the loads on surface were observed in Zone Z2. On the other hand, Zone Z5 showed a large increase in compressive stresses in comparison to any other zones. Zone Z8 has largely high values of shear stresses. The remaining six zones on either side of the pavement are not as nearly critical as the three zones right underneath the loading contact area. The figure also shows the effect of thickness on each zones' cumulative strain values. A clear reduction in Z5 strain values is observed with increasing thickness; however, the other zones do not show a consistent reduction with increasing thickness. This can be attributed to the accuracy of FE solution in the elements of subdomains at the surface and bottom (Z2 and Z8) where there could be insufficient number of integration points to describe stress and strain fields. When the sections with and without milling are compared, an increase in the strain response is observed for the sections where thin overlay was applied after milling (sections with quote mark ').

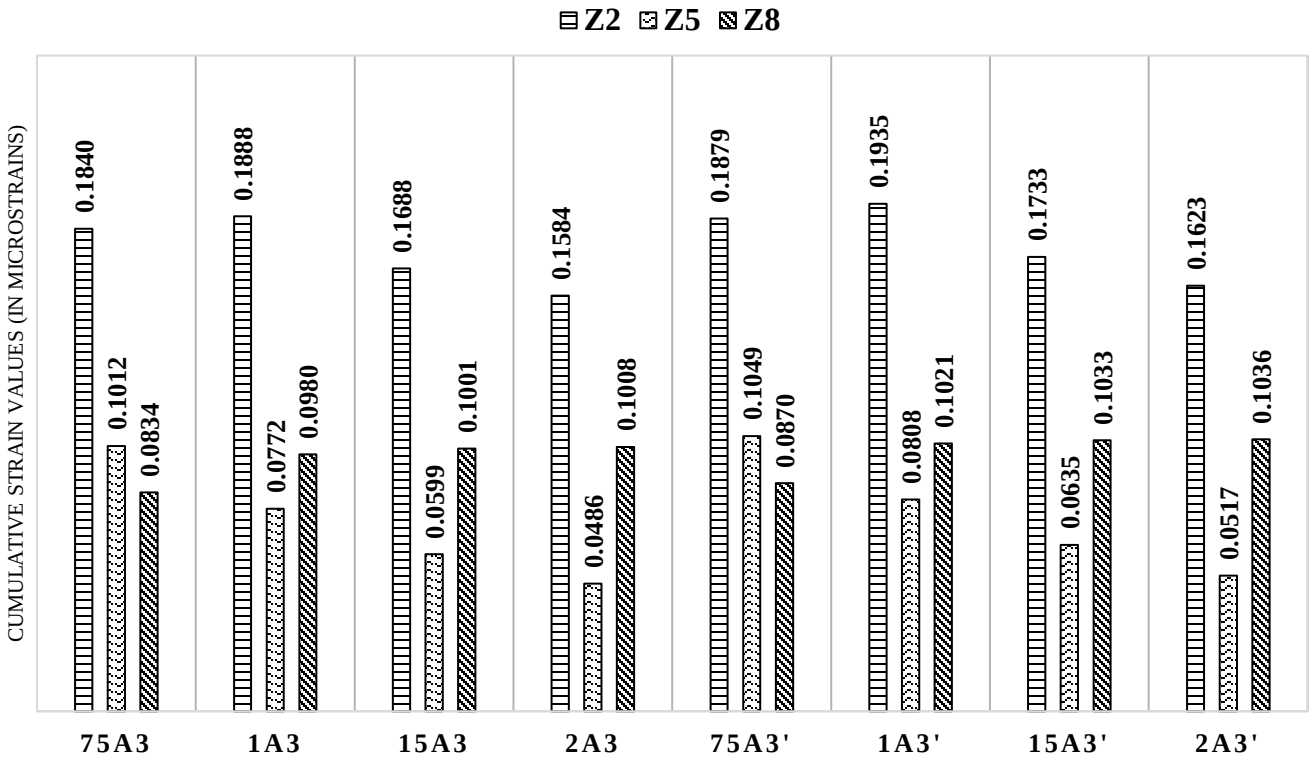

Figure 5-6 Cumulative strain results for the ALF material.

Similarly, Figure 5-7 shows the results for the domain analysis conducted on R27-42 AC mix type for the original pavement structure without milling. Cumulative strain values decrease as the thin overlay thickness increases from .75 in to 2 in. The critical zones are under the influence compressive and shear stresses.

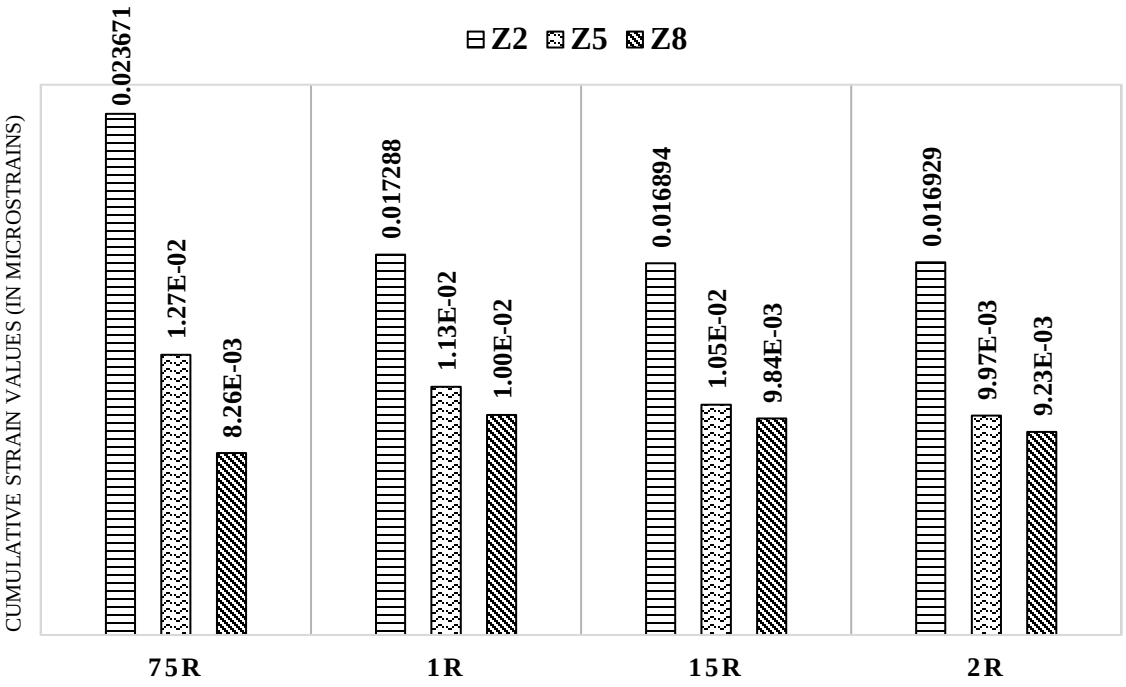

Figure 5-7 Cumulative strain responses for R27-42 mix.

It is noticed that reliable domain analysis results could not be obtained for some of the subdomains within the thin overlays. This could be due to insufficient integration points and mesh refinement especially for the elements on the surface. Therefore, the domain analysis was extended to additional cases where the thin overlay constitutes one subdomain (with Zones Z1, Z2, and Z3) and other subdomains remain within the rest of existing AC layers. The total domain depth is made of all of AC layers, including thin overlay and exiting AC layers (thin overlay + AC2 (1.9 in) + AC3 (1.9 in) + AC4 (9.8 in)). Iterations were also performed considering 1-in milled surface. One such mean strain plot for the R 27-42 mixes is shown in Figure 5-8. As shown in Figure 5-8, for R 27-42 AX mixes, Zone Z2 has a thickness of 0.75 in and the full domain has a thickness of 14.5 in. In this case, the domain analysis would allow the structural contribution of thin overlays (if any) as discussed in the next section.

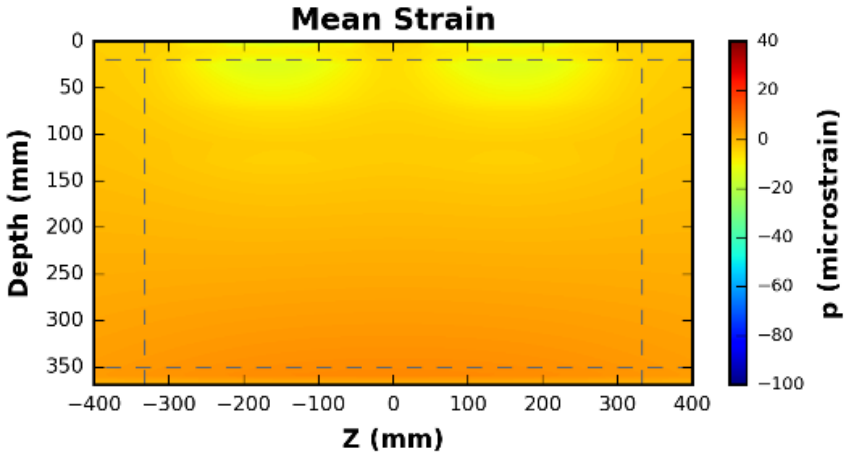

Figure 5-8 Mean strain responses for the AC mix R 27-42 at 0.75-in overlay.

5.2.1 Thin Overlay Contribution to the Pavement Structure

The domain analysis was modified to cover the entire AC layers with the near-surface subdomains (Z1, Z2, and Z3) assigned to thin overlay. This is necessary to determine and evaluate more precisely the profile of the responses developed when a thin overlay is laid on the surface. A typical contour profile of the responses captured is shown in Figure 5-9.

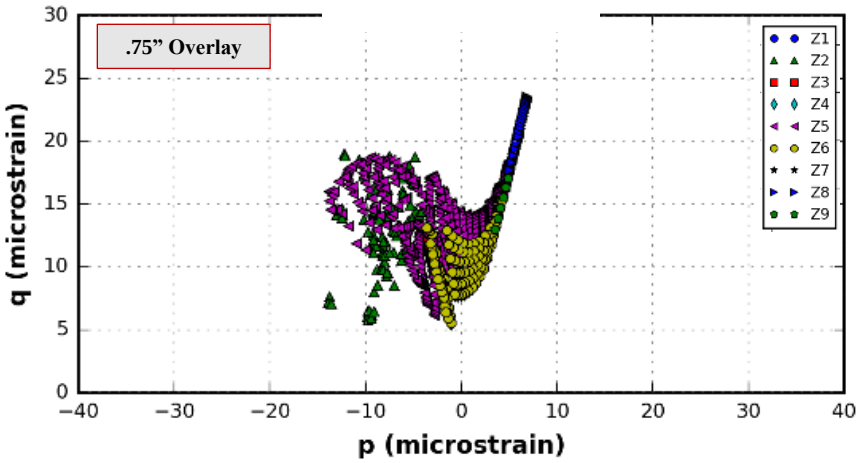

Figure 5-9 Normal and shear strain responses for R 27-42 AC mix with 0.75-in thick overlay.

It is clear from the plot that Zone Z2 which comprises the thin overlay section has the high compression and shear strains. Quite similarly, Zone Z3 has compressive responses within the layer. However, strains gradually transformed from compressive to tensile as depth increased within the domain. Zone 6 primarily demonstrates tensile strain behavior. The zones lying at the bottom of the domain (at the bottom of AC structure) has high shear and tensile strain values. These values could be compared to a case where there is no thin overlay on the surface (a reference case). After a visual comparison of the strain values in Figures 5-9 and 5-10, it is quite evident that the pavement without thin overlay has higher values of the compressive strains. In addition, the shear strains in general are much higher.

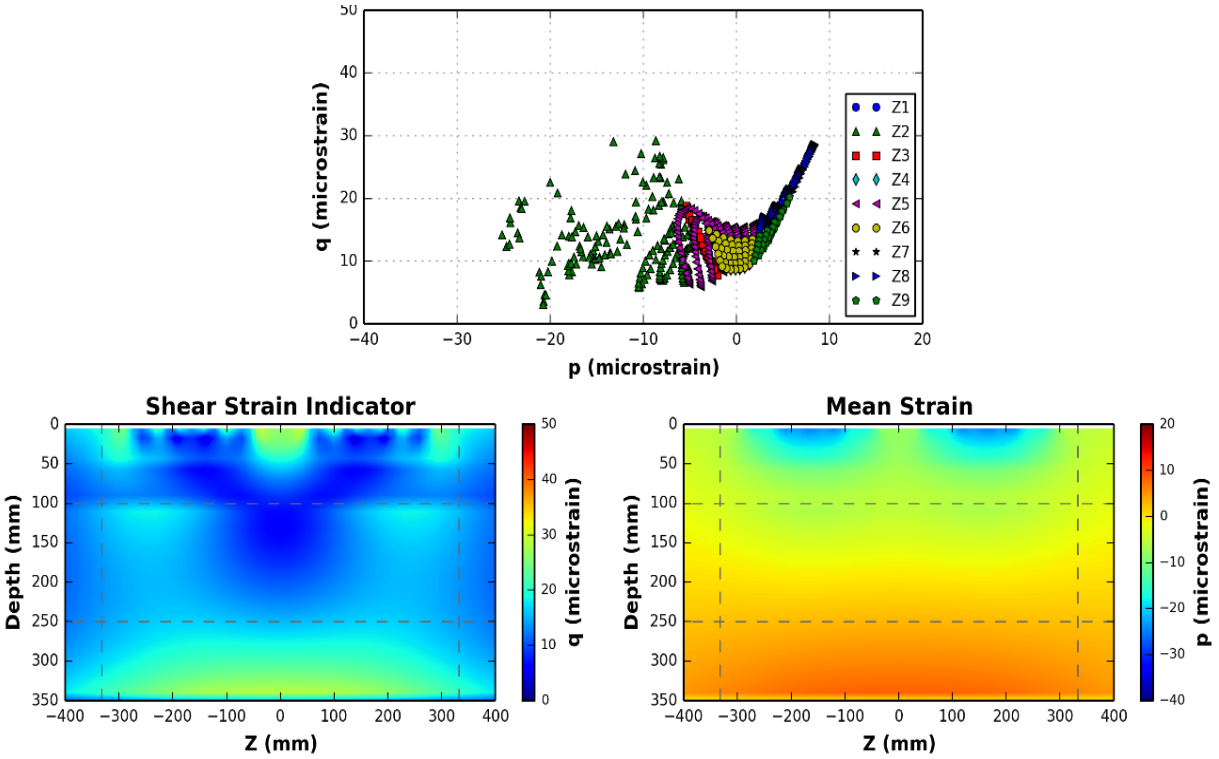

Figure 5-10 Normal and shear strain responses for the pavement structure without thin overlay (R27-42 AC mix).

In order to evaluate the impact of increase in thickness of thin overlays on the strain responses within the subdomains, a comparison of contour profiles for one of the mixes with increasing thickness values is presented in Figure 5-11. The results for the smallest thickness of overlay is presented in Figure 5-9 for the same mix. With an increase in the thickness of the overlay, compressive as well as shear strains in the overlay (zone Z2) are decreased. Normal strains are decreased in Zone Z5 too, but there is a gradual increase in the shear components observed in Zone Z5. This behavior of shear strains continued as the thickness of the overlay kept increasing. Tensile and shear forces are decreased in the region at the bottom of the defined domain (in Regions Z8 and Z9). Zone Z6 also shows a slight decrease in the tensile forces. To summarize, almost all the critical responses show a decrease in value with increasing overlay thickness, except for an increase in the shear strains at the zone constituting the middle part of the AC structure.

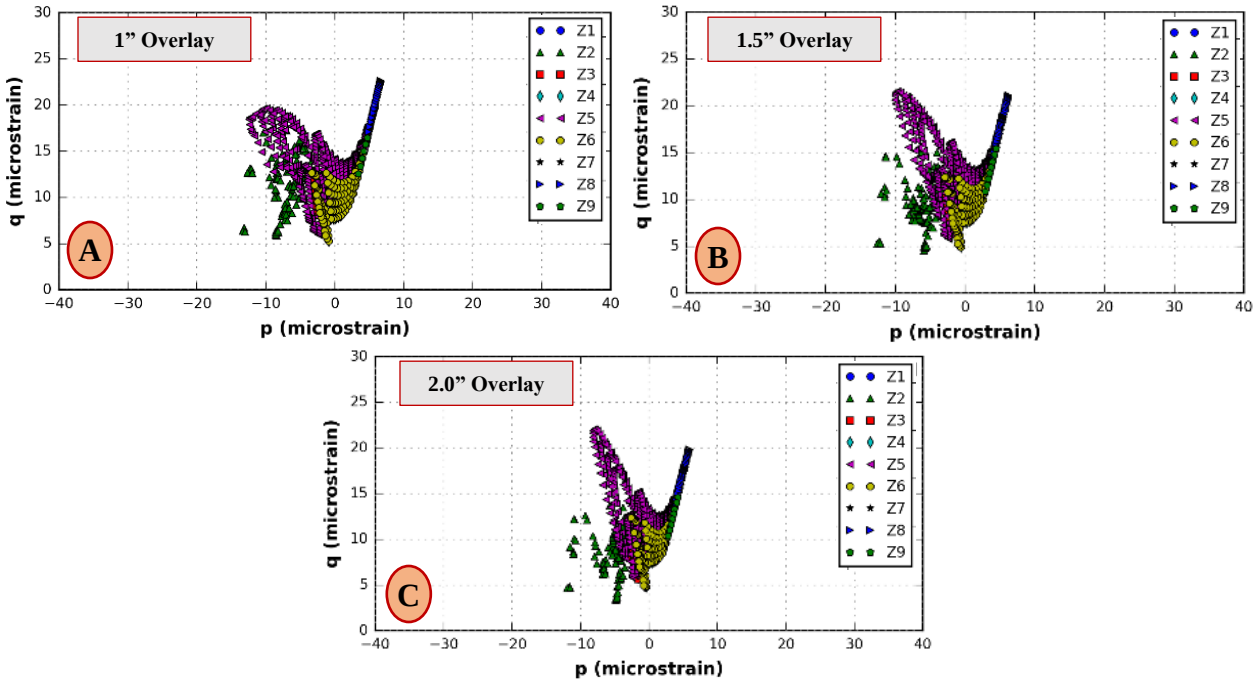

Figure 5-11 Contour plots for different overlay thicknesses.

Figure 5-12 compares the contour profiles of domains with and without 1 in removal from the existing AC layer.

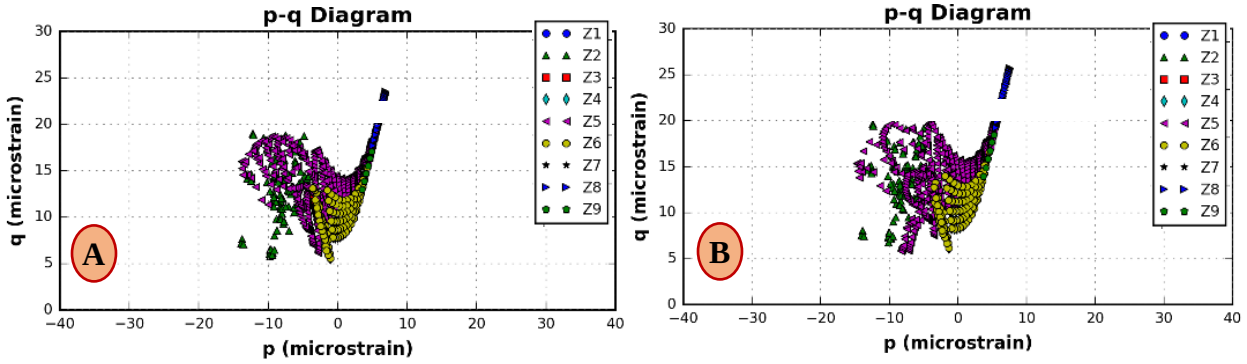

Figure 5-12 Strain profile comparison of the pavement structures (a) with and (b) without a 1-in milling of the original AC layer surface when 0.75-in thick AC is applied.

From Figure 5-12, almost all major zones analyzed show an increase in the shear strains when 1 in is milled from the existing pavement. While this increase is minimal for the surface zone (Z2) and a slightly higher for zone Z5, it is significant for the bottom Zone Z8. In addition, some regions in the Zones Z5 and Z6 of Figure 5-12 (b) experience an increase in compressive strains as compared to those in Figure 5-12 (a).

Figure 5-13 shows results for the same thin overlay AC mix and increasing overlay thickness for a pavement with existing deterioration in the surface layer. A major reduction in the shear and mean components of compressive and shear strains were noticed with increasing thickness except an increase in shear strains in some regions of Zone Z5.

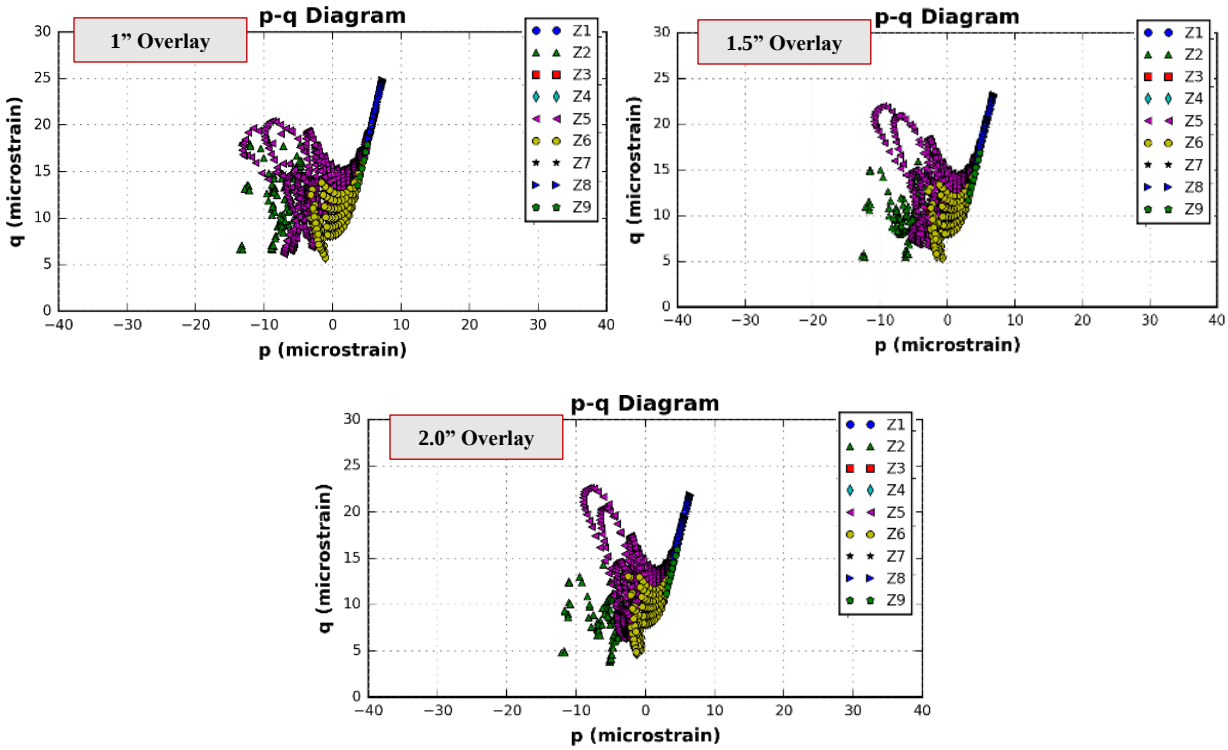

Figure 5-13 Critical responses for different overlay thicknesses.

It is, therefore, concluded that although the magnitude of response changes, the pattern of variation of responses for a single mix is almost the same within varying thicknesses of overlays. Hence, a similar analysis was conducted using the ALF (Lane 3) AC mix.

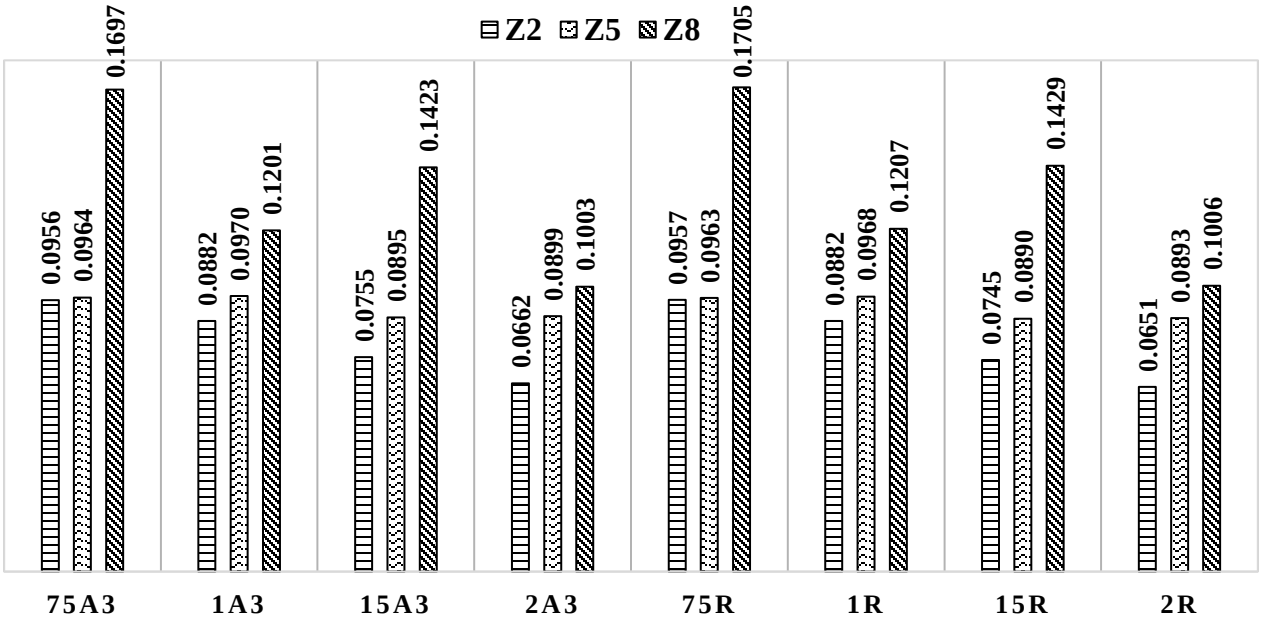

Figure 5-14 Cumulative strain results for the R 27-42 and ALF AC mixes.

Cumulative strain results from the domain analysis are shown for the two mixes in Figure 5-14. The results showed the zoning scenario where surface subdomains (Z1, Z2, and Z3) remained completely within the thin overlay, and the rest of the subdomains were within the existing AC layers. Figure 5-14 shows that Zone Z8 at the bottom of the pavement structure has greater cumulative strain values than any of the other zones. Variation in these values within the zone does not correspond to overlay thickness change. The middle zone, which has a lower strain magnitudes, does not follow a specific pattern of change. Hence, with the exception of the overlay area, the structural contribution of thin overlays appears to be insignificant. Although values are slightly greater for the R27-42 mix in some zones, the values are material-independent.

In summary, although the initial stress or strain response does not significantly change when two different materials are used, pavement performance can be drastically different if the damage potential of these two materials are different. This is a limitation of some of the mechanistic models considering only linear elastic or viscoelastic properties. Further evaluation of critical responses using the concept of failure envelope (as described earlier) is presented in the next chapter.

The change in overlay thickness did not seem to change the variation of the strains in different zones with respect to each other; however, a reduction in the maximum strains at the bottom zone of the AC layer are observed with the increasing overlay thickness. This is consistent with critical point analysis presented in Chapter 4. Therefore, based on the results of the mechanistic analysis presented, it can be concluded that presence of thin overlays may have some influence on structural capacity of flexible pavements. In addition, changing the thickness of the thin overlay has significant impact on the responses within the overlay which may initiate and govern the failure before bottom-up fatigue cracking occurs.

CHAPTER 6 - BRIDGING PAVEMENT AND MICROMECHANICAL FE MODELS

One of the major objectives of this research project was to develop a computationally efficient method to link micromechanical features of AC (introduced in Volume I) and thin overlay response and mechanisms of failure as presented in this volume. The domain analysis method introduced as a concept to consider the failure criteria of the pavement sections with a thin surface layer. In the domain analysis technique, a fictitious failure envelope is designed to define the failure characteristics of the AC mixture used in the overlays. However, to develop a more realistic scenario, it is necessary that the envelope reflect the actual failure behavior of the mixes studied in this project. In this regard, it is technically appropriate to obtain these values from either some actual laboratory or field experimental results or values derived from simulations created using FEs methods. The micromechanical model was developed for a commonly used fracture test and was presented in Volume 1 Report of this project. The intent of the micromechanical models is to evaluate the cracking potential for the AC mixes used in the pavement analysis and domain method. Therefore, the scenario that the failure surface used in the domain method could be altered, based on the cracking potential of AC mixes determined using micromechanical simulations, is presented in this chapter. The concept of polar plots is presented and the impact of the parameters, used to define a failure envelope, on the critical responses.

6.1 POLAR PLOT AND FAILURE ENVELOPE CONCEPT

The failure envelope and its development, as part of the domain analysis method, is presented in Chapter 5. Defining a failure envelope requires determination of the mode in which a particular stress or strain value might yield or in other words starts developing inelastic strains. Failure envelope should ideally be determined using proper experimental techniques. Each AC mixture, depending on some volumetric, micromechanical features, or loading conditions may have different failure potentials. Considering some changes in the failure envelope, the impact of the position of the failure envelope on the cumulative strain values in different zones could be studied.

The domain introduced in Section 5.2 was considered. In this case the thin overlay was subdivided into different subregions. For the ALF Lane 3 AC mix at a thickness of 1 in, polar plots for the thin overlay layer with different properties were generated. The analysis was conducted by keeping the failure envelope properties as presented in Chapter 5. However, as the weight factors for different sectors on the polar plot remained the same, the position of the point cloud to the envelope was altered by simply changing the maximum limit of the horizontal axis in order to study the impact of changes in the defined material damage potential. As a result, this can be implemented as a change in the position of the failure envelope indicating a material with different damage capacity for each case. Four different axis limits with a fixed failure envelope are presented in Figure 6-1. It can be noticed that as the failure envelope shrinks, the cloud of stress points get closer to the failure surface indicating higher potential of damage.

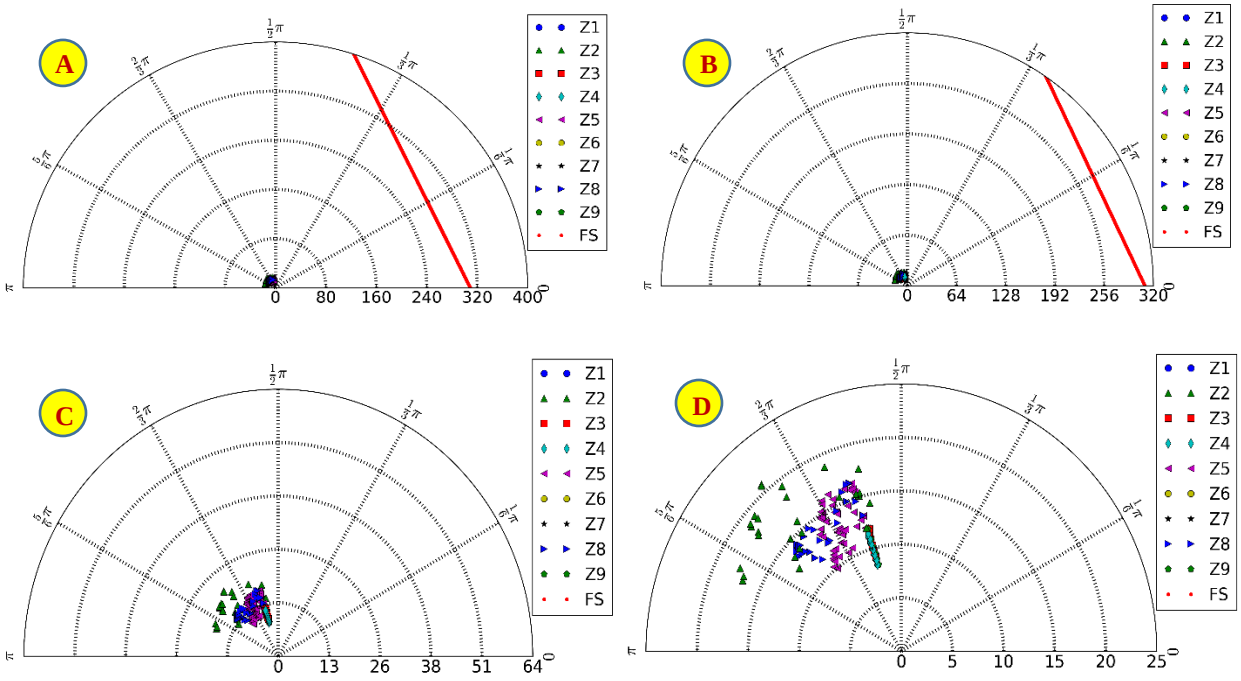

Figure 6-1 Sensitivity analysis for the failure criteria defined in 1-in thick overlays illustrating the variations in the failure potential of a material (A: lowest damage potential and D: highest damage potential).

The corresponding value of the cumulative strains for each zone for the four different cases of failure envelop is given in Table 6-1. As expected, with the failure envelope moving closer to the cloud of points, cumulative strain values exhibit a significant increase and approach a value of 1.0.

Table 6-1 Cumulative Strains for the Cases Defined in Figure 6-1

Case	Z1	Z2	Z3	Z4	Z5	Z6	Z7	Z8	Z9
A	0.14	0.0	0.19	0.0	0.14	0.0	0.06	0.08	0.06
B	0.24	0.0	0.33	0.0	0.24	0.0	0.11	0.13	0.11
C	0.71	0.0	1.0	0.0	0.71	0.0	0.33	0.4	0.33
D	0.74	0.0	1.03	0.0	0.74	0.0	0.34	0.41	0.34

Figure 6-2 shows the results for the analysis carried out for the two different thin overlay AC mix types (R 27-42 and ALF Lane 3). The effect of existing damage in the AC2 layer (1.9 in existing surface layer) was also accounted for.

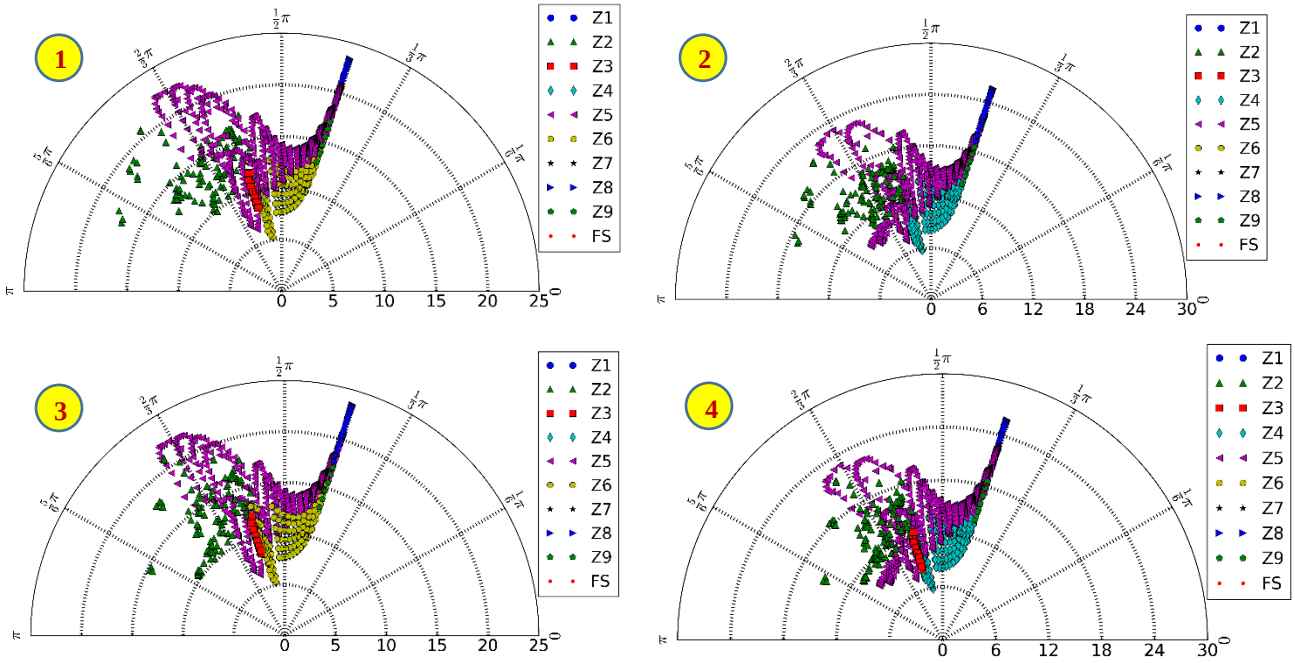

Figure 6-2 Polar plot analysis for two different AC mixes without and with the impact of existing damage to the AC layer.

where:

Case 1 = ALF Lane 3 AC mix without the damage in existing AC Layer

Case 2 = ALF Lane 3 AC mix with damage in existing AC Layer

Case 3 = R 27-42 AC mix without the damage in existing AC Layer

Case 4 = R 27-42 AC mix with damage in existing AC Layer

Corresponding cumulative strain values for all the four cases are given in Table 6-2.

Table 6-2 Cumulative Strains for the Cases Defined in Figure 6-2

Case	Z1	Z2	Z3	Z4	Z5	Z6	Z7	Z8	Z9
1	0.35	0.37	0.48	0.45	0.35	0.37	0.37	0.50	0.37
2	0.36	0.37	0.49	0.47	0.36	0.37	0.40	0.53	0.4
3	0.36	0.38	0.48	0.42	0.36	0.38	0.37	0.50	0.37
4	0.36	0.37	0.49	0.44	0.36	0.37	0.40	0.53	0.40

The values in Table 6-2 confirm the initial assumption of this analysis that the value of weight factors remained the same for all the sectors since pavement structural response was not significantly altered due to overlay thickness change and different material modulus. As the point cloud for the pavement structure did not drastically change in position, the cumulative strain values

presented in the table are not different from each other. However, a change in the failure envelope properties for any one of the cases made a remarkable difference in the cumulative strain values calculated. For example, Figure 6-3 shows the effect of change in failure envelope properties for the thin overlay with ALF Lane 3 AC mix properties and an existing damaged AC2 layer.

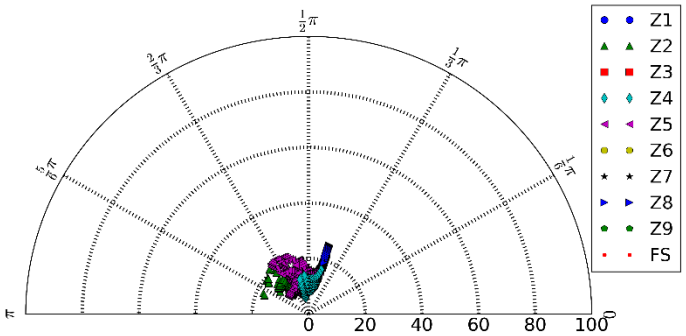

Zone	CE AC
Z1	0.34
Z2	0.35
Z3	0.46
Z4	0.45
Z5	0.34
Z6	0.35
Z7	0.37
Z8	0.49
Z9	0.37

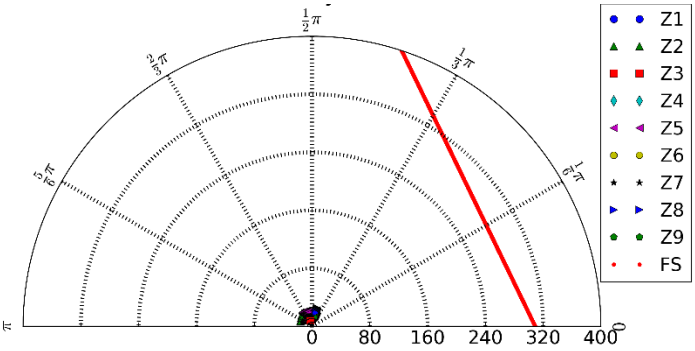

Zone	CE AC
Z1	0.07
Z2	0.07
Z3	0.09
Z4	0.09
Z5	0.07
Z6	0.07
Z7	0.08
Z8	0.1
Z9	0.08

Figure 6-3 Sensitivity analysis for the failure criteria defined for the ALF Lane 3 AC mix type considering deterioration in the existing AC layer.

Comparing Figures 6-2 and 6-3 shows that an increase in the values of cumulative strains was observed when a change in the failure criteria was made and the point cloud moved closer to the envelope defined. An additional observation regarding the responses recorded for different zones could also be made. In Chapter 5, it was shown that Zones Z2, Z5 and Z8, out of all the nine separate zones, displayed the highest variation in the critical response values as per the contour plot.

6.2 SENSITIVITY OF RESPONSE TO CHANGES IN FAILURE ENVELOPES

For the purpose of comparing changes to the polar plot for a certain thickness of the thin overlay and a fixed failure envelope, the approach adopted in preceding sections was sufficient. However, in order to carry out a more robust analysis across different thicknesses of the overlay, simply changing the axis limits produces inconclusive and unreliable results. To solve this problem, a fixed value is kept for the horizontal axis limit and the properties of the failure envelope are changed. In this project, no actual experimental or field results were available to obtain failure properties for a particular mix, therefore, a hit and trial method was adopted to manually generate different envelopes. In this process, values were assumed for the basic envelope parameters for

every case, signifying the damage capacity of a specific overlay material. Table 6-3 gives basic attributes of the different cases considered.

Table 6-3 Properties of Different Failure Envelopes in the AC Layer for Strain Domain

Failure Surface Parameter	Case 1	Case 2	Case 3	Case 4
β	50°	50°	50°	50°
d $[\mu\varepsilon]$	5.0	20.0	50.0	100.0
R	0.30	0.30	0.30	0.69
α	0.15	0.32	0.32	0.32

For all the four cases in Figure 6-4, the failure envelope is visibly seen expanding farther from the p-q point cloud as shown.

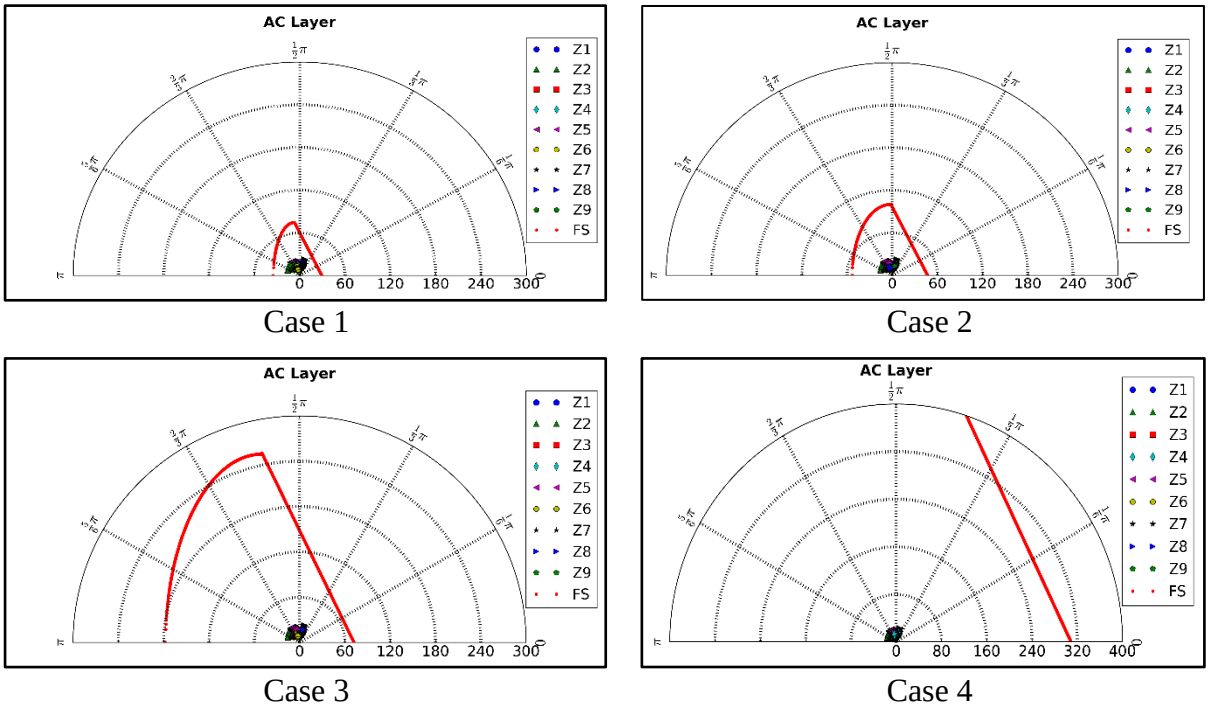

Figure 6-4 Different failure envelopes generated for the thin overlay analysis.

As seen in Figure 6-4, all four cases theoretically represent four different thin overlay materials for a specific overlay thickness. It should be kept in mind that the input details in the Drucker-Prager Cap Model involved the influence of elastic behavior, shear failure surface, cap parameters (R and α), hydrostatic pressure, and the inelastic volumetric strain relationship. However, the subdomain analysis conducted in the previous chapter showed that the tensile and compressive distresses were more significant in comparison with the shear forces for a pavement with thin asphalt overlay. For the purposes of this analysis, a failure envelope as shown in Figure 6-5 was developed for the four cases.

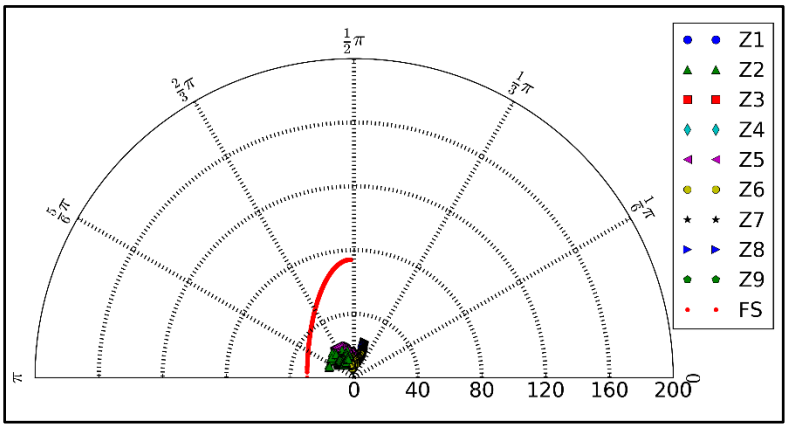

Figure 6-5 Modified failure envelope generated for the thin overlay analysis.

To figure out the actual impact of each case, cumulative strain values for a full AC section along a single 2-D layer were compared. Figure 6-6 compares the strains in different zones of one of the 2-D layers in the traveling direction for a thin overlay thickness of 1 in. This layer was selected based on the maximum value of the cumulative strains generated in a layer calculated on the basis of equation (9) as follows:

$$C\varepsilon_{case} = \frac{\sum_{l=1}^{z}\sum_{j=1}^{e}\sum_{i=1}^{s}\left|(pq)_{\sigma,\varepsilon}\right|_{jl} a_{jl} * w_i}{A_z} \tag{6.1}$$

where: $C\varepsilon_{case}$ = cumulative stress/strain of the specific load case

$\left|(pq)_{\sigma,\varepsilon}\right|_{jl}$ = vector magnitude of the element j for a total of e elements within the zone l for a total of z zones

a_{jl} = area of element j within zone l

w_i = weight of the specific sector i for a total of s sectors

A_z = total area of zone z

In the previous analysis, the 2-D plane for calculating the strains was situated at the mid-length of the subdomain structure. However, a comparison of $C\varepsilon_{case}$ values for the 2-D planes in the traveling direction showed that the maximum strain states occurred right behind the middle of the tire footprint. This might be caused by the viscoelasticity of AC layers which results in a delay between the loading and related strain response.

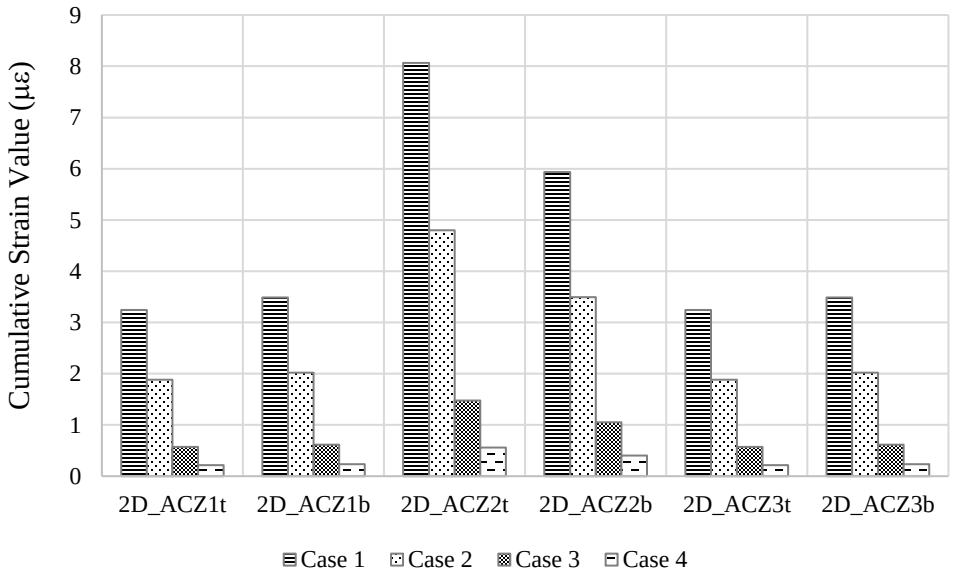

Figure 6-6 Comparison of strains in Zones Z1, Z2 and Z3.

The ‘t’ and ‘b’ in the legend represent the “top” and “bottom” of a given zone. It was observed that the strain values decreased from Case 1 to 4. Similar comparisons for other zones are made in Figures 6-7 and 6-8.

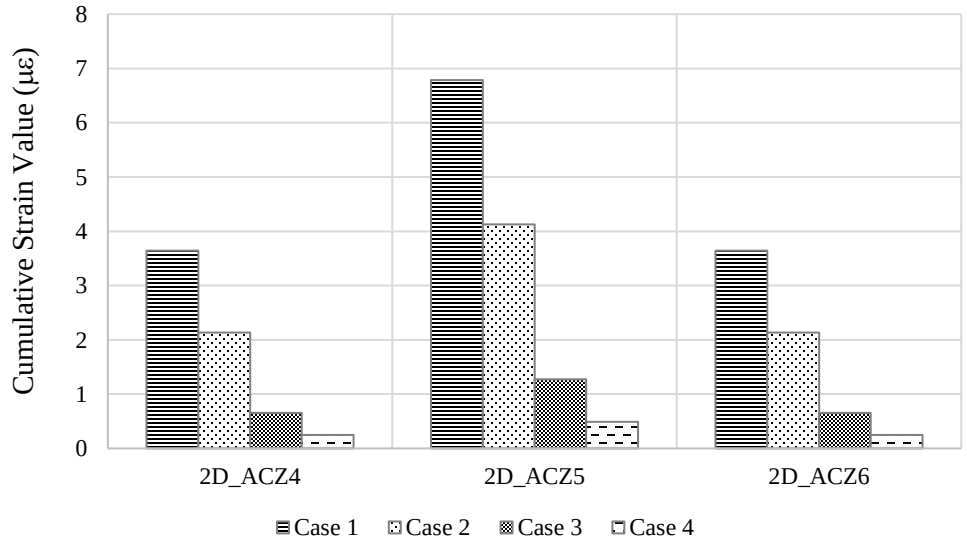

Figure 6-7 Comparison of strains in Zones Z4, Z5 and Z6.

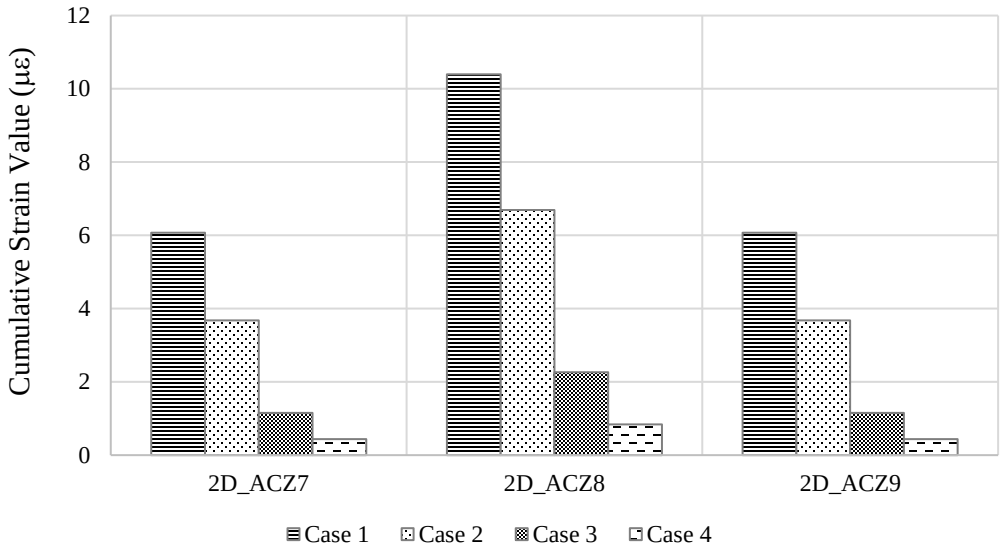

Figure 6-8 Comparison of strains in Zones Z7, Z8 and Z9.

Zones Z4 to Z6 also show a response reduction from Cases 1 to 4. A similar pattern of variation was observed for the bottommost Zones Z7 to Z9. As mentioned in Chapter 5, maximum strains were generated in Zones Z2, Z5, and Z8. Based on this analysis, it could be suggested that the material represented by Case 1 for a specific overlay thickness was the one with the highest damage potential. Similar conclusions were made for other thicknesses of the thin AC overlay as well. Figures 6-9 and 6-10 provide the values of overall strains in the 2-D pavement section and 3-D strains below the AC layer, respectively.

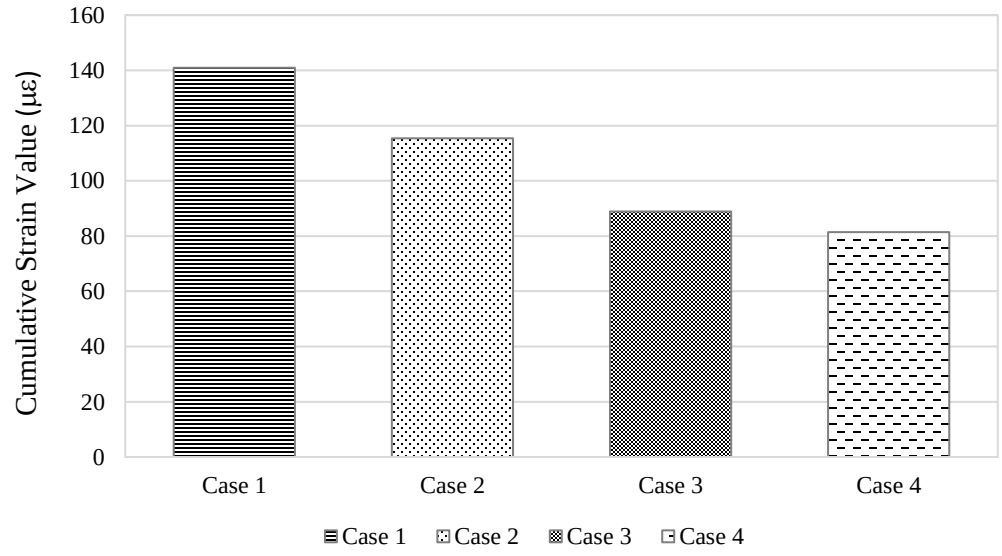

Figure 6-9 Comparison of overall strains in the 2-D pavement section.

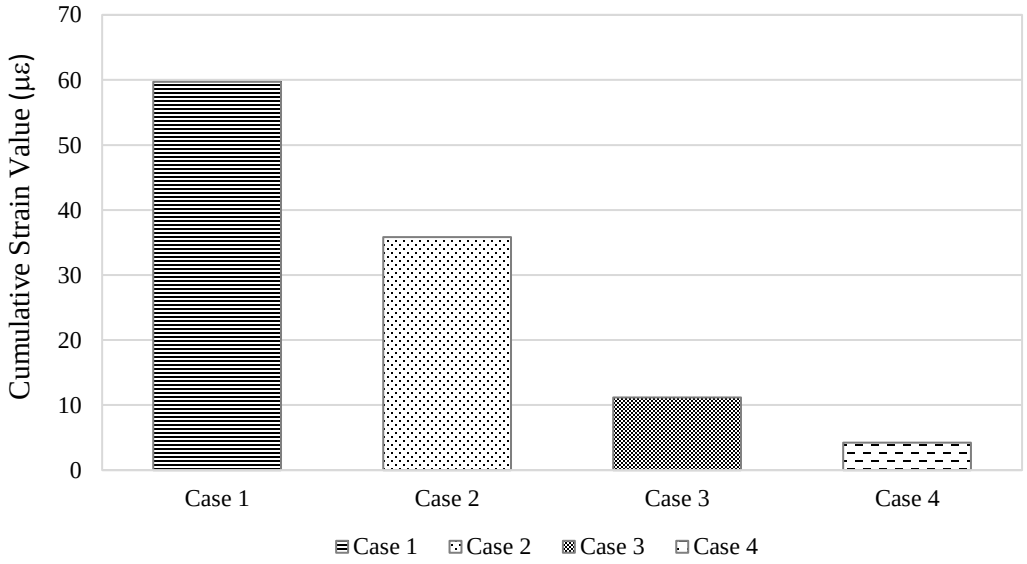

Figure 6-10 Comparison of 3-D strains below the AC layer.

As a result, Case 1 material with the highest value of strains might represent an overlay structure with the least service life. Table 6-4 gives the numerical values of maximum cumulative strains for a 2-D layer for different cases and overlay thicknesses.

Table 6-4 Maximum Cumulative Strain ($\mu\varepsilon$) Values for a 2D Layer in The Traveling Direction

Overlay Thickness (in)	Case 1	Case 2	Case 3	Case 4
0.75	163	130	96	87
1.0	141	115	89	81
1.5	130	106	81	74
2.0	113	93	74	68

In confirmation with the theoretical assumptions of a failure envelope made earlier, Case 1 had the highest value of strains. Also, in accordance with the conclusions made in Chapter 5, the thickest overlay had the least value of strains. If it were considered that the case with minimum strains had the highest service life (L), then the respective L values would be easily mapped out.

6.3 SERVICE LIFE ESTIMATION

Based on information in the literature, the service life of thin overlays ranges from 7 to 11 years. Therefore, if the case with least thickness and worst material is given an ‘L’ value of seven years, then rest of the values for L would be mapped accordingly. Table 6-5 shows a clear progression in the service life values as the thickness of thin overlay increases. With the increasing thickness of the thin overlay and better AC mix type used, the pavement requires less frequent maintenance. The values range from a minimum of seven to a maximum of approximately 15

years, see Figure 6-11. If the case with the highest service life is considered the Best (B) performer, then the rest would be indicated as Worst (W) or Intermediate (I(1) and I(2)) performers.

Table 6-5 Expected Service Lives (L) for Different Cases

Overlay Thickness (in)	Case 1	Case 2	Case 3	Case 4
0.75	7.0	8.5	11.2	12.4
1.0	7.9	9.5	12.1	13.2
1.5	8.5	10.2	13.3	14.3
2.0	9.7	11.6	14.4	15.5

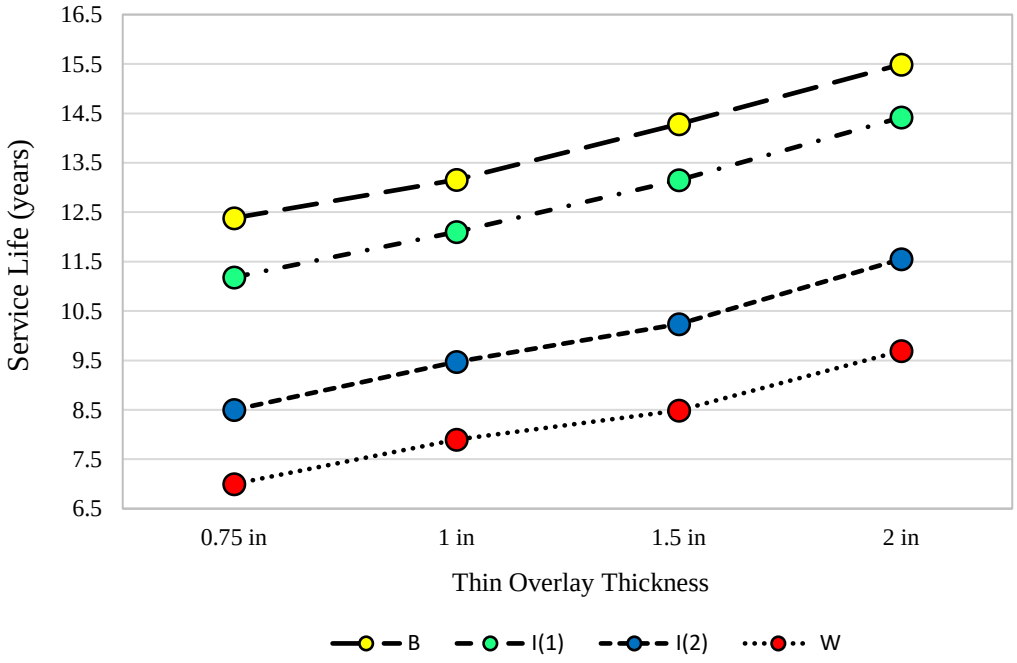

Figure 6-11 Service life vs. thin overlay thickness for different material types.

CHAPTER 7 - FINAL REMARKS

A mechanistic evaluation of thin overlay as a pavement preservation treatment method is presented. A three-dimensional (3-D) finite element (FE) pavement model was developed to understand mechanics of thin overlays and their overall contribution to pavement system. The 3-D FE model was coupled with the domain analysis to better understand potential failure mechanisms in thin overlays as well as to incorporate various mixture characteristics to overlay performance. In order to incorporate asphalt concrete (AC) mixture characteristics other than modulus, a micromechanical model was developed for the AC mixes commonly used in surface overlays and modeled using a fracture test. The micromechanical model development and analysis results for various AC overlay mixes were presented in Volume 1 Report of this project. The AC mixes' fracture characteristics were determined using the micromechanical models. The output of micromechanical models was used to bridge microscale modeling to the 3-D FE pavement models to predict overlay life cycle. The following findings may be drawn from this study:

1. Based on critical point stress and strain analysis, the longitudinal strains are always greater than transverse strains at the bottom of the overlay as well as other AC layers.

2. Thin overlays up to 2 in are usually under compression and shear type stresses.

3. As thin overlay thickness increase, the pavement responses decrease, suggesting the structural value of thin overlays.

4. Point stress and strain analysis is inadequate to describe complex stress and strain states within the thin overlays. Therefore, analysis results may be inconclusive to predict thin overlay service life.

5. The effect of material modulus properties on the thin AC overlay responses appeares to be minimal. Hence, failure characteristics of materials may need to be incorporated into the analysis.

6. Using domain analysis, a uniform decrease in the cumulative strains in the overlay section (zone Z2) was observed with the increasing thickness of the overlay. In general, high compressive and shear strains were observed in the surface AC layers. A shift from compressive to tensile behavior was noticed in the AC layers below the surface overlay.

7. Deterioration in existing AC layers was considered. In that case, shear strains increased considerably for most of the AC layer zones beneath the overlay. The increase was, however, more significant at the bottom of the AC section.

8. Using the range of service lives expected from thin overlays and domain analysis output, it was demonstrated that allowable service lives can be between 7 to approximately 15 years with the thickest overlay and strongest AC mix type having highest value of service life.

The following conclusions are made:

1. Current experimental methods used to characterize AC mixes may not be adequate to describe the structural response and damage occurring in thin overlays.

2. It is recommended to utilize domain analysis in lieu of critical point responses. Domain analysis allows better characterization of complex stress and strain states within the thin overlays. In addition, it allows the incorporation of material's failure characteristics that can be used in predicting the thin overlay service life.

3. Domain analysis shows that the thickness of thin AC overlays can govern the responses within the thin overlay and, therefore, would be a dominant factor in pavement performance.

REFERENCES

ABAQUS. (2014). Version 6.14. Dassault Systems.

Al-Qadi, I., M. Elseifi, and D. Leonard. (2003). Development of an Overlay Design Model for Reflective Cracking with and without Steel Reinforcing Nettings. Journal of the Association of Asphalt Paving Technologists, Vol. 72, pp. 388-423.

Al-Qadi, I., Wang, H., Yoo, P., and Dessouky, S. (2008). "Dynamic analysis and in situ validation of perpetual pavement response to vehicular loading." Transportation Research Record: Journal of the Transportation Research Board, 2087, 29–39.

Al-Qadi, I. L. and Yoo, P. J. (2007). "Effect of surface tangential contact stresses on flexible pavement response (with discussion)." Journal of the Association of Asphalt Paving Technologists.

Al-Qadi, I., S. Son, and T. Zehr. (2013). Development of an economical, thin, quiet, long lasting and high friction surface layer. Volume 2: Field construction, field testing, and engineering benefit analysis. Illinois Center for Transportation FHWA-ICT-13-006, F04S05.

Al-Qadi, I. L., Ozer, H., Lambros, J., El-Khatib, A., Singhvi, P., Khan, T., Rivera J. , and Doll, B. (2015). Testing Protocols to Ensure Performance of High Asphalt Binder Replacement Mixes Using RAP and RAS. Final Report no. FHWA-ICT-15-017, Illinois Center of Transportation, Project Sponsored by Illinois Department of Transportation.

Al-Qadi, I. L., Ozer, H., Gamez, A., and Hernandez, J. (2016). Influence of Tire Parameters on Roadway Structures. Research Report No. ICT-16-017, Illinois Center for Transportation.

American Association of State Highway and Transportation Officials (AASHTO). (1999). Pavement Preservation in the United States. Survey by the Lead States Team on Pavement Preservation. American Association of State Highway and Transportation Officials. Washington DC.

Anderson, K., Russell, M., Ulhmeyer, J., Luhr, D., Dias, B., and Weston, J. (2014). Trinidad Lake Asphalt Overlay Performance Final Report. Washington State Department of Transportation, Report No. WA-RD 710.2.

Baek. J., and Al-Qadi, I. L.. (2011). Sand Mix Interlayer to Control Reflective Cracking in Hot-Mix Asphalt Overlay. Transportation Research Record: Journal of the Transportation Research Board, No. 2227, Transportation Research Board of the National Academies, Washington, D.C., pp. 53–60.

Barker, R. W., Bianchini, A., and Brown, E. R. (2011). Minimum Thickness Requirements for Asphalt Surface Course and Base Layer in Airfield Pavements. Final report, ERDC/GSL TR-11-27, US Army Engineer Research and Development Center.

Bausano, J. P., Chatti, K., and Williams, R. C. (2004). Determining Life Expectancy of Preventive Maintenance Fixes for Asphalt-Surfaced Pavements. Transportation Research Record, Journal of the Transportation Research Board, No. 1866, National Research Council, Washington, D. C., pp. 1-8.

Belshe, M., Kaloush, K. E., Golden, J. S., Mamlouk, M., and Phelan, P. E. (2007). Asphalt-Rubber Asphalt Concrete Friction Course Overlays as Pavement Preservation Strategy for Portland Cement Concrete Pavement. TRB Annual Meeting Compendium, Paper No. 07-1916, Transportation Research Board, Washington, DC, 2007.

Bennert, T., Fee, F., Sheehy, E., Jumikis, A. and Sauber, R. (2005). Comparison of Thin-Lift Hot-Mix Asphalt Surface Course Mixes in New Jersey. Transportation Research Record: Journal of the Transportation Research Board, No. 1929, Transportation Research Board of the National Academies, Washington, D.C., pp. 59–68.

Brown, E. R., Hainin, M. R., Cooley, A., and Hurley. G. (2004). Relationships of HMA In-Place Air Voids, Lift Thickness, and Permeability. Volumes I through IV. NCHRP Report No. 531. National Cooperative Highway Research Program.

Brown, E. R., M. Hainin, and L. Cooley, Jr. (2005). Determining Minimum Lift Thickness for Hot Mix Asphalt (HMA) Mixtures. Journal of the Association of Asphalt Paving Technologists 74:23-66. Long Beach, CA.

Cable, J. K., Fanous, F. S., Ceylan, H., Wood, D., Frentress, D., Tabbert, T., Oh, S. Y. and Gopalakrishnan, K. (2005). Design and Construction Procedures for Concrete Overlay and Widening of Existing Pavements. FHWA DTFH61-01-X-00042 (Project 6), IHRB Project TR-511, Center for Portland Cement Concrete Pavement Technology, Iowa State University.

Coetzee, N. and Monismith, C. (1979). Analytical Study of Minimization of Reflection Cracking in Asphalt Concrete Overlays by Use of a Rubber-Asphalt Interlayer. Transportation Research Record, pp. 100-108.

Cewe, J. (1966). Thin Overlays in the Greater Vancouver Area. Proceedings of the Canadian Technical Asphalt Association, Vol. 11, pp. 199–203.

Cooley, L. A., Jr. and Brown E.R. (2003). Potential of Using Stone Matrix Asphalt (SMA) for Thin Overlays. NCAT Report 03-01, National Center for Asphalt Technology, Auburn, Alabama.

Chen, N., Vito, J. D., and Gene, R. (1982). Finite Element Analysis of Arizona's Three-Layer Overlay System of Rigid Pavements to Prevent Reflective Cracking. Proceedings of Association of Asphalt Paving Technologists, Vol. 51, pp. 150-168.

Chou, E. Y., Datta, D. and Pulugurta, H. (2008). Effectiveness of Thin Hot Mix Asphalt Overlay on Pavement Ride and Condition Performance. Report No. FHWA/OH-2008/4. Ohio Department of Transportation.

Cuelho, E., Mokwa, R. and Akin, M. (2006). Preventive Maintenance Treatments of Flexible Pavements: A Synthesis of Highway Practice, Report No. FHWA/MT-06-009/ 8117-26, Western Transportation Institute, 36 pp., Oct. 2006.

Eckman, B. (1990). ESSO MOEBIUS Computer Software for Pavement Design Calculations, User's manual. Centre de Recherche ESSO. Mont Saint Aignan. France. June, Vol. 19, pp. 190-198.

Elseifi, M., Al-Qadi, I. L., and Yoo, P. J. (2006). "Viscoelastic modeling and field validation of flexible pavements." Journal of engineering mechanics, 132(2), 172–178.

Eshan, D. (2009). Asphalt Pavement Aging and Temperature Dependent Properties Using Functionally Graded Viscoelastic Model. PhD Dissertation, University of Illinois at Urbana-Champaign.

Federal Highway Administration. (2005). Pilot Program Evaluates Quiet Pavements in Arizona. Focus. FHWA-HRT-05-027, Washington, DC.

Frank, B. (2013). Plant Diagnostic Tool. http://www.pahotmix.org/images/bobfrank.swf [last accessed Jan. 31, 2013].

Francken, L. and Vanelstraete, A. (1992). Interface Systems to Prevent Reflection Cracking, Proceedings of 7th International Conference on Asphalt Pavement, Nottingham, UK, Vol. 1, pp. 45-60.

Gamez, A., Hernandez, J. A., Ozer, H., and Al-Qadi, I. L. (2018). Development of Domain Analysis for Determining Potential Pavement Damage. Journal of Transportation Engineering, Part B: Pavements, 144(3), 04018030.

Geoffroy, D. (1998). Thin-surfaced Pavements: Synthesis of Highway Practice 260. Transportation Research Board, Washington DC.

Hall, K., Connor, J., Darter, M. and Carpenter, S. (1989). Rehabilitation of Concrete Pavements, Vol. 3, Concrete Pavement Evaluation and Rehabilitation System, Publication FHWA-RD-88-073. FHWA, US Department of Transportation.

Hernandez, J. A., Gamez, A., and Al-Qadi, I. L. (2016). Effect of wide-base tires on nationwide flexible pavement systems: Numerical modeling. Transportation Research Record: Journal of the Transportation Research Board, (2590), 104-112.

Joseph, P., Haas, W. A. P.and Rothenburg, L. (1987). Low Temperature Reflection Cracking through Asphalt Overlays. In Proceedings 6th International Conference on Structural Design of Asphalt Pavements, pp. 935-945.

Ozer, H., Al-Qadi, I. L., Singhvi, P., Bausano, J., Carvalho, R., Li, X., & Gibson, N. (2018). Prediction of pavement fatigue cracking at an accelerated testing section using asphalt mixture performance tests. International Journal of Pavement Engineering, 19(3), 264-278.

NCHRP (National Cooperative Highway Research Program) 1-37A. (2007). Mechanistic Empirical Design of New and Rehabilitated Pavement Structures. http://www.trb.org/mepdg/guide.htm.

Jayawickrama, P. and Lytton, R. (1987). Methodology for Predicting Asphalt Concrete Overlay Life Against Reflection Cracking. Proceedings 6th International Conference on Structural Design of Asphalt Pavements, pp. 912-924.

Kandhal, P. S. and Cooley, L. A. (2002). Coarse Versus Fine-Graded Superpave Mixtures: Comparative Evaluation of Resistance to Rutting. NCAT Report 02-02, National Center for Asphalt Technology, Auburn, Alabama.

Keenan, C., Sprung, M., Strocko, E., Schmidt, R.C. and Sedor, J. (2012). Freight Facts and Figures, Report FHWA-HOP-13-001. Federal Highway Administration, Office of Freight Management and Operations, Washington D.C., 2012.

Kim, J. and Buttlar, W.G. (2002). Analysis of Reflective Crack Control System Involving Reinforcing Grid over Base-Isolating Interlayer Mixture. Journal of Transportation Engineering, Vol. 128, pp. 375-384.

Kim, M., Buttlar, W. G., Baek, J. and Al-Qadi, I. L. (2009). Field and Laboratory Evaluation of Fracture Resistance of Illinois Hot-Mix Asphalt Overlay Mixtures. Transportation Research Record: Journal of the Transportation Research Board, No. 2127, Transportation Research Board of the National Academies, Washington, D.C., pp. 146–154.

Labi, S., Lamptey, G., Konduri, S. and Kumares, C. S. (2005). Analysis of Long-Term Effectiveness of Thin Hot-Mix Asphaltic Concrete Overlay Treatments. Transportation Research Record, Journal of the Transportation Research Board, No. 1940, National Research Council, Washington, D. C., pp. 3-12.

Lee, H. J., Park, H. M. and Lee, J. H. (2007). Development of a Simplified Design Procedure for Determining Layer Thickness in Long-Life Pavements. Transportation Research Record, Journal of the Transportation Research Board, No. 2037, National Research Council, Washington, D. C., pp. 76-85.

Luelmo, F. S., Boccaleri, S. R. and Alonzo, L. V. (1971). Flexible Pavements, Spain. Presented at the XIVth World Road Congress, Prague, Czechoslovakia.

McCullough, B. F., and Seeds, S. B. (1982). Field Validation of an Overlay Design Procedure to Prevent Reflection Cracking. Proceedings 5th International Conference on Structural Design of Asphalt Pavements, Vol. I, pp. 780-791.

Newcomb, D. E. (2009). Thin Asphalt Overlays for Pavement Preservation. Information Series 135, National Asphalt Pavement Association.

Owusu-Antwi, E., Khazanovich, L. and Titus-Glover, L. (1998). Mechanistic-Based Model for Predicting Reflective Cracking in Asphalt Concrete-Overlaid Pavements, Transportation Research Record, Journal of the Transportation Research Board, Vol. 1629, pp. 234-241.

Pavement Preservation Journal (2014). Thin Overlays, ADA Guidance.

Parker, R. (1993). Evaluation of Performance and Cost-Effectiveness of Thin-Pavement Surface Treatments, Oregon Department of Transportation, Salem.

Rahman, F., Hossain, M., Romanoschi, S. A. and Hobson, C. (2011). Experience with Thin Superpave Mixture Overlay of Small Aggregate Top Size in Kansas. Transportation Research Record, Journal of the Transportation Research Board, No. 2205, National Research Council, Washington, D. C., pp. 3-10.

Rymer, B. and Donavan, P. (2005). California Tests Show Pavement Selection Influences Noise Levels. Hot Mix Asphalt Technology, National Asphalt Pavement Association.

Sauber, R. W. (2009). Thin Overlays: Pavement Preservation. New Jersey Department of Transportation.

Scullion, T., Zhou, F., Walubita, L. and Sebesta, S. (2009). Design and Performance Evaluation of Very Thin Overlays in Texas. FHWA/TX-09/0-5598-2, Texas Transportation Institute, College Station, Texas.

Shin, H., and Kim, J. B. (2015). Physical Interpretation for Cap Parameters of the Modified Drucker-Prager Cap Model in Relaxation to the Deviator Stress Curve of a Particulate Compact in Conventional Triaxial Testing. Journal of Powder Technology, Vol. 280, pp. 94-102.

Smith, R. E., Darter, M. I., and Lytton, R. L. (1986). Mechanistic overlay design procedures available to the design engineer (No. 1060).

Son, S. and Al-Qadi, I. L. (2014). Engineering Cost-Benefit Analysis of Thin, Durable Asphalt Overlays. Transportation Research Record: Journal of the Transportation Research Board, (2456), 135-145.

Sousa, J., Pais, J., Saim, R., Way, G. and Stubstad, R. (2001). Development of a Mechanistic Overlay Design Method Based on Reflective Cracking Concepts. Final Report for Rubber Pavements Association, Consulpav International.

Thompson, M. R., and Elliott, R. P. (1985). ILLI-PAVE based response algorithms for design of conventional flexible pavements. Transportation Research Record, 1043, 50-57.

Thompson, M. (1996). Mechanistic-empirical flexible pavement design: An overview. Transportation Research Record: Journal of the Transportation Research Board, (1539), 1-5.

USDOT. (2013). Status of the Nation's Highways, Bridges, and Transit: Conditions and Performance: Report to the Congress, U.S. Department of Transportation, Washington D.C., 2014.

Van Gurp, C. and Molenaar, A. (1989). Simplified Method to Predict Reflective Cracking in Asphalt Overlays, in RILEM Conference on Reflective Cracking in Pavements, Leige, Belgium, pp. 190–198.

Walubita, F. L., and Scullion, T. (2008). Thin HMA Overlay in Texas: Mix Design and Laboratory Material Property Characterization. FHWA/TX-08/0-5598-1, Texas Transportation Institute, College Station, Texas, January 2008.

Wang, Y., Wang, G. and Mastin, N. (2012). Cost and Effectiveness of Flexible Pavement Treatments: Experience and Evidence. Journal of Performance of Constructed Facilities, ASCE, Vol. 26, No. 4, 2012.

Watson, D. E., Zhang, J. and Powell, R. B. (2004). Analysis of Temperature Data for the National Center for Asphalt Technology Test Track. Transportation Research Record: Journal of the Transportation Research Board, No. 1891, Transportation Research Board of the National Academies, Washington, D.C.

Watson, D.E., Vargas-Nordcbeck, A., Moore, J. R., Jared, D. and Wu, P. (2008a). Evaluation of the Use of Reclaimed Asphalt Pavement in Stone Matrix Asphalt Mixtures. Transportation Research Record, Journal of the Transportation Research Board, No. 2051, Transportation Research Board of the National Academies, Washington, D.C., pp. 64–70.

Watson, D.E., Moore, J.R., Heartsill, J., Jared, D. and Wu, P. (2008b). Verification of Superpave Number of Design Gyration Compaction Levels for Georgia. Transportation Research Record: Journal of the Transportation Research Board, No. 2057, Transportation Research Board of the National Academies, Washington, D.C., pp. 75–82.

Watson, D., and Heitzman, M. (2014). Thin Asphalt Concrete Overlays: A Synthesis of Highway Practice. NCHRP Synthesis 464, Transportation Research Board, Washington D.

West, R., Rausch, R. and Takahashi, O. (2006). Refinement of Mix Design Criteria for 4.75 mm Superpave Mixes. Proceedings of 10th International Conference on Asphalt Pavements, Quebec City, Canada, International Society for Asphalt Pavements, pp. 161–170.

Wilson, B., Scullion, T. and Estakhri, C. (2012). Design and Construction Recommendations for Thin Overlays in Texas. FHWA/TX-13/0-6615-1, Texas Transportation Institute, College Station, Texas.

Wu, R., Harvey, J. and Monismith, C. (2006). Towards a Mechanistic Model for Reflective Cracking in Asphalt Concrete Overlays. Journal of the Association of Asphalt Paving Technologists, Vol. 75, pp. 491–534.

Xie, H., Cooley, L. A., and Huner, M. H. (2005). 4.75 mm NMAS Stone Matrix Asphalt (SMA) Mixtures. NCAT Report 03-05. National Center for Asphalt Technology, Auburn University, Alabama.

Yoo, P. J., Al-Qadi, I. L., Elsefi, M. A. and Janajreh, I. (2006). Flexible Pavement Responses to Different Loading Amplitudes Considering Layer Interface Condition and Lateral Shear Forces. International Journal of Pavement Engineering, Vol. 7, No. 1, pp. 73-86.

Zhu, D., and Jia, X. (2011). Analysis and Simulation of Interlayer Damages in Asphalt Pavement Overlay Cement Concrete Slab. Geotechnical Special Publications, American Society of Civil Engineers, Vol. 212, pp. 192-199.

Zhou, F., Hu, S., Hu, X. and Scullion, T. (2009). Mechanistic-Empirical Asphalt Overlay Thickness Design and Analysis System. FHWA/TX-09/0-5123-3, Texas Transportation Institute, College Station, Texas, October.
Zimmerman, K. A. (1995). Pavement management methodologies to select projects and recommend preservation treatments (Vol. 222). Transportation Research Board.
Zubeck, H., Mullin, A. and Liu, J. (2012). Survey on Pavement Preservation Treatments in Cold Regions. Swedish National Road and Transport Research Institute, VTI, Linkoeping, Sweden.

APPENDIX A: SUMMARY OF MIXES USED

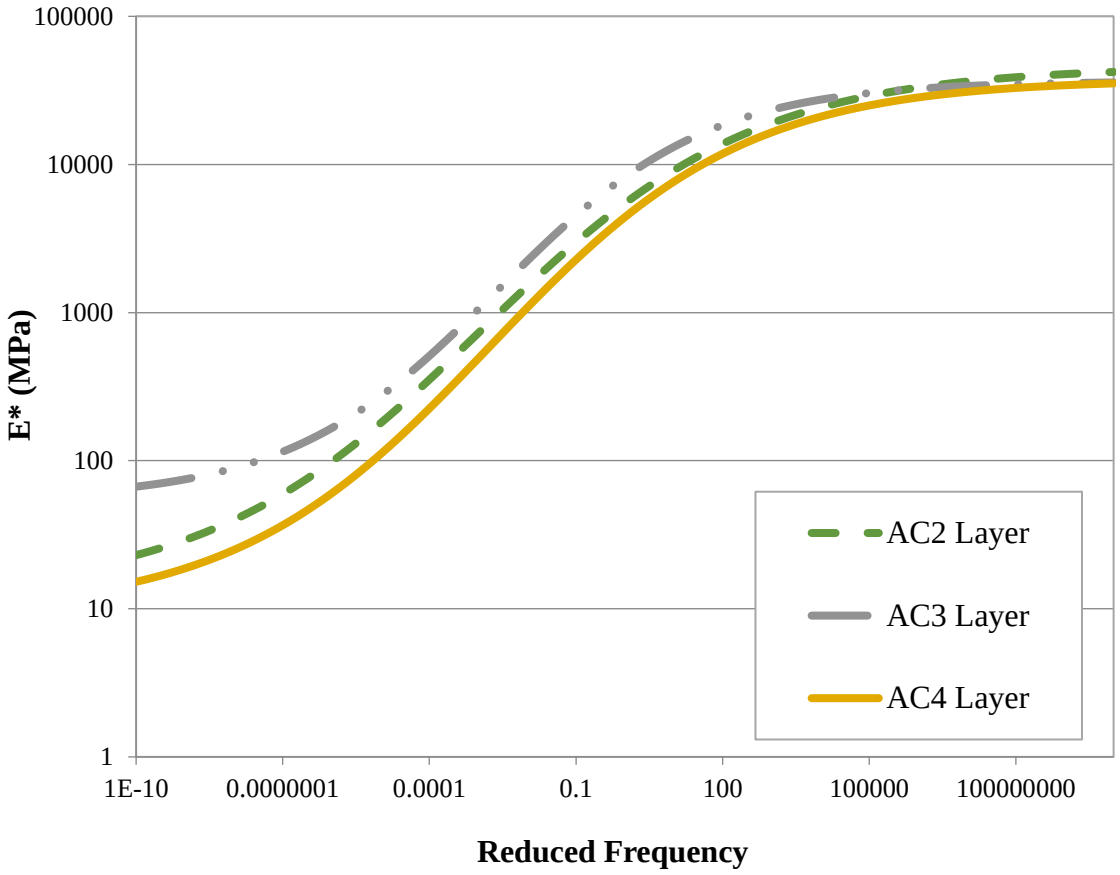

Figure 0-1 Curves for the AC layers below thin AC overlay.

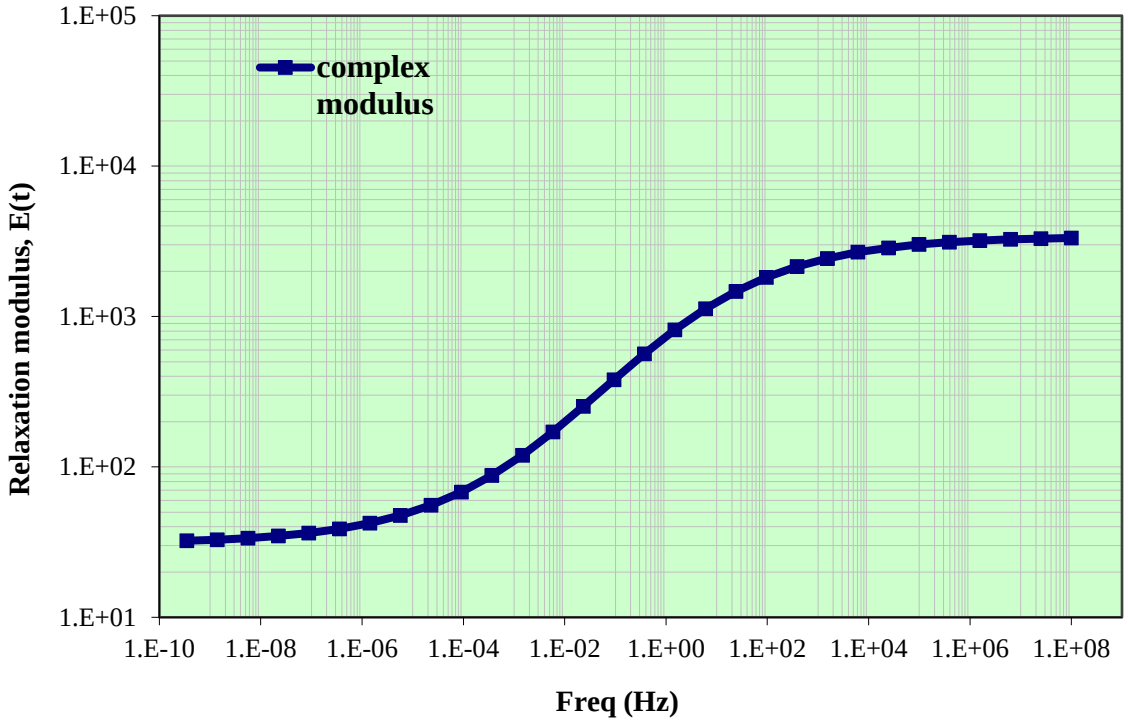

Figure 0-2 Master curve for the R27-42 AC mix type.

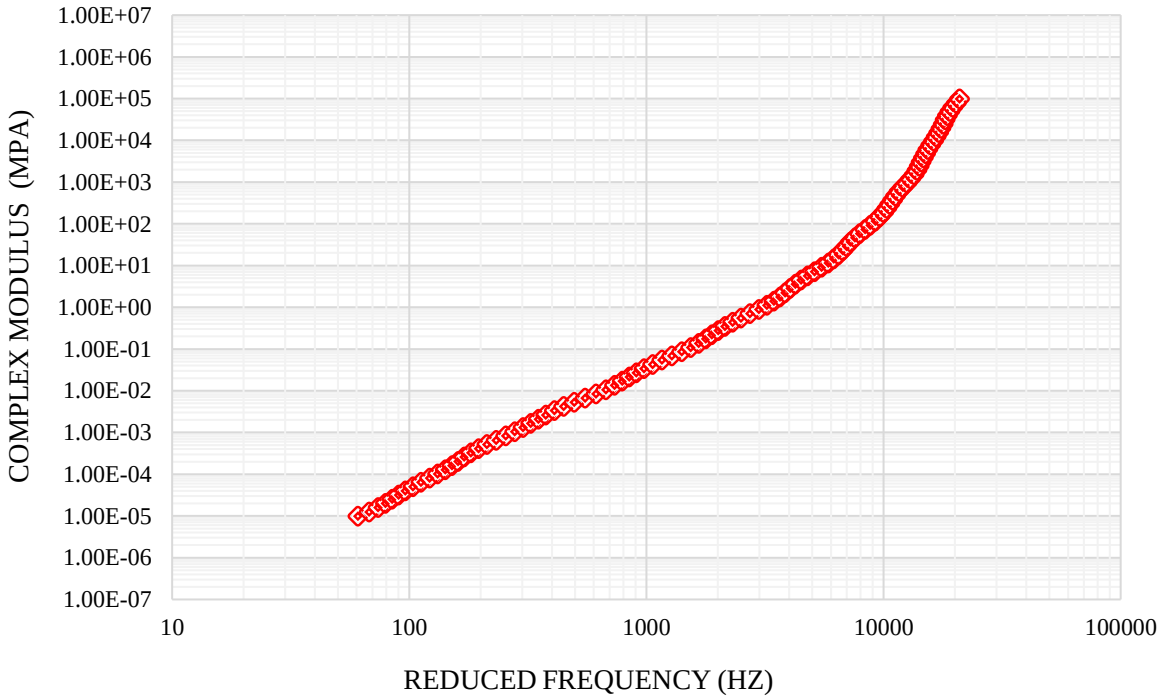

Figure 0-3 Master curve for ALF (Lane 3) AC mix type.

APPENDIX B: PATH ANALYSIS RESULTS FOR 3D PAVEMENT FE MODELS

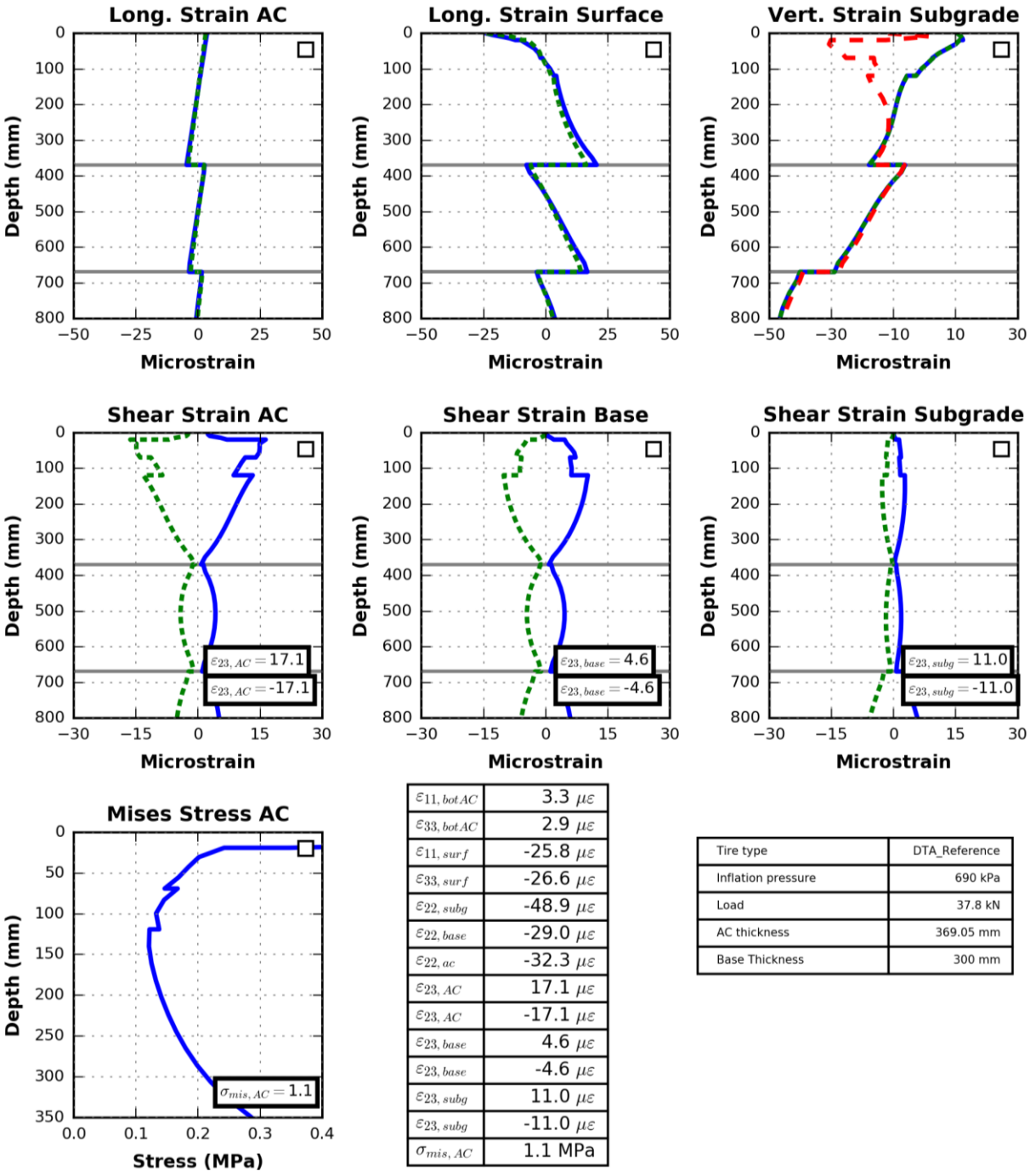

$\varepsilon_{11,botAC}$	3.3 $\mu\varepsilon$
$\varepsilon_{33,botAC}$	2.9 $\mu\varepsilon$
$\varepsilon_{11,surf}$	-25.8 $\mu\varepsilon$
$\varepsilon_{33,surf}$	-26.6 $\mu\varepsilon$
$\varepsilon_{22,subg}$	-48.9 $\mu\varepsilon$
$\varepsilon_{22,base}$	-29.0 $\mu\varepsilon$
$\varepsilon_{22,ac}$	-32.3 $\mu\varepsilon$
$\varepsilon_{23,AC}$	17.1 $\mu\varepsilon$
$\varepsilon_{23,AC}$	-17.1 $\mu\varepsilon$
$\varepsilon_{23,base}$	4.6 $\mu\varepsilon$
$\varepsilon_{23,base}$	-4.6 $\mu\varepsilon$
$\varepsilon_{23,subg}$	11.0 $\mu\varepsilon$
$\varepsilon_{23,subg}$	-11.0 $\mu\varepsilon$
$\sigma_{mis,AC}$	1.1 MPa

Tire type	DTA_Reference
Inflation pressure	690 kPa
Load	37.8 kN
AC thickness	369.05 mm
Base Thickness	300 mm

Figure B-1 Mix: R 27-42, Case: 0.75 in overlay thickness.

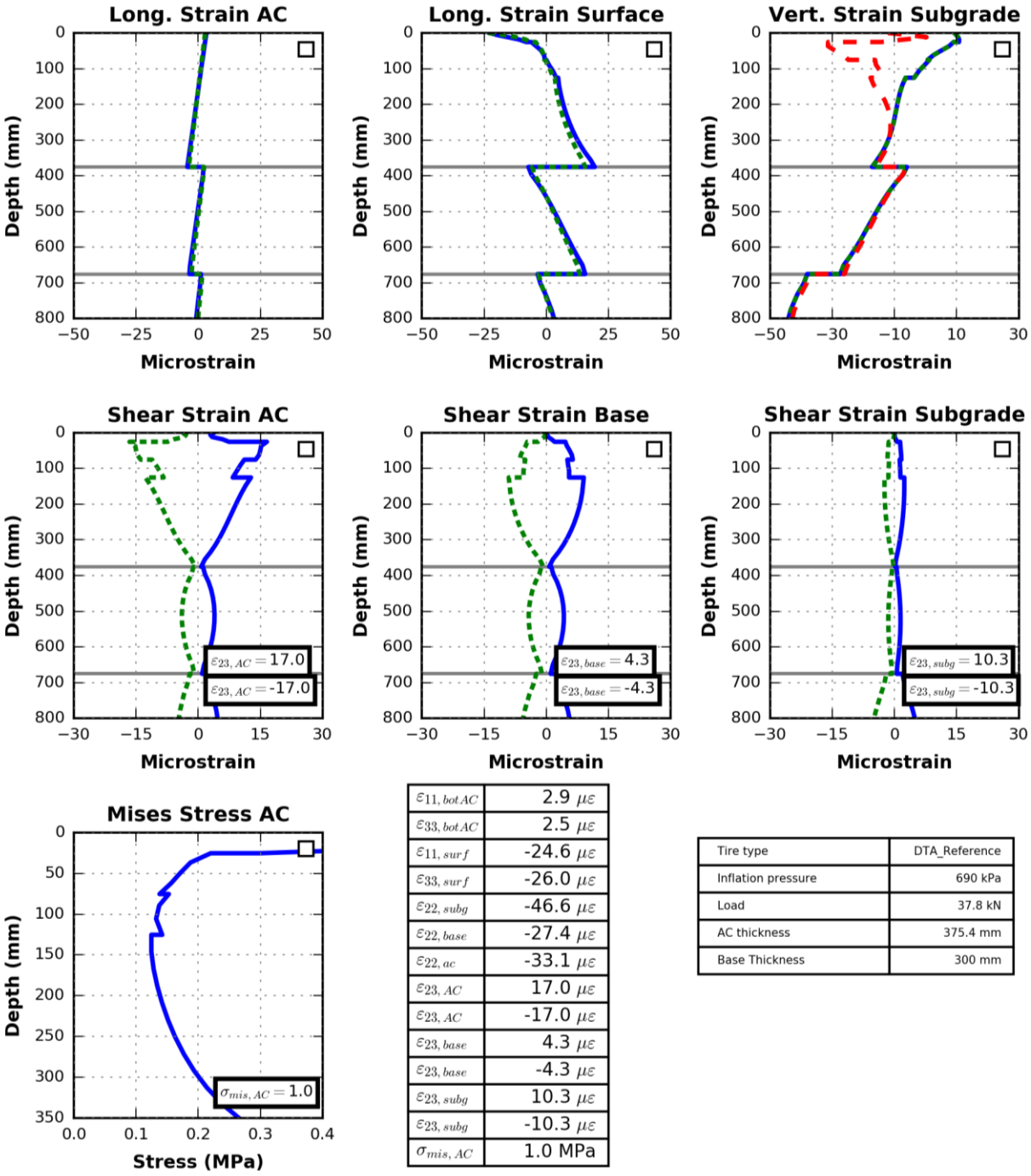

$\varepsilon_{11,botAC}$	2.9 $\mu\varepsilon$
$\varepsilon_{33,botAC}$	2.5 $\mu\varepsilon$
$\varepsilon_{11,surf}$	-24.6 $\mu\varepsilon$
$\varepsilon_{33,surf}$	-26.0 $\mu\varepsilon$
$\varepsilon_{22,subg}$	-46.6 $\mu\varepsilon$
$\varepsilon_{22,base}$	-27.4 $\mu\varepsilon$
$\varepsilon_{22,ac}$	-33.1 $\mu\varepsilon$
$\varepsilon_{23,AC}$	17.0 $\mu\varepsilon$
$\varepsilon_{23,AC}$	-17.0 $\mu\varepsilon$
$\varepsilon_{23,base}$	4.3 $\mu\varepsilon$
$\varepsilon_{23,base}$	-4.3 $\mu\varepsilon$
$\varepsilon_{23,subg}$	10.3 $\mu\varepsilon$
$\varepsilon_{23,subg}$	-10.3 $\mu\varepsilon$
$\sigma_{mis,AC}$	1.0 MPa

Tire type	DTA_Reference
Inflation pressure	690 kPa
Load	37.8 kN
AC thickness	375.4 mm
Base Thickness	300 mm

Figure B-2 Mix: R 27-42, Case: 1.0 in overlay thickness.

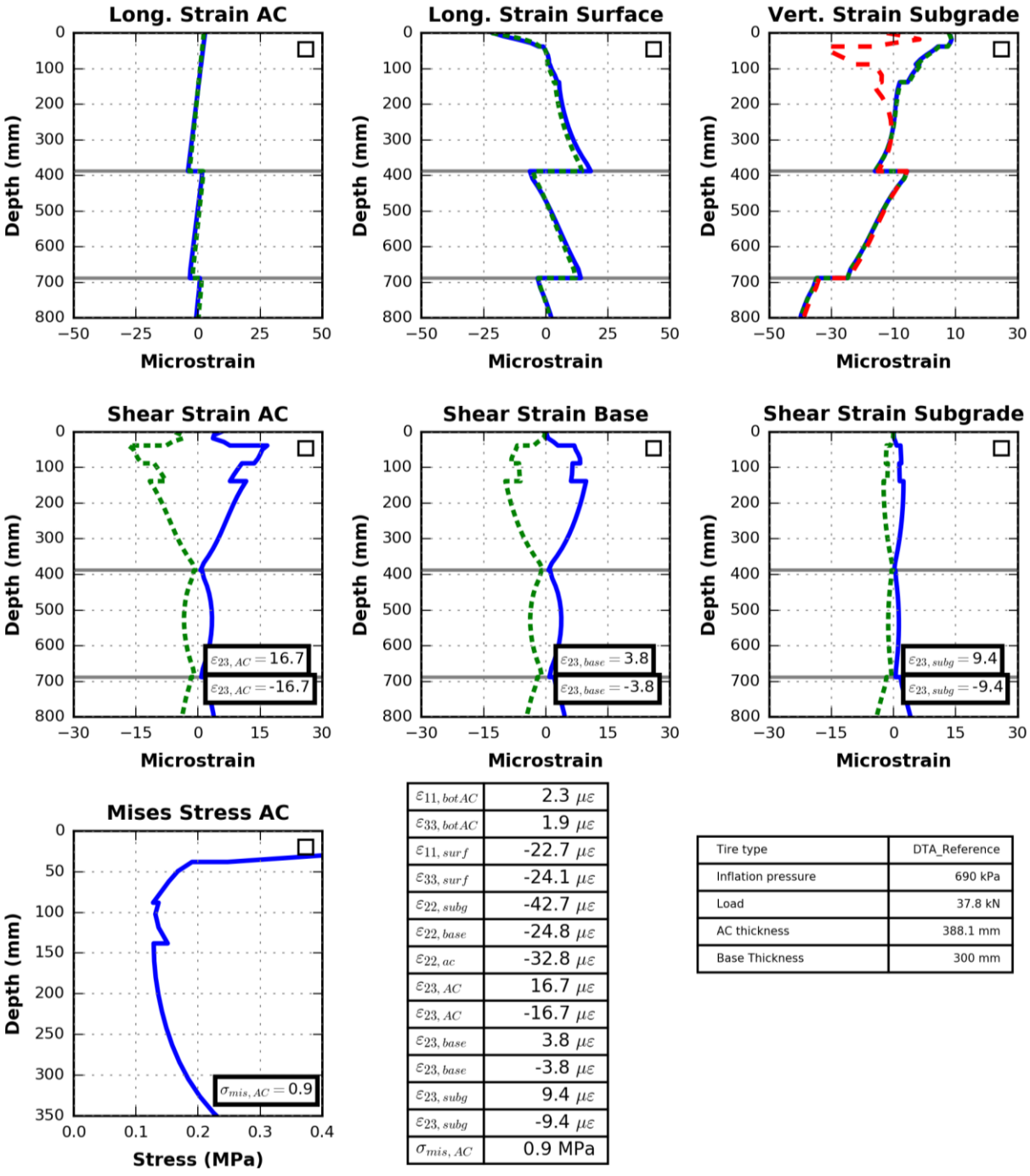

$\varepsilon_{11,botAC}$	2.3 $\mu\varepsilon$
$\varepsilon_{33,botAC}$	1.9 $\mu\varepsilon$
$\varepsilon_{11,surf}$	-22.7 $\mu\varepsilon$
$\varepsilon_{33,surf}$	-24.1 $\mu\varepsilon$
$\varepsilon_{22,subg}$	-42.7 $\mu\varepsilon$
$\varepsilon_{22,base}$	-24.8 $\mu\varepsilon$
$\varepsilon_{22,ac}$	-32.8 $\mu\varepsilon$
$\varepsilon_{23,AC}$	16.7 $\mu\varepsilon$
$\varepsilon_{23,AC}$	-16.7 $\mu\varepsilon$
$\varepsilon_{23,base}$	3.8 $\mu\varepsilon$
$\varepsilon_{23,base}$	-3.8 $\mu\varepsilon$
$\varepsilon_{23,subg}$	9.4 $\mu\varepsilon$
$\varepsilon_{23,subg}$	-9.4 $\mu\varepsilon$
$\sigma_{mis,AC}$	0.9 MPa

Tire type	DTA_Reference
Inflation pressure	690 kPa
Load	37.8 kN
AC thickness	388.1 mm
Base Thickness	300 mm

Figure B-03 Mix: R 27-42, Case: 15.0 in overlay thickness.

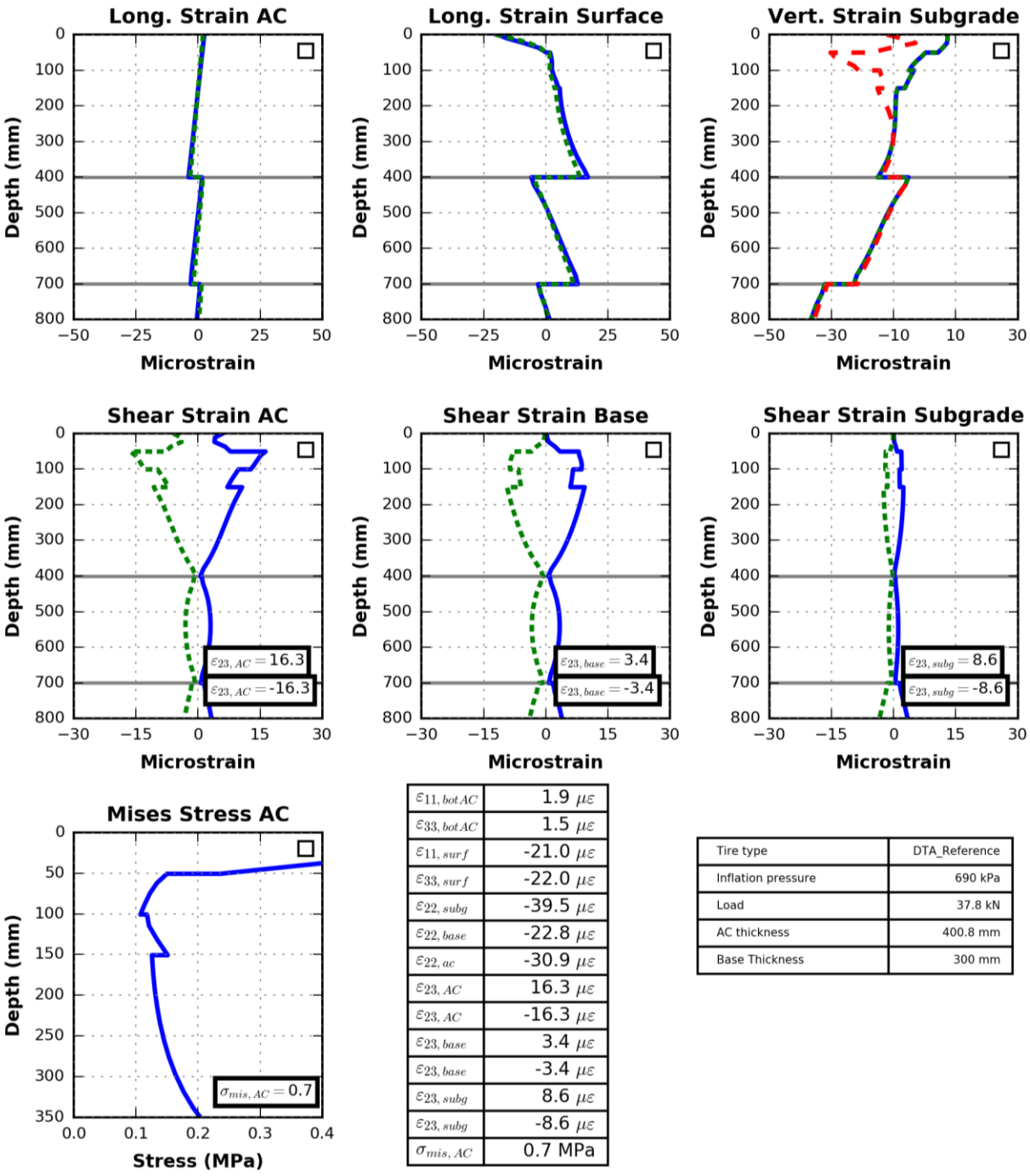

$\varepsilon_{11,botAC}$	1.9 $\mu\varepsilon$
$\varepsilon_{33,botAC}$	1.5 $\mu\varepsilon$
$\varepsilon_{11,surf}$	-21.0 $\mu\varepsilon$
$\varepsilon_{33,surf}$	-22.0 $\mu\varepsilon$
$\varepsilon_{22,subg}$	-39.5 $\mu\varepsilon$
$\varepsilon_{22,base}$	-22.8 $\mu\varepsilon$
$\varepsilon_{22,ac}$	-30.9 $\mu\varepsilon$
$\varepsilon_{23,AC}$	16.3 $\mu\varepsilon$
$\varepsilon_{23,AC}$	-16.3 $\mu\varepsilon$
$\varepsilon_{23,base}$	3.4 $\mu\varepsilon$
$\varepsilon_{23,base}$	-3.4 $\mu\varepsilon$
$\varepsilon_{23,subg}$	8.6 $\mu\varepsilon$
$\varepsilon_{23,subg}$	-8.6 $\mu\varepsilon$
$\sigma_{mis,AC}$	0.7 MPa

Tire type	DTA_Reference
Inflation pressure	690 kPa
Load	37.8 kN
AC thickness	400.8 mm
Base Thickness	300 mm

Figure B-4 Mix: R 27-42, Case: 2.0 in overlay thickness.

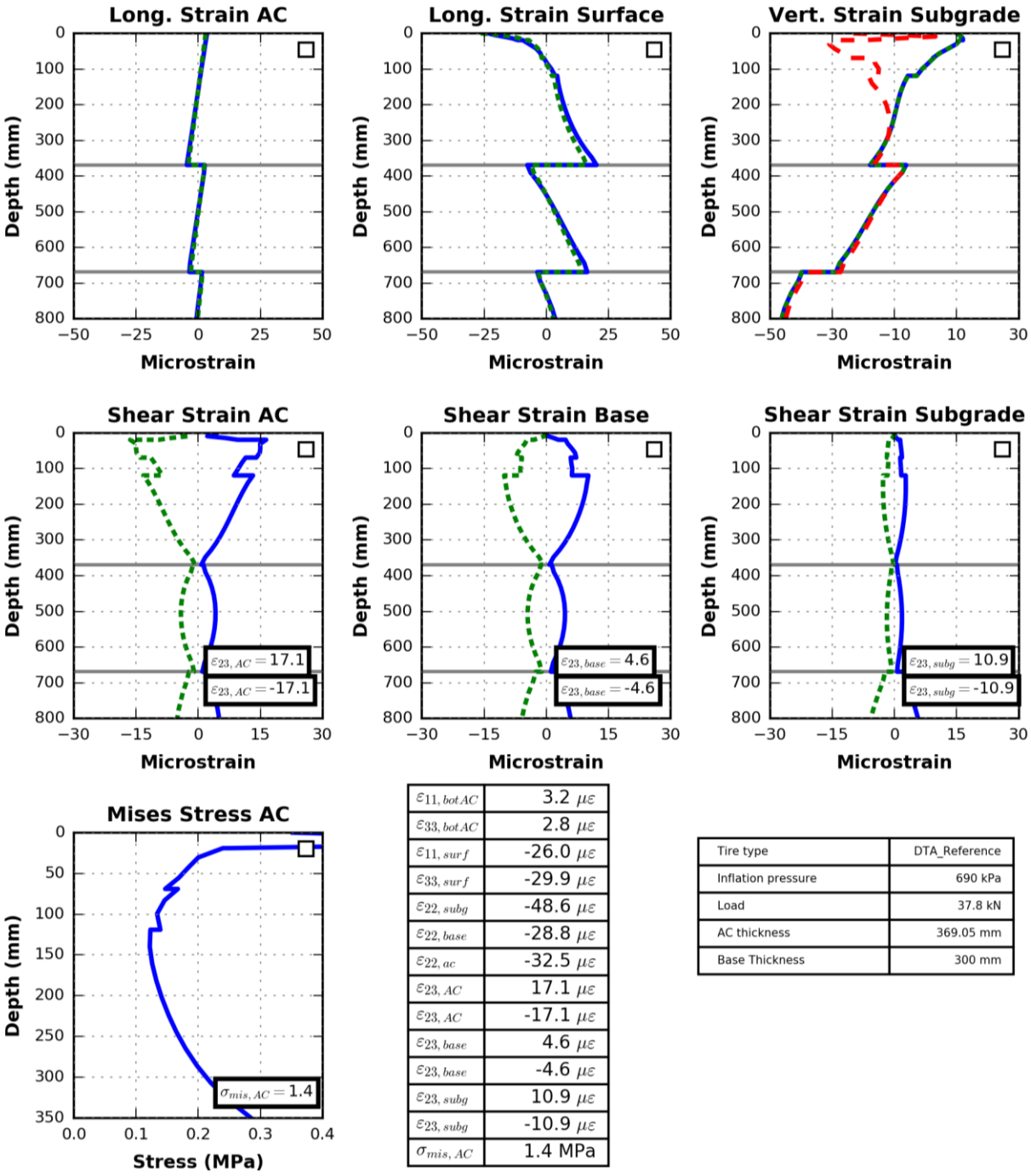

$\varepsilon_{11,botAC}$	3.2 $\mu\varepsilon$
$\varepsilon_{33,botAC}$	2.8 $\mu\varepsilon$
$\varepsilon_{11,surf}$	-26.0 $\mu\varepsilon$
$\varepsilon_{33,surf}$	-29.9 $\mu\varepsilon$
$\varepsilon_{22,subg}$	-48.6 $\mu\varepsilon$
$\varepsilon_{22,base}$	-28.8 $\mu\varepsilon$
$\varepsilon_{22,ac}$	-32.5 $\mu\varepsilon$
$\varepsilon_{23,AC}$	17.1 $\mu\varepsilon$
$\varepsilon_{23,AC}$	-17.1 $\mu\varepsilon$
$\varepsilon_{23,base}$	4.6 $\mu\varepsilon$
$\varepsilon_{23,base}$	-4.6 $\mu\varepsilon$
$\varepsilon_{23,subg}$	10.9 $\mu\varepsilon$
$\varepsilon_{23,subg}$	-10.9 $\mu\varepsilon$
$\sigma_{mis,AC}$	1.4 MPa

Tire type	DTA_Reference
Inflation pressure	690 kPa
Load	37.8 kN
AC thickness	369.05 mm
Base Thickness	300 mm

Figure B-05 Mix: ALF Lane 3, Case: 0.75 in overlay thickness.

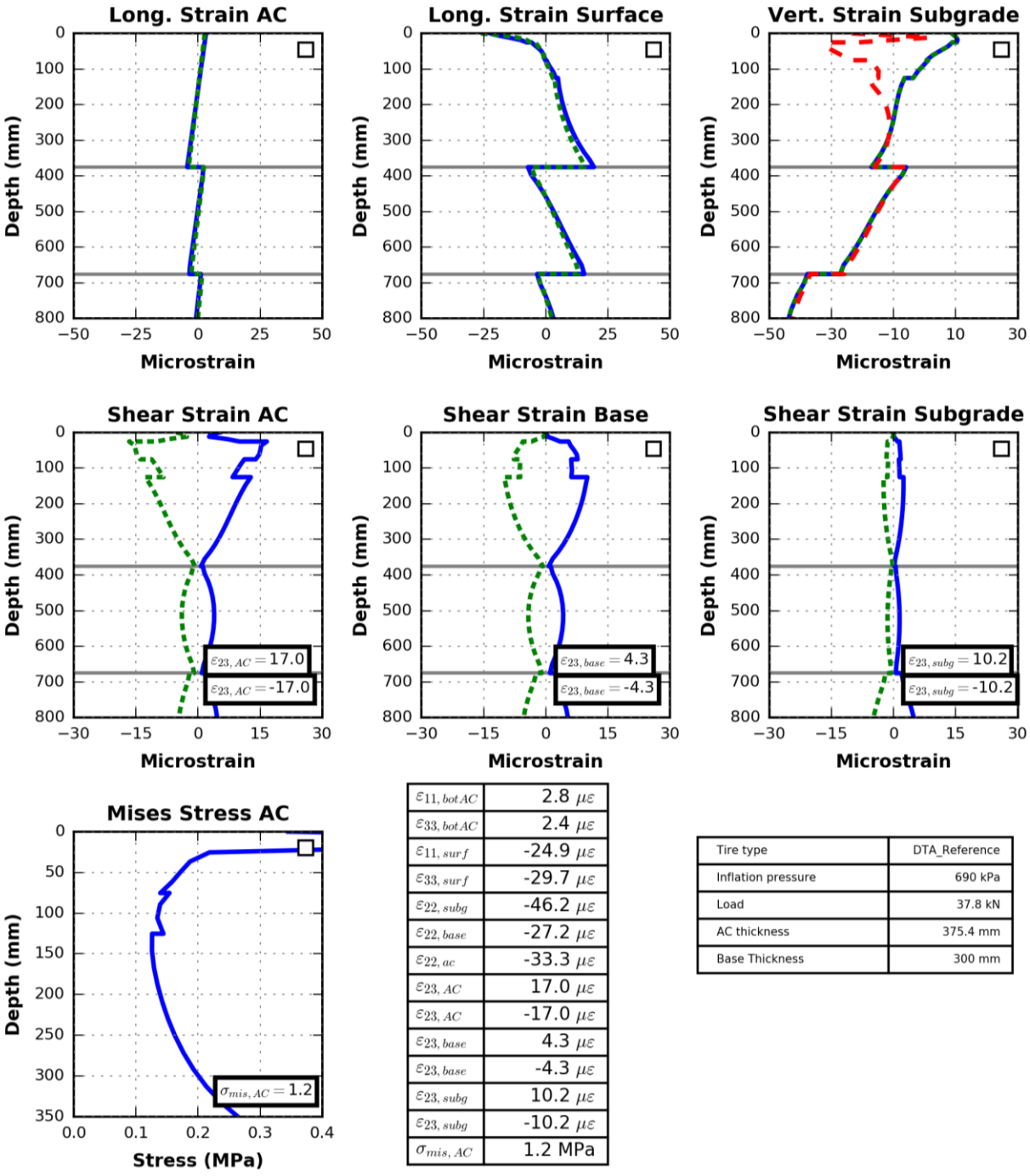

$\varepsilon_{11,botAC}$	2.8 $\mu\varepsilon$
$\varepsilon_{33,botAC}$	2.4 $\mu\varepsilon$
$\varepsilon_{11,surf}$	-24.9 $\mu\varepsilon$
$\varepsilon_{33,surf}$	-29.7 $\mu\varepsilon$
$\varepsilon_{22,subg}$	-46.2 $\mu\varepsilon$
$\varepsilon_{22,base}$	-27.2 $\mu\varepsilon$
$\varepsilon_{22,ac}$	-33.3 $\mu\varepsilon$
$\varepsilon_{23,AC}$	17.0 $\mu\varepsilon$
$\varepsilon_{23,AC}$	-17.0 $\mu\varepsilon$
$\varepsilon_{23,base}$	4.3 $\mu\varepsilon$
$\varepsilon_{23,base}$	-4.3 $\mu\varepsilon$
$\varepsilon_{23,subg}$	10.2 $\mu\varepsilon$
$\varepsilon_{23,subg}$	-10.2 $\mu\varepsilon$
$\sigma_{mis,AC}$	1.2 MPa

Tire type	DTA_Reference
Inflation pressure	690 kPa
Load	37.8 kN
AC thickness	375.4 mm
Base Thickness	300 mm

Figure 0-6 Mix: ALF Lane 3, Case: 1.0 in overlay thickness.

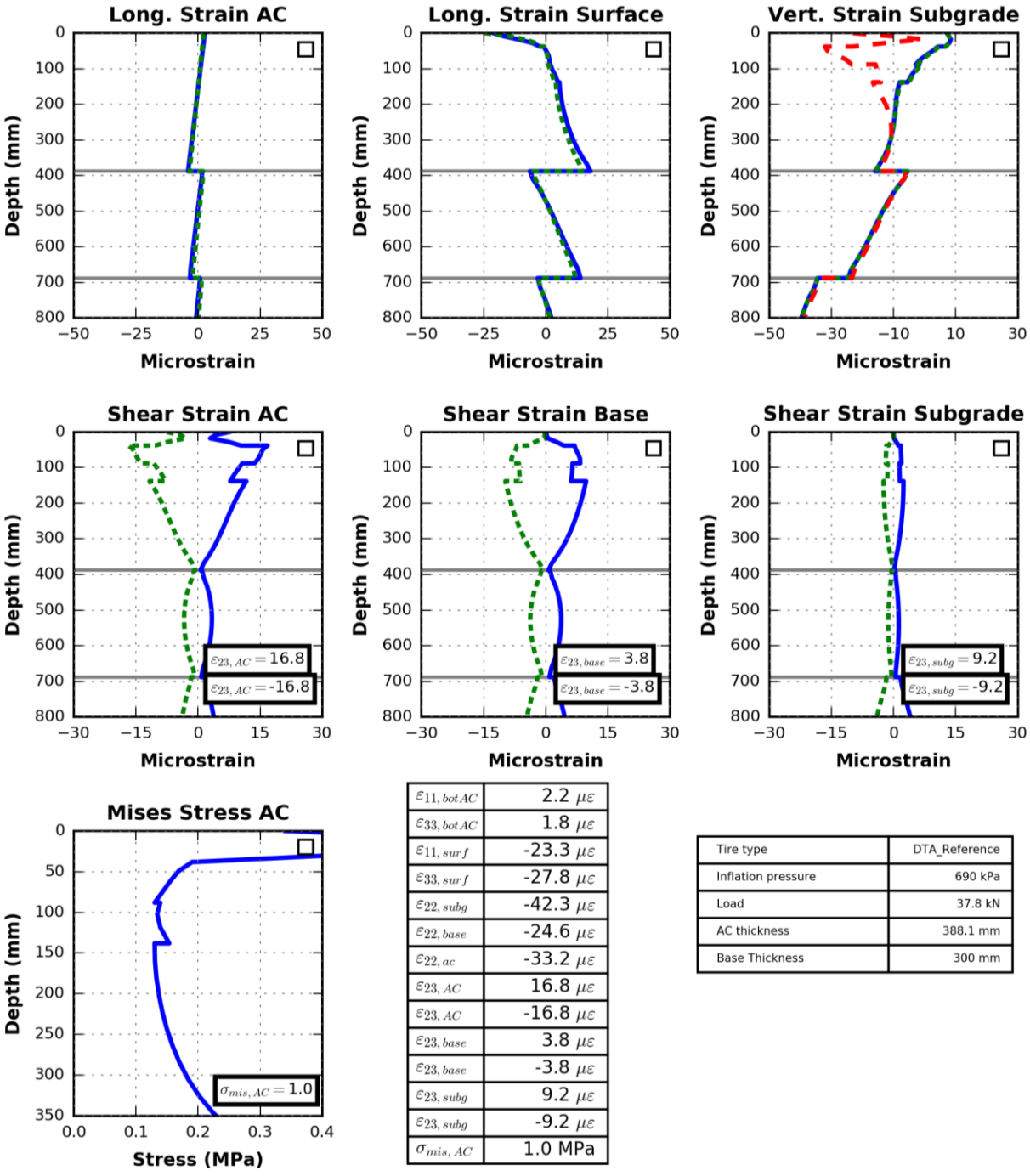

$\varepsilon_{11,botAC}$	2.2 $\mu\varepsilon$
$\varepsilon_{33,botAC}$	1.8 $\mu\varepsilon$
$\varepsilon_{11,surf}$	-23.3 $\mu\varepsilon$
$\varepsilon_{33,surf}$	-27.8 $\mu\varepsilon$
$\varepsilon_{22,subg}$	-42.3 $\mu\varepsilon$
$\varepsilon_{22,base}$	-24.6 $\mu\varepsilon$
$\varepsilon_{22,ac}$	-33.2 $\mu\varepsilon$
$\varepsilon_{23,AC}$	16.8 $\mu\varepsilon$
$\varepsilon_{23,AC}$	-16.8 $\mu\varepsilon$
$\varepsilon_{23,base}$	3.8 $\mu\varepsilon$
$\varepsilon_{23,base}$	-3.8 $\mu\varepsilon$
$\varepsilon_{23,subg}$	9.2 $\mu\varepsilon$
$\varepsilon_{23,subg}$	-9.2 $\mu\varepsilon$
$\sigma_{mis,AC}$	1.0 MPa

Tire type	DTA_Reference
Inflation pressure	690 kPa
Load	37.8 kN
AC thickness	388.1 mm
Base Thickness	300 mm

Figure 0-7 Mix: ALF Lane 3, Case: 15.0 in overlay thickness.

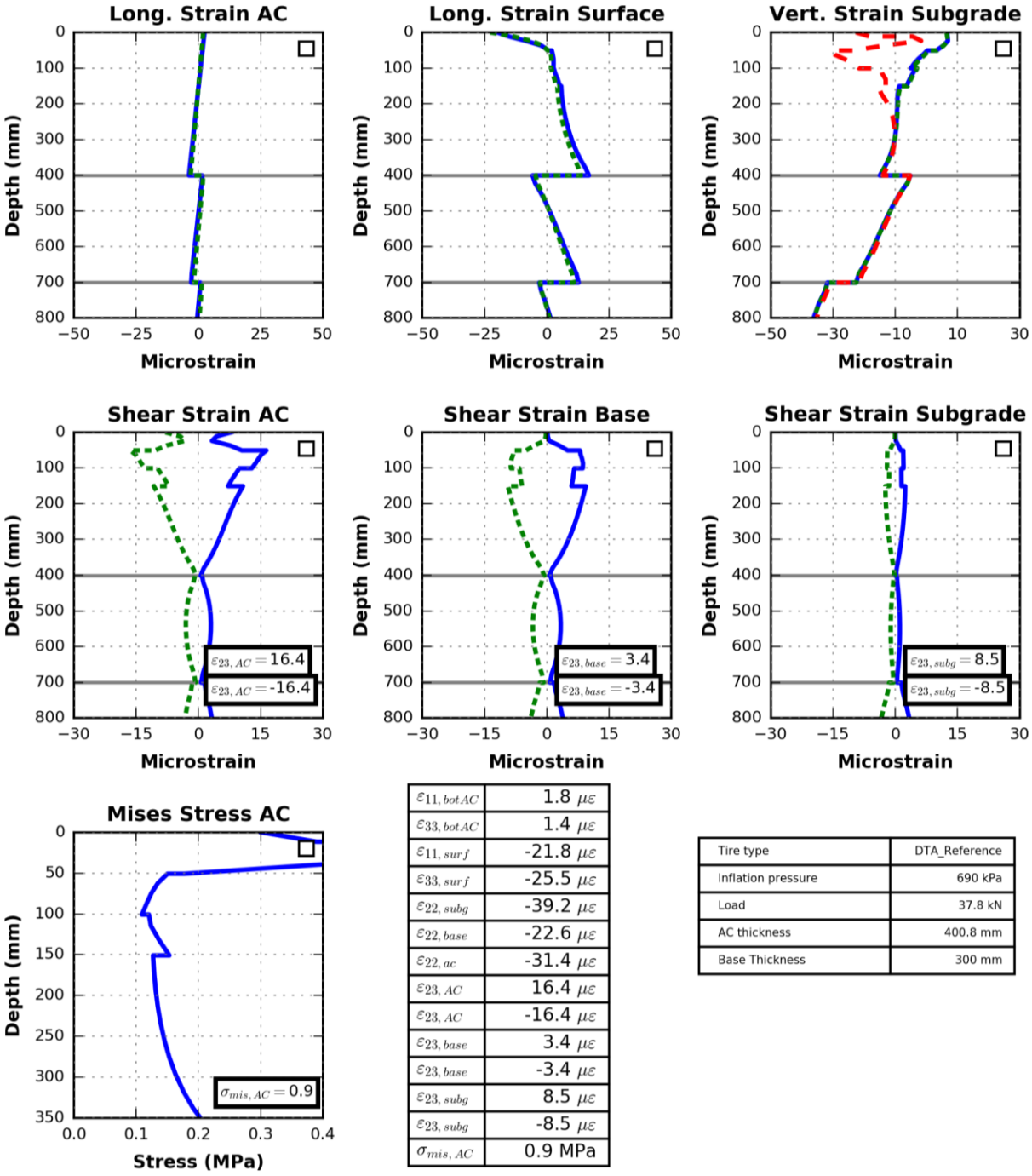

$\varepsilon_{11,botAC}$	1.8 $\mu\varepsilon$
$\varepsilon_{33,botAC}$	1.4 $\mu\varepsilon$
$\varepsilon_{11,surf}$	-21.8 $\mu\varepsilon$
$\varepsilon_{33,surf}$	-25.5 $\mu\varepsilon$
$\varepsilon_{22,subg}$	-39.2 $\mu\varepsilon$
$\varepsilon_{22,base}$	-22.6 $\mu\varepsilon$
$\varepsilon_{22,ac}$	-31.4 $\mu\varepsilon$
$\varepsilon_{23,AC}$	16.4 $\mu\varepsilon$
$\varepsilon_{23,AC}$	-16.4 $\mu\varepsilon$
$\varepsilon_{23,base}$	3.4 $\mu\varepsilon$
$\varepsilon_{23,base}$	-3.4 $\mu\varepsilon$
$\varepsilon_{23,subg}$	8.5 $\mu\varepsilon$
$\varepsilon_{23,subg}$	-8.5 $\mu\varepsilon$
$\sigma_{mis,AC}$	0.9 MPa

Tire type	DTA_Reference
Inflation pressure	690 kPa
Load	37.8 kN
AC thickness	400.8 mm
Base Thickness	300 mm

Figure B-08 Mix: ALF Lane 3, Case: 2.0 in overlay thickness.

APPENDIX C: PAVEMENT DOMAIN ANALYSIS RESULTS (STRAINS) USING 3D FE MODELS

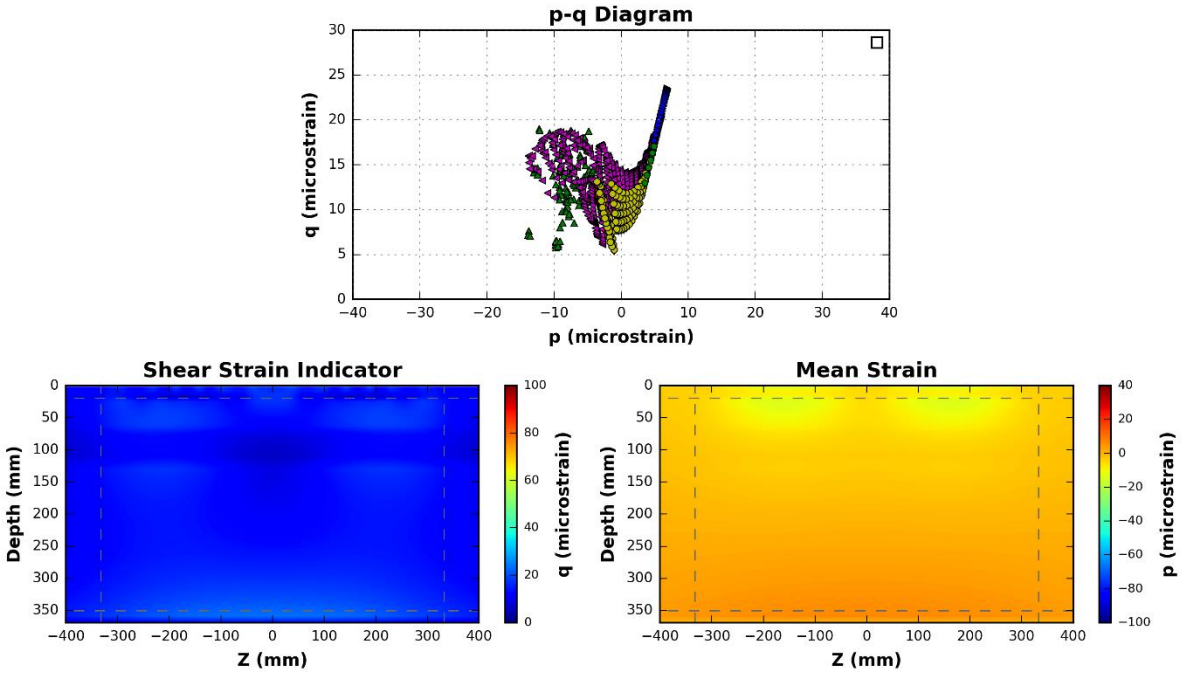

Figure 0-1 Mix: R 27-42, Case: 0.75 in overlay thickness.

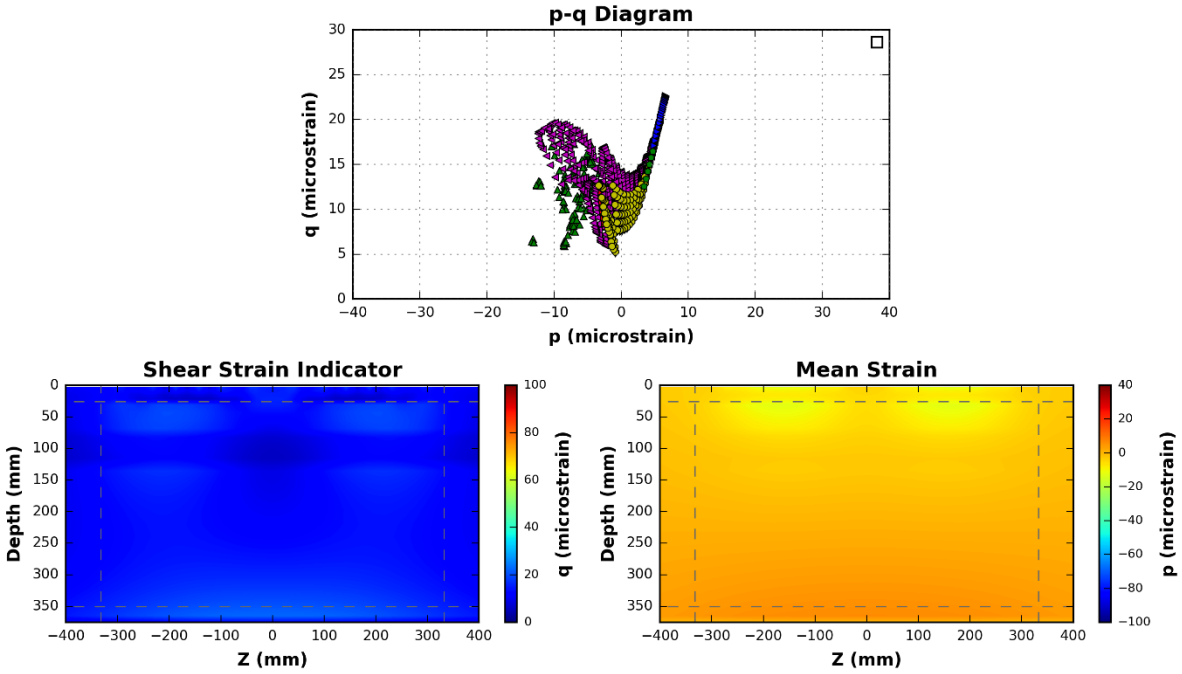

Figure 0-2 Mix: R 27-42, Case: 1.0 in overlay thickness.

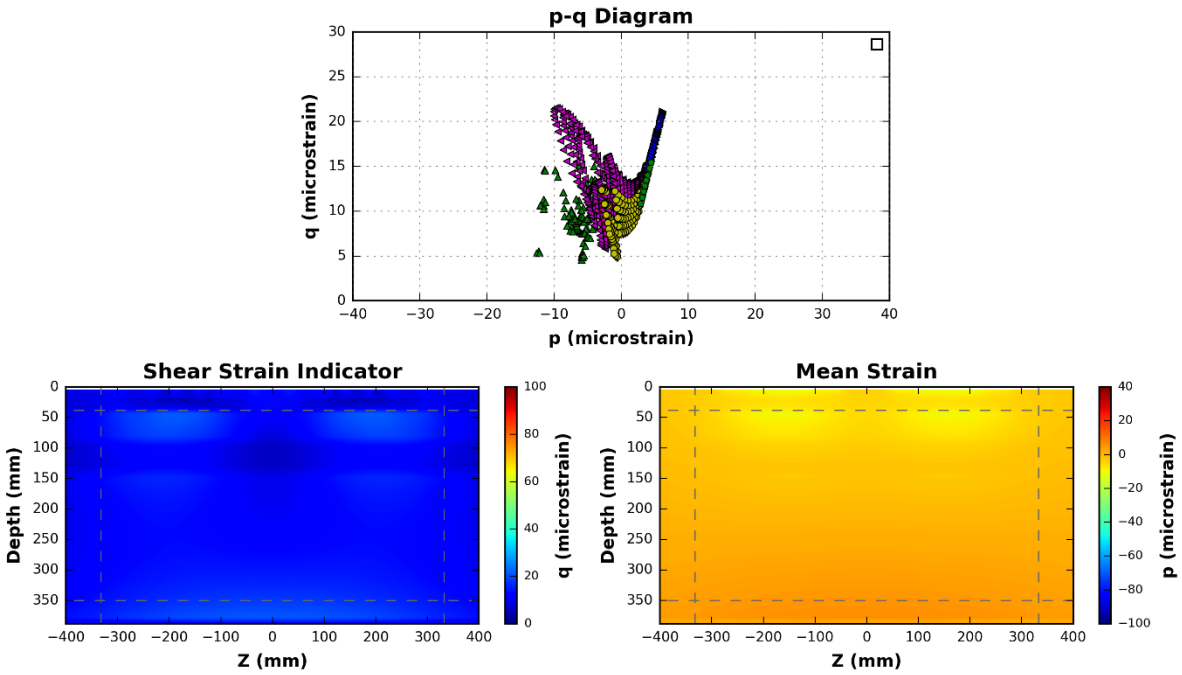

Figure 0-3 Mix: R 27-42, Case: 15.0 in overlay thickness.

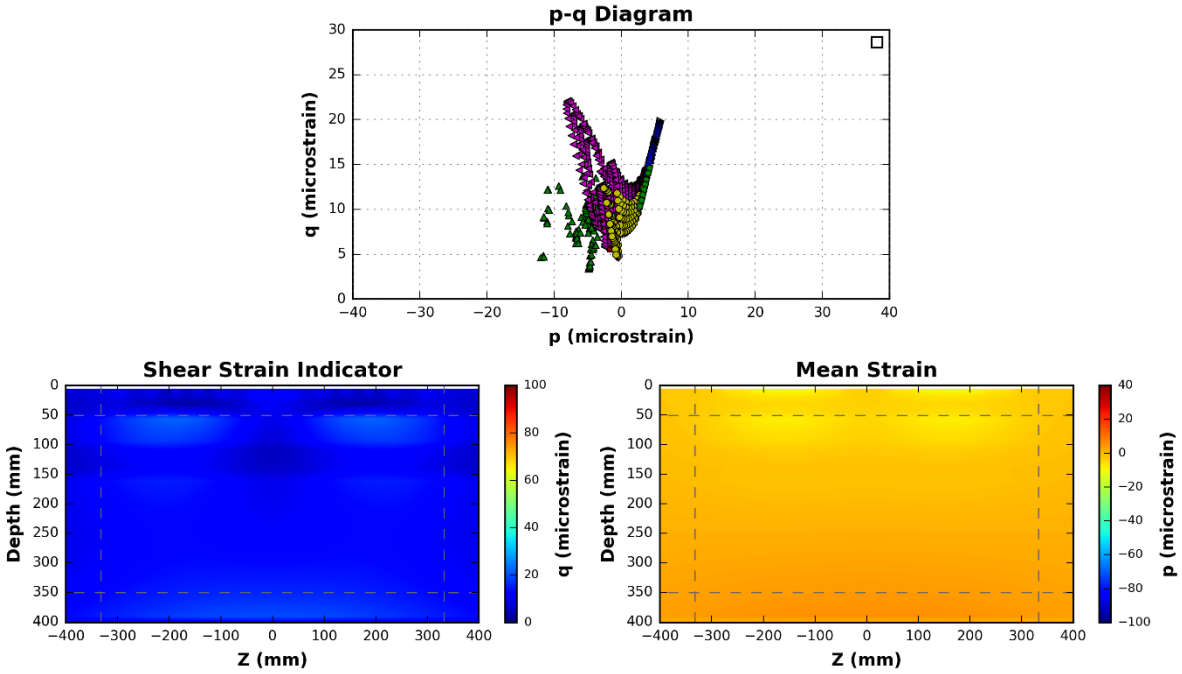

Figure 0-4 Mix: R 27-42, Case: 2.0 in overlay thickness.

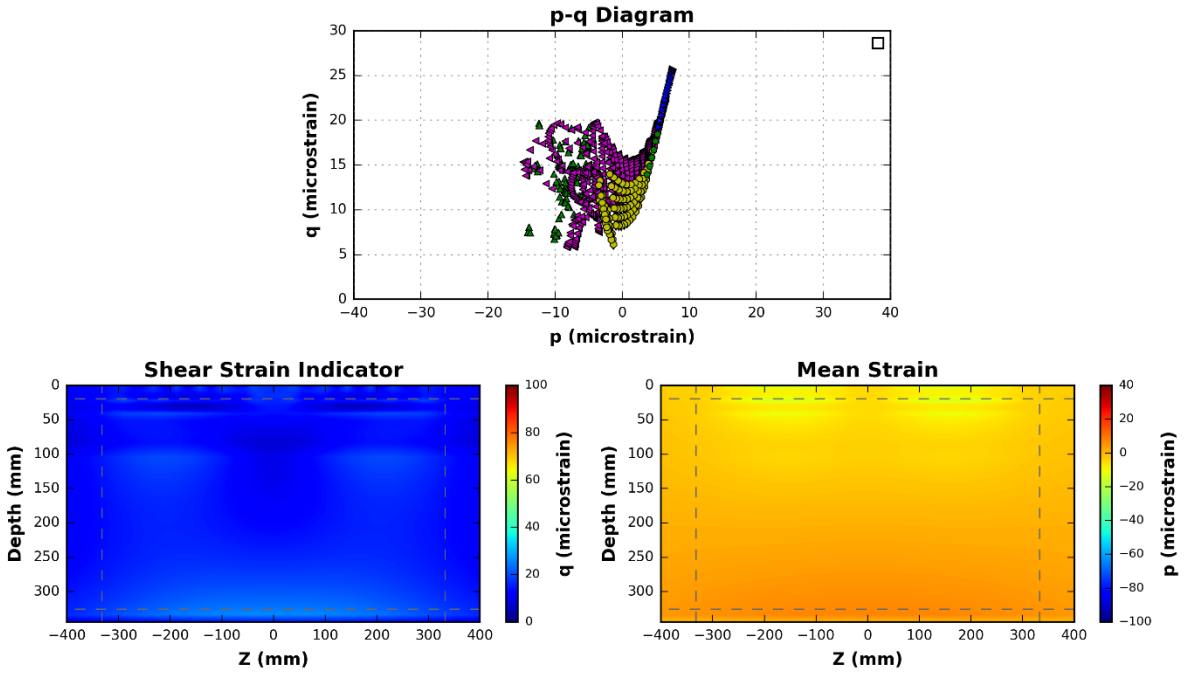

Figure 0-5 Mix: R 27-42, Case: 0.75 in overlay thickness (with a reduced thickness of the AC section).

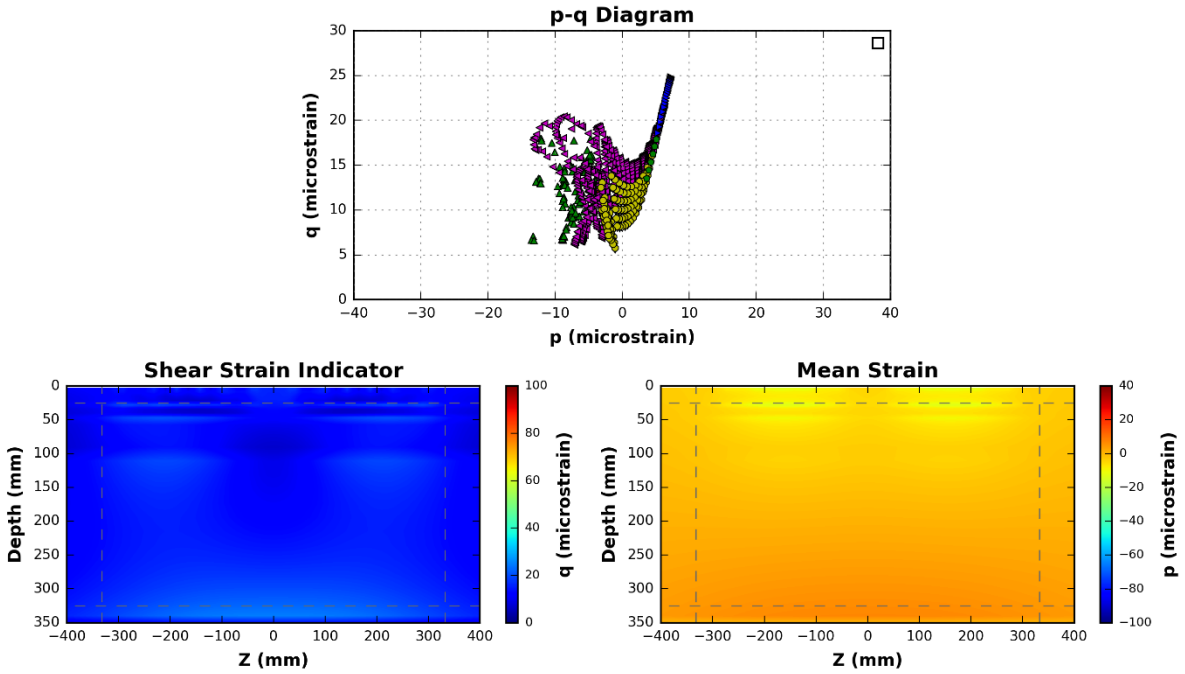

Figure C-6 Mix: R 27-42, Case: 1.0 in overlay thickness (with a reduced thickness of the AC section).

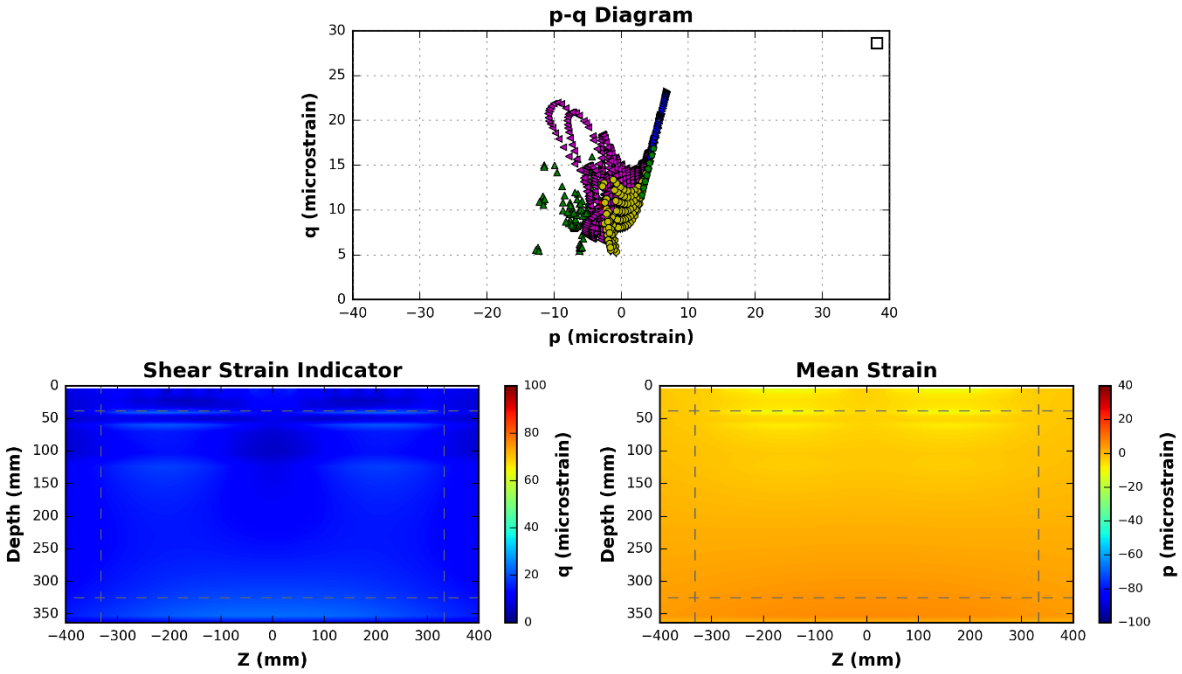

Figure C-07 Mix: R 27-42, Case: 15.0 in overlay thickness (with a reduced thickness of the AC section).

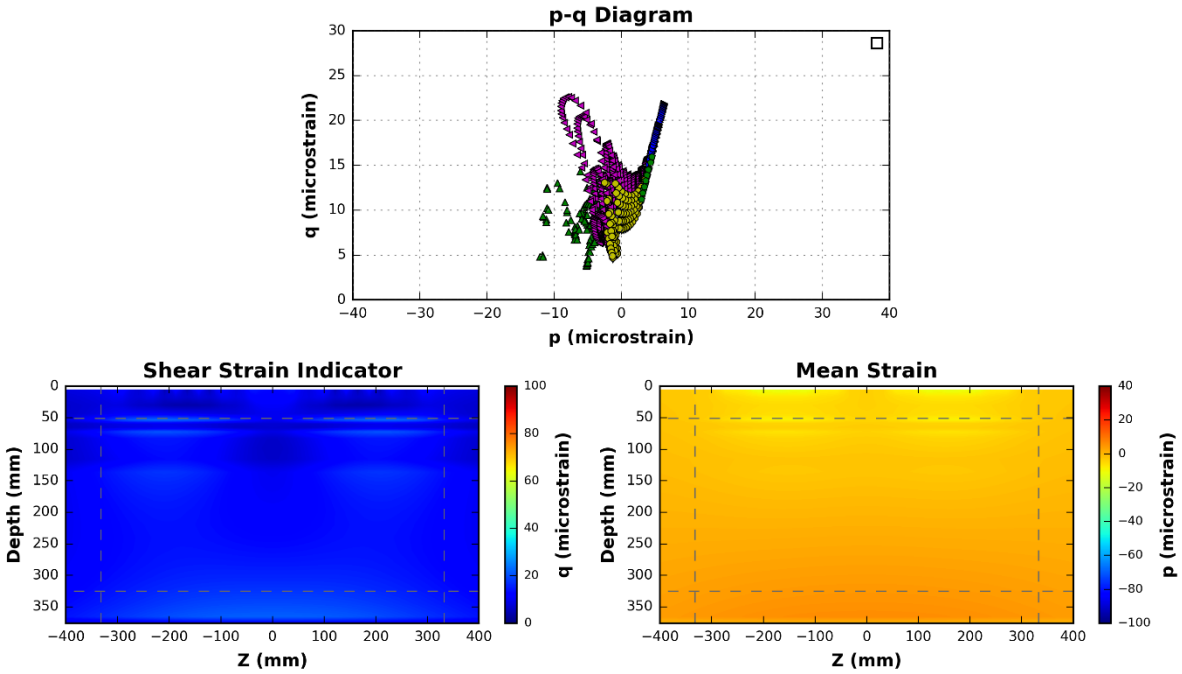

Figure C-8 Mix: R 27-42, Case: 2.0 in overlay thickness (with a reduced thickness of the AC section).

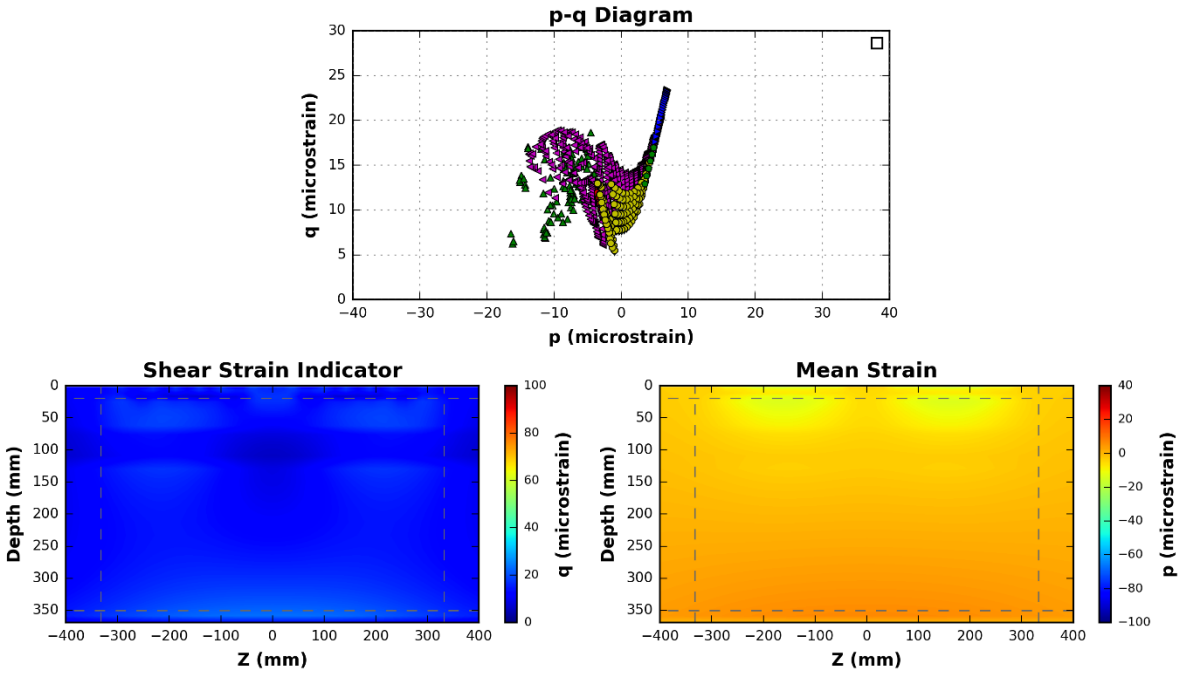

Figure C-9 . Mix: ALF Lane 3, Case: 0.75 in overlay thickness.

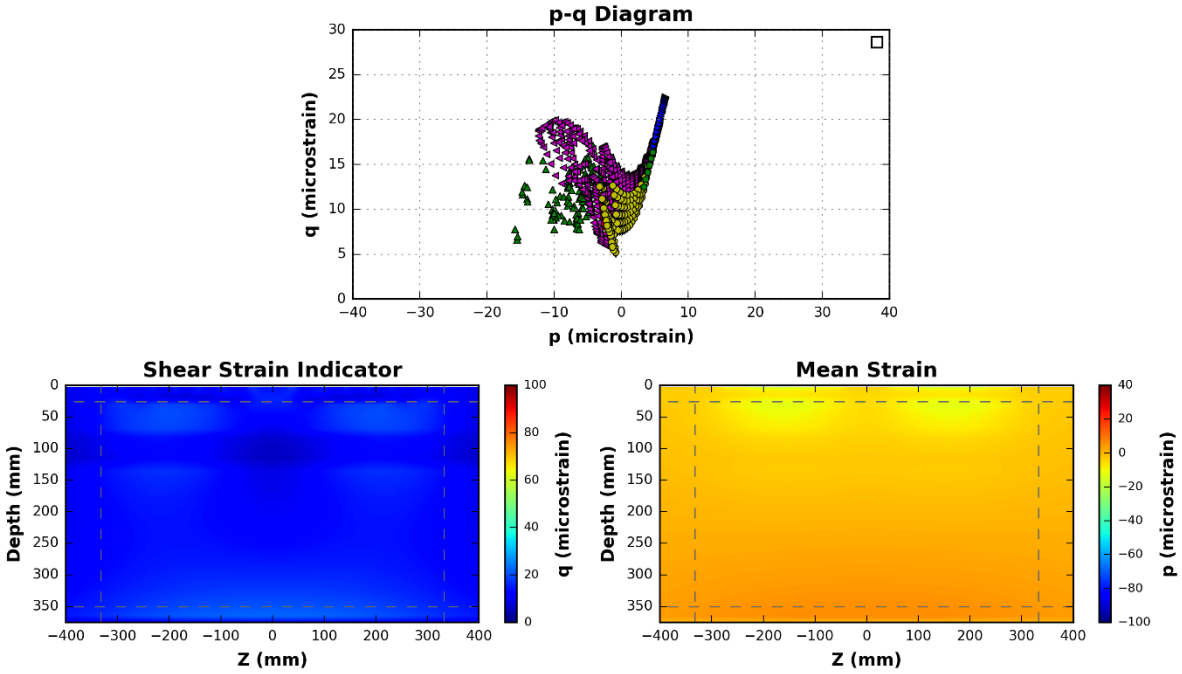

Figure C-010 Mix: ALF Lane 3, Case: 1.0 in overlay thickness.

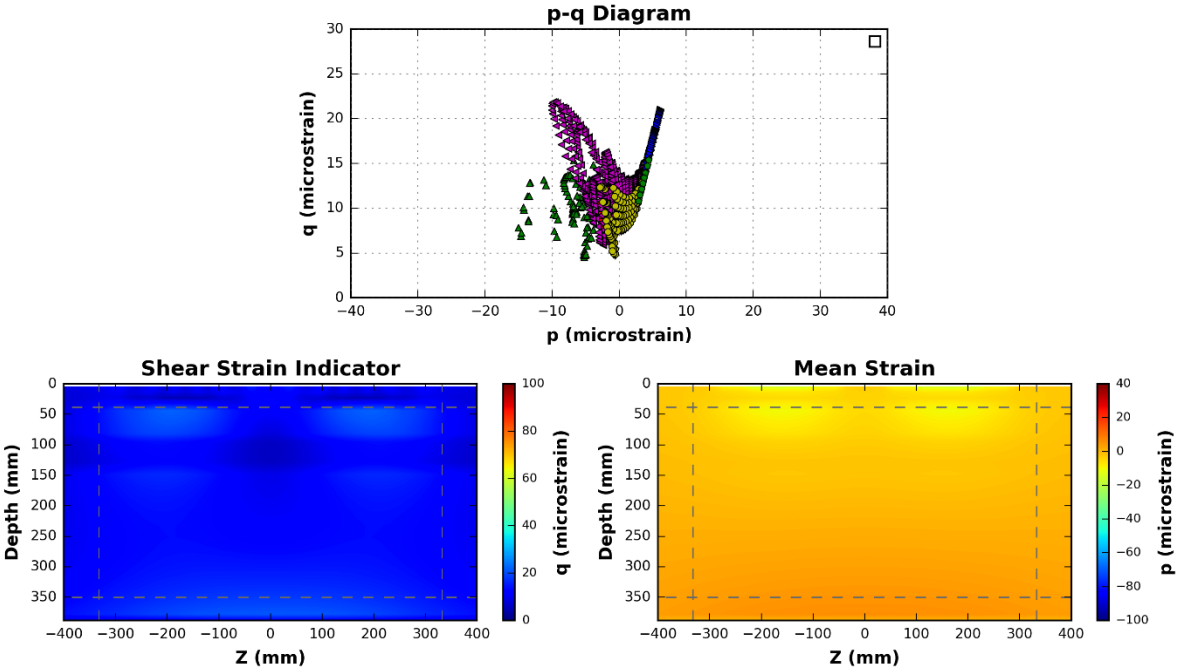

Figure C-11 Mix: ALF Lane 3, Case: 15.0 in overlay thickness.

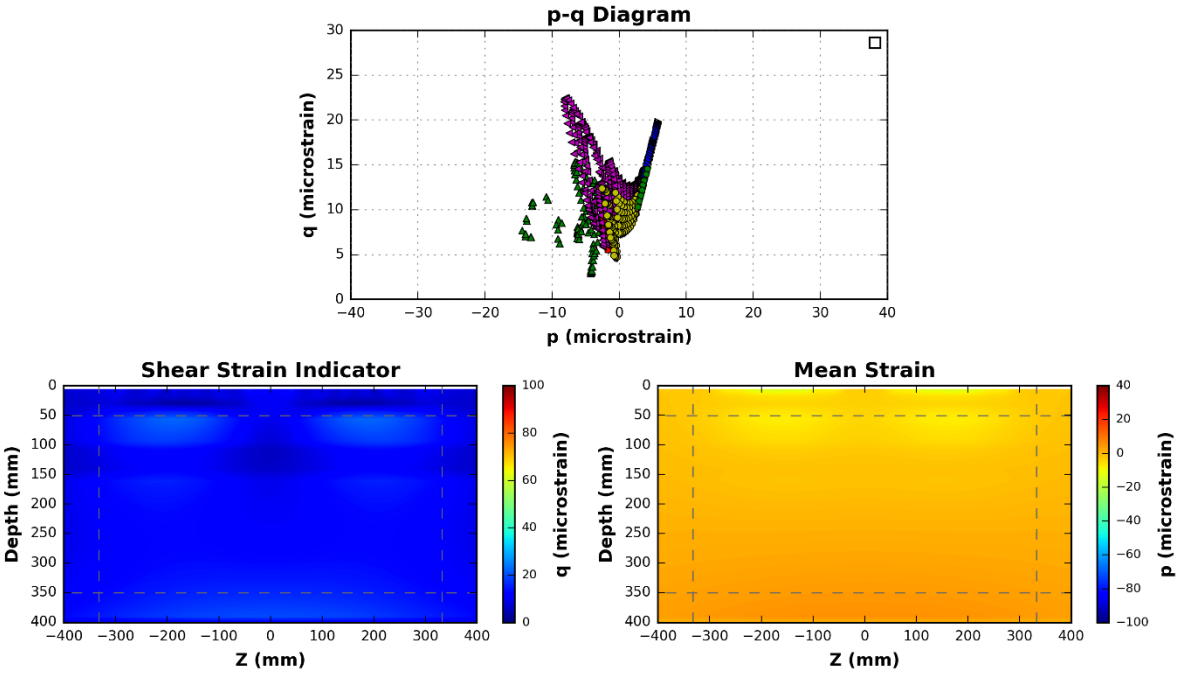

Figure C-12 Mix: ALF Lane 3, Case: 2.0 in overlay thickness.

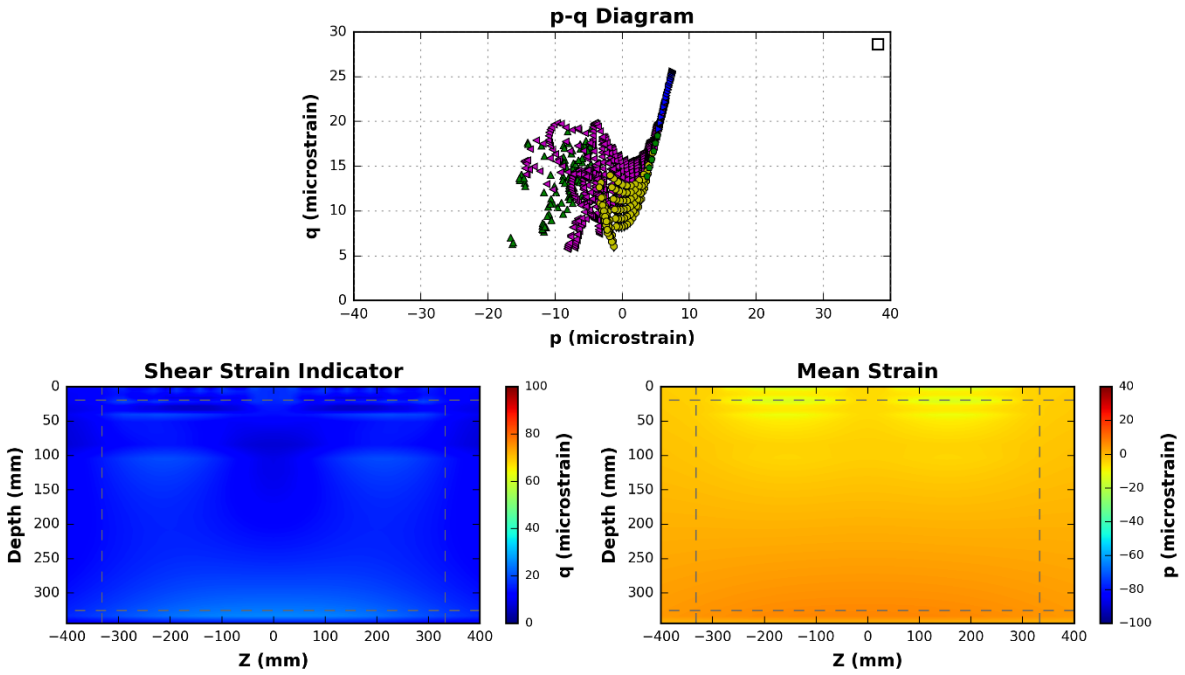

Figure 0-13 Mix: ALF Lane 3, Case: 0.75 in overlay thickness (with a reduced thickness of the AC section).

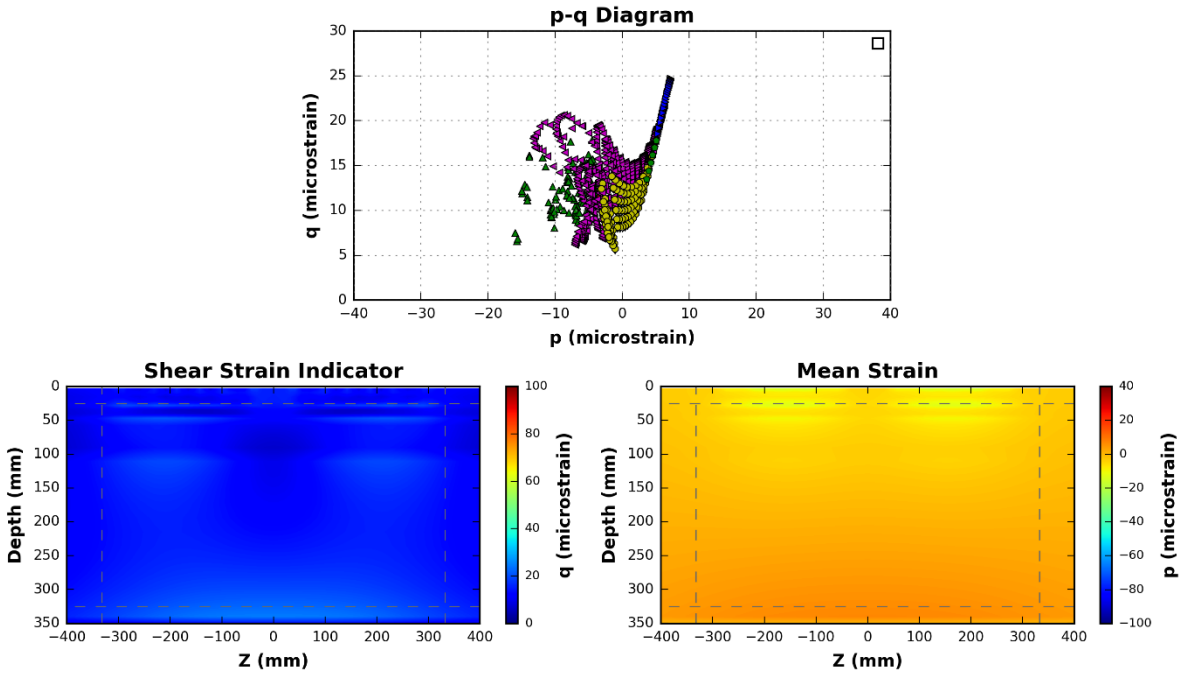

Figure 0-14 Mix: ALF Lane 3, Case: 1.0 in overlay thickness (with a reduced thickness of the AC section).

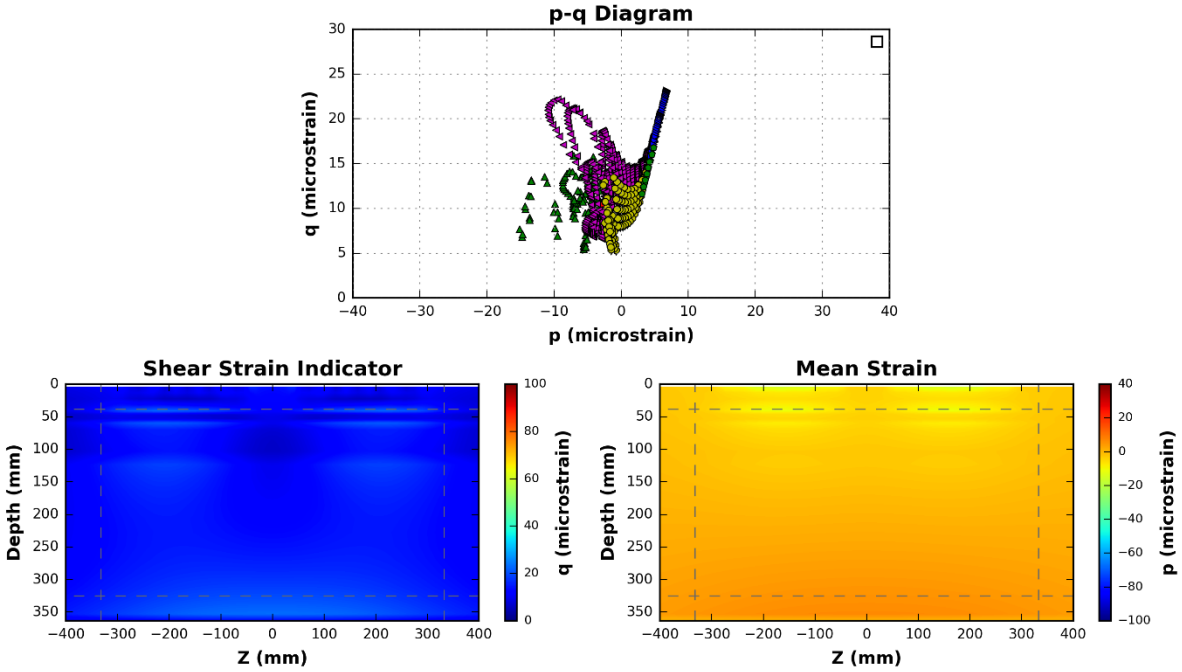

Figure 0-15 Mix: ALF Lane 3, Case: 15.0 in overlay thickness (with a reduced thickness of the AC section).

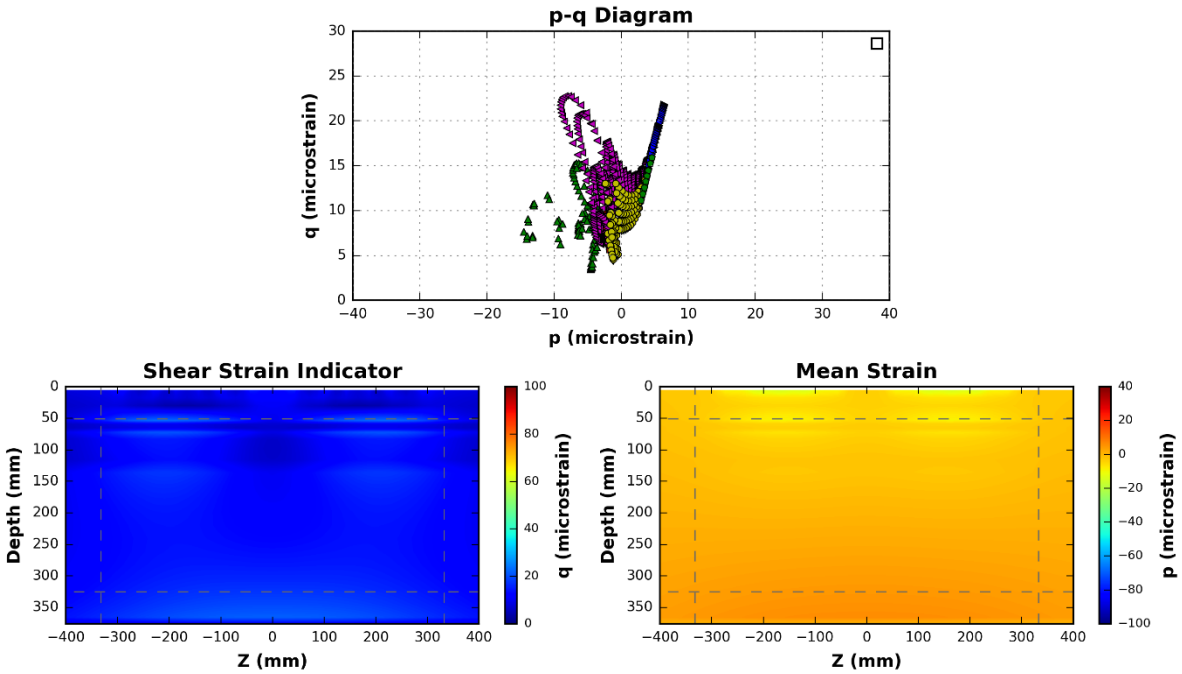

Figure C-16 Mix: ALF Lane 3, Case: 2.0 in overlay thickness (with a reduced thickness of the AC section).